

# Mapping change in rice cultivation using geospatial science in the Paro Valley, Bhutan from 1995-2011

Thesis submitted by

**Dorji Tashi**

**2172009**

October 2018

For the degree of Master of Science in GIS

In College of Science and Engineering

Flinders University, Adelaide, South Australia

Supervisors: Professor Andrew Millington and Professor David Bruce

## DECLARATION

I **Dorji Tashi**, hereby declare that this thesis is my own work with the help of my supervisors. I certify that this thesis does not incorporate without acknowledgment any material previously submitted for a degree or diploma in any university; and that to the best of my knowledge and belief, does not contain any material previously published or written by another person except where due reference is made in the text.

Signature 

Date 19<sup>th</sup> of October 2018

# ABSTRACT

Rice is the major agricultural land use in the world which feeds about 50 percent of its population. This thesis demonstrated an approach to map the change in the spatial extent of rice cultivation using the Remote Sensing (RS) and Geographical Information System (GIS) techniques. The temporal and spatial pattern of change in rice fields from 1995 to 2011 in the Paro valley, Bhutan was analysed with relevant ancillary data to discover some of its major causes (drivers). The conservation of the natural environment is one of the four pillars of Bhutan's development philosophy – Gross National Happiness (GNH); and the 71 percent of the country which is forested provides a habitat for some of the world's endangered species of flora and fauna. Since early 2000, urbanization in Bhutan has expanded rapidly, with this posing a potential threat to both environmental conservation and the supply of agricultural land which is the main source of livelihood for almost 60 percent of the population.

Because information, especially at a local scale, on the change in rice cultivation is not available in Bhutan, this project utilised satellite imagery to derive estimates of rice cultivation in the Paro valley over 16 years. The project employed three broad areas of geospatial science; viz. i) satellite image pre-processing, ii) Land use land cover (LULC) change mapping and iii) spatial analysis to discover some of the causes behind the change in rice fields. Level-2 processed Landsat-5 Thematic Mapper (TM) images of September 1995, August 2005 and August 2011 (summer growing season) were used. Other suitable imagery (satellite or airborne) were not available especially in 1995. Pre-processing and data preparation steps covered verification of geometric registration of images, cloud masking, principal component analysis (PCA), normalized difference vegetation index (NDVI), and extraction of relative heights from the major rivers using a Digital Elevation Model (DEM) from the Panchromatic Remote-sensing Instrument for Stereo Mapping (PRISM) sensor on board Advanced Land Observation Satellite (ALOS). Supervised and unsupervised classifications were performed on five data sets: i) PC1-NDVI-DEM, ii) PC1-PC2-NDVI-DEM, iii) PC1-PC2-NDVI-Relative DEM, iv) PC1-PC2-NDVI-DEM-Relative DEM and v) the original Landsat-5 TM image. Accuracies of ten different LULC classification were compared on a pixel-by-pixel basis with the field cadastral survey data of 2011 which also recorded LU. All geospatial analyses were carried out in ERDAS Imagine 2018 and ArcGIS version 10.6.

Contrary to the findings from the previous literature, none of the composite data of using PCAs, NDVI and or DEM yielded better accuracy than classifications from the original image. Supervised classification of the original TM image produced the highest accuracy. Hence, the maximum likelihood classifier was used for supervised classification of the 1995 and 2005 TM images. Classification accuracies for rice and other crops from the 2011 TM image were 81.4% and 66.6%

respectively, with very high confidences. After applying the same methodology of image classification to earlier dates, a trend of change in LULC from 1995 to 2011 was determined. Despite relatively low accuracy ( $\approx 70\%$ ) for the post-classification change detection, the rice showed an increase in total area of about 500 hectares. This result for the change in rice field was analysed with available ancillary data to explain the possible causes of the increase in the Paro valley. It was found that substantial increase in rice from 1995 to 2011 correlated to the population increase and economic development that occurred during the study period. The coarser spatial resolution of the Landsat imagery and small plot size of rice field created mixed spectral and thus degraded the classification accuracy. Landsat imagery does not seem to be suitable for this type of study in similar terrain.

# **DEDICATION**

To all my Teachers of past, present, and future.

# **ACKNOWLEDGEMENT**

There are many individuals and institutions who contributed to the final form of thesis project. Firstly, to my two supervisors – Professor Andrew Millington and Professor David Bruce of Flinders University. Their vast knowledge, experiences and unwavering support and guidance helped me to complete my Thesis. It is beyond words to express my gratitude to them. Thank you, a lot.

Robert Keane, GIS Specialist, School of the Environment, Flinders University has been kind enough to help me during any technical issue, especially related to GIS. You owe my credit. My thank also goes to Dr Ilka Wallis, for coordinating the Master students' research smoothly.

It would not have been possible without the support from my beloved wife, Lucky Wangmo, who supported my study both financially and morally. An equal share of credit goes to my three children who had sacrificed their parental love and care and coping up with the hard times in our absence. An immense thank also goes to their two Aunts, Dechen Peldon and Jigme Choden who looked after them with utmost love.

I would like to thank Mr. Tashi, Chief Survey Engineer, National Land Commission who has put lot of efforts to mobilise data from different sources and managed to send them to me on time. Lastly, I cannot afford to forget to thank the administration of School of the Environment and Flinders University for facilitating a conducive learning environment.

# ACCRONYMS

6S	Second Simulation of a Satellite Signal in the Solar Spectrum
ANN	Artificial Neural Network
AOI	Area of Interest
AVHRR	Advanced Very High-Resolution Radiometer
DGPS	Differential Global Positioning System
EnMAP	Environmental Mapping and Analysis Programme
ERDAS	Earth Resources Data Analysis System
ERTS	Earth Resource Technology Satellite
GCP	Ground Control Point
GDP	Gross Domestic Product
GIS	Geographic Information System
GNH	Gross National Happiness
IGBP	International Geosphere Biosphere Programme
IHDP	International Human Dimensions Programme
IRS	Indian Remote Sensing
ISODATA	Iterative Self-Organizing Data Analysis
L1T	Level 1 Terrain-corrected
LDCM	Landsat Data Continuity Mission
LEDAPS	Landsat Ecosystem Disturbance Adaptive Processing System
LTS	Landsat Time Series
LULC	Land Use Land Cover

MLC	Maximum Likelihood Classifier
MODIS	Moderate Resolution Imaging Spectro-radiometer
MSS	Multispectral Scanner System
NASA	National Aeronautics and Space Administration
NDVI	Normalized Difference Vegetation Index
NLCD	National Land Cover Database
NLCS	National Land Commission Secretariat
OLI	Operational Land Imager
PCA	Principal Component Analysis
PRISM	Panchromatic Remote-sensing Instrument for Stereo Mapping
RS	Remote Sensing
SOM	Self-Organizing Map
SVM	Support Vector Machine
SWIR	Short Wave Infrared
TCT	Tasselled Cap Transformation
TIR	Thermal Infrared Region
TIRS	Thermal Infrared Sensor
TM	Thematic Mapper
USD	United States Dollar
USGS	United States Geological Survey
VHR	Very High Resolution

# TABLE OF CONTENTS

Declaration .....	i
Abstract.....	ii
Dedication .....	iv
Acknowledgement.....	v
Accronyms.....	vi
Table of contents .....	viii
List of Figures .....	xiii
List of Tables .....	xiv
Chapter One .....	1
1 Introduction.....	1
1.1 General overview of land use land cover change and drivers .....	1
1.2 The specifics of land use change related to rice in Bhutan.....	2
1.3 Overview of Bhutan .....	2
1.3.1 Location and extent .....	2
1.3.2 Topography.....	3
1.3.3 Climate .....	3
1.3.4 Economy and agriculture .....	4
1.3.5 Environmental laws and policies .....	5
1.4 Study area .....	6
1.5 Aims and objectives.....	8
1.6 Thesis structure.....	8
Chapter Two .....	9
2 Literature review .....	9
2.1 Land use land cover change .....	9
2.2 General insights on sectoral causes of land use change.....	10
2.2.1 Natural factors.....	10

2.2.2	Economic factors .....	11
2.2.3	Demographic factors .....	11
2.2.4	Institution factors.....	12
2.3	General causes of land use change in Bhutan.....	12
2.3.1	Natural factors.....	12
2.3.2	Economic factors .....	13
2.3.3	Demographic factors .....	13
2.3.4	Institutional factors.....	13
2.4	Rice production system in Bhutan .....	15
2.4.1	Wet subtropical (low altitude) zone .....	16
2.4.2	Humid subtropical (mid altitude) zone.....	16
2.4.3	Warm temperate (high altitude) zone .....	16
2.5	Remote sensing data sources .....	16
2.6	Image processing techniques .....	17
2.7	Change detection techniques.....	18
2.8	Integration of remote sensing data with other spatial data.....	19
Chapter Three.....		20
3	Methods .....	20
3.1	Data collection .....	20
3.1.1	Brief background on the Landsat series.....	20
3.1.2	Data from Bhutan Government.....	23
3.2	Software used .....	23
3.3	Image pre-processing .....	24
3.3.1	Geometric correction .....	24
3.3.2	Projection.....	25
3.3.3	Clipping study area .....	25
3.3.4	Cloud masking .....	25
3.3.5	Topographic normalization.....	27
3.3.6	Generation of the river network.....	28

3.3.7	Extraction of relative digital elevation model (DEM).....	29
3.3.8	Principal Component Analysis (PCA).....	29
3.3.9	Normalized Difference Vegetation Index (NDVI) .....	30
3.3.10	Layer Stack .....	31
3.4	Digital image processing .....	31
3.4.1	Unsupervised classification.....	32
3.4.2	Supervised classification .....	33
3.4.3	Post-classification smoothing processes .....	35
3.4.4	Accuracy assessment .....	36
3.4.5	Land use land cover mapping.....	37
3.5	Change detection .....	38
3.6	Geospatial analyses for drivers of rice-land .....	38
Chapter Four.....		39
4	Results .....	39
4.1	Image pre-processing .....	39
4.1.1	Geometric verification.....	39
4.1.2	Cloud masking .....	40
4.1.3	Topographic normalization.....	42
4.1.4	Generation of river network .....	43
4.1.5	Extraction of relative digital elevation model.....	43
4.1.6	Principal Component Analysis.....	44
4.1.7	Normalized Difference Vegetation Index .....	45
4.1.8	Layer stack.....	46
4.2	Digital image processing .....	47
4.2.1	Supervised classification .....	47
4.2.2	Post-classification processes .....	47
4.2.3	Accuracy assessment .....	47
4.2.4	Accuracy assessment for unsupervised classification .....	47
4.2.5	Accuracy assessment for supervised classification .....	49

4.2.6	Land use land cover mapping.....	52
4.3	Change detection .....	56
4.3.1	Change from 1995 to 2005 .....	56
4.3.2	Change from 2005 to 2011 .....	57
4.3.3	Change from 1995 to 2011 .....	57
4.4	Accuracy of post-classification change detection.....	60
4.4.1	Statistical method .....	60
4.4.2	Visual assessment of change detection accuracy.....	60
4.5	Drivers of LULC change.....	62
4.5.1	Natural factors.....	62
4.5.2	Economic factors .....	65
4.5.3	Demographic factors .....	65
4.5.4	Policy factors .....	66
Chapter Five	.....	67
5	Analysis and Discussion .....	67
5.1	Image pre-processing .....	67
5.1.1	Geometric verification.....	67
5.1.2	Generation of river network .....	67
5.1.3	Extraction of relative Digital Elevation Model .....	67
5.1.4	Normalized Difference Vegetation Index .....	68
5.2	Digital image processing .....	68
5.2.1	Unsupervised classification.....	68
5.2.2	Supervised classification .....	68
5.2.3	Accuracy assessment .....	69
5.2.4	Accuracy of PC1-NDVI-DEM composite data .....	70
5.2.5	Accuracy of original TM image.....	71
5.3	Change detection .....	74
5.3.1	Change in rice fields from 1995 – 2005.....	74
5.3.2	Change in rice fields from 2005-2011.....	74

5.3.3	Change in rice fields from 1995-2011.....	74
5.3.4	Change detection accuracy .....	74
5.4	Drivers for change in rice cultivation .....	75
5.4.1	Socio-economic factors.....	75
5.4.2	Demographic factors .....	76
5.4.3	Institutional factors .....	76
5.5	Limitations of the study.....	76
Chapter Six.....		78
6	Conclusion and Recommendation .....	78
6.1	Key findings.....	78
6.1.1	Challenge to acquire suitable satellite data .....	78
6.1.2	Highest accuracy by supervised classification of original TM image.....	78
6.1.3	Overall increase in rice cultivation during the study period.....	79
6.1.4	Possible drivers of increase in the rice cultivation.....	79
6.2	Recommendations .....	79
6.2.1	Higher spatial resolution imagery .....	79
6.2.2	Higher spectral resolution .....	80
6.2.3	More specific ancillary data .....	80
6.2.4	Change trajectory analysis.....	80
6.2.5	Control illegal cropping .....	80
References.....		81
Appendix A: Crop calendar for Paro district .....		96
Appendix B: Encapsulated Postscript for cloud masking model.....		97
Appendix C: Python script of the model to extract relative DEM .....		99
Appendix D: Encapsulated Postscript for accuracy assessment model .....		101
Appendix E: Land use land cover change map from 1995-2005 .....		102
Appendix F: Land use land cover change map from 2005-2011 .....		103
Appendix G: Land use land cover change map from 1995-2011 .....		104

# LIST OF FIGURES

Figure 1. 1 Global map of rice production in million metric tons .....	2
Figure 1. 2 Location of Bhutan in the South East Asia region .....	3
Figure 1. 3 Bhutan: climatic zones.....	4
Figure 1. 4 Location of Paro Valley and map of Bhutan with reference to world map. ....	6
Figure 1. 5 Red rice produced from Paro Valley. ....	7
Figure 1. 6 Paro valley showing Paro Dzong in the front and Paro town in the background and rice field on left and right centre in light green/yellow tones. ....	7
Figure 2. 1 Photograph of a scarecrow to prevent wild animals from entering the paddy field in the Paro valley.....	15
Figure 2. 2 Terraced rice farming in Bhutan. ....	15
Figure 3. 1 Landsat Time Series. The red lines indicate the year of images used for the current study .....	21
Figure 3. 2 Cross section profile of Paro valley .....	24
Figure 3. 3 Cloud masking model .....	27
Figure 3. 4 Model in the ArcTool box to extract relative DEM. The Python script for this model is given in the Appendix B. ....	29
Figure 3. 5 Flow diagram of main processes.....	32
Figure 3. 6 Histogram of distance file in MLC for rice class; threshold set at 39.972.....	35
Figure 3. 7 Spatial model to subtract two thematic images used for accuracy assessment.....	37
Figure 4. 1 Cloud quality bands (subsets) for (a) 1995, (b) 2005 and (c) 2011 Landsat TM images .....	41
Figure 4. 2 Image of (a) combined cloud QA band, (b) 2011 TM image with cloud cover (BGR=543) and (c) output of cloud masking (BGR=543).....	41
Figure 4.3 (a) 2011 TM image before topographic normalization and (b) 2011 TM image after topographic normalization; band combination 5,4,3 RGB.....	42
Figure 4. 4 Spectral profiles of two locations for (a) original 2011 TM image (b) Topo normalized image.....	43
Figure 4. 5 Relative DEM with values of relative height from the nearest river points .....	44
Figure 4. 6 Percentage of information content in different PCs.....	45
Figure 4. 7 Classification output images after (a) MLC, (b) Threshold, (c) Majority filter and (d) Clump and Eliminate .....	47

Figure 4. 8 Error map of rice classification on 2011 TM image using supervised classification. Most of the errors were seen to occur along the edges of LU as marked by A and rarely in larger clumps as labelled by B. ....	51
Figure 4. 9 Error map of other crops classification on 2011 TM image using supervised classification .....	52
Figure 4. 10 Land use land cover map of Paro Valley, 1995 .....	53
Figure 4. 11 Land use land cover map of Paro Valley, 2005 .....	54
Figure 4. 12 Land use land cover map Paro Valley, 2011. ....	55
Figure 4. 13 Total area of rice in study area for 1995, 2005 and 2011 .....	56
Figure 4. 14 Maps showing change in rice cultivation between different years.....	59
Figure 4. 15 The increment of rice from 1995 – 2005 from change detection analysis.....	61
Figure 4. 16 The red boundary line shows the increase in rice from the classification maps.....	61
Figure 4. 17 The area marked by black polygon is shown as decrease in rice from 1995 to 2005 due to the error of omission in the 2005 image classification. ....	62
Figure 4. 18 Annual rainfall from 1995 to 2011 in the study area .....	63
Figure 4. 19 Rainfall during the rice growing months (June-September) from 1995 -2011.....	63
Figure 4. 20 Mean monthly temperatures for 1995, 2005 and 2011 in the Paro valley.....	64
Figure 4. 21 Mean temperatures of rice growing months (June-September) of 1995, 2005 and 2011 .....	64
Figure 4. 22 Growth in GDP for Bhutan, 1990 to 2012 .....	65
Figure 4. 23 Total population of Bhutan in 1995, 2005 and 2011 .....	66
Figure 5. 1 Sample spectral signature showing two spectrally different rice class and rice class overlapping with other crop.....	69
Figure 5. 2 Mean values of forest and rice classes in the PC1-NDVI-DEM composite image.....	71
Figure 5. 3 Spectral signatures of forest and rice in the original Landsat image for the same pixels used to calculate mean values in Figure 5. 2. ....	71
Figure 5. 4 Mismatch of edges between the rice raster and the polygon rice.....	72
Figure 5. 5 Histogram showing number of rice plots of varied sizes.....	73
Figure 5. 6 A typical example of rice plots interspersed by other land uses (white areas). The area of each plot in m <sup>2</sup> is labelled.....	73

## LIST OF TABLES

Table 3. 1 Outline of Landsat-5 TM bands and their corresponding spatial resolution .....	22
Table 3. 2 List of Landsat scenes used for the study (Path 138, Row 41).....	23
Table 3. 3 List of ancillary data from the government of Bhutan .....	23
Table 3. 4 Surface reflectance values of cloud quality assessment (sr_cloud_qa) band. ....	26
Table 3. 5 Minnaert constant .....	28
Table 4. 1 The Root Mean Square Error (RMSE in pixels) of geo-rectification of three date images done by USGS .....	39
Table 4. 2 Results of geo-registration of Landsat-5 TM 2011 image with Google Earth 2012.....	40
Table 4. 3 Comparison of pixel values for two locations for original and topographic normalization image.....	42
Table 4. 4 Amount of information in different PCs expressed in terms of eigenvalues and percentages. ....	45
Table 4. 5 Ranges of values in different datasets.....	46
Table 4. 6 Different data type selected while combining different layers of datasets .....	46
Table 4. 7 Comparison of classification accuracy of rice (unsupervised) among different datasets	48
Table 4. 8 Comparison of classification accuracy of other crop (unsupervised) among different datasets.....	48
Table 4. 9 Comparison of classification accuracy of rice (supervised) among different datasets ...	49
Table 4. 10 Comparison of classification accuracy of other crop (supervised) among different datasets.....	49
Table 4. 11 Change matrix of land cover from 1995-2005 .....	56
Table 4. 12 Change matrix of land cover from 2005-2011 .....	57
Table 4. 13 Change matrix of land covers from 1995-2011.....	58

# CHAPTER ONE

## 1 INTRODUCTION

### 1.1 General overview of land use land cover change and drivers

Significant modification of land surface has taken place over thousands of years since humans started domesticating animals and plants for their food and services (Mittermeier et al. 2002). It has resulted in the serious alteration in patterns of land use and land cover (LULC). It is known that the ramifications of LULC change exerts negative impacts on the environment and climate (Lambin, Geist & Lepers 2003). However, LULC change benefits are also experienced, especially in the form of increased production of food, fibre, and services. Therefore, studies on LULC change are gaining continued attention from diverse research communities, especially in order to try to strike a balance between environmental degradation and intensification of food production (Foley et al. 2005; Kleemann et al. 2017; Lambin, Geist & Lepers 2003; Manakos & Braun 2014). International organizations like the International Geosphere Biosphere Programme (IGBP) and International Human Dimensions Programme on Global Climate Change (IHDP) play active roles in global LULC change mapping, studying the causes and even developing predictive models for LULC change (Goldewijk 2001).

Initially, scientists thought that LULC changes occurred in a progressive, linear and irreversible manner caused by the growth in human populations, but recent findings have dispelled this simplistic notion and it is now understood that LULC change is driven by more complex and interdependent spatio-temporal factors (Lambin, Geist & Lepers 2003). Lambin, Geist and Lepers (2003) classified the drivers of LULC change into two broad categories of proximate (direct) and underlying (indirect). The proximate drivers are direct human activities that immediately contribute to the change in land use decisions locally, whereas underlying drivers are fundamental forces that influence the proximate factors; these underlying decisions are often made far away from the site of land use change. Underlying drivers can also be biophysical factors, as well as the economic, institutional, demographic and cultural factors alluded to above. More recently, it has been realised that many of these underlying factors combine into what can be termed the forces of globalization. Depending on the different spatial and temporal natures of human-environment interaction, the drivers can be reshaped to form a unique pathway for LULC change (Lambin et al. 2001) for a particular area at a particular instant in time.

## 1.2 The specifics of land use change related to rice in Bhutan

Despite the rapid expansion of global agricultural land that has been occurring over the last one and a half centuries (Goldewijk 2001), the issue of global food security still remains a critical challenge in the wake of ever increasing population (Dong & Xiao 2016). Rice is the staple cereal for more than half of the world's population, although it accounts to only about 12 percentage of global agriculture land area (FAO 2013). Rice cultivation has huge environmental effects in the form of increased fresh water consumption, more evapotranspiration from the flooded paddy fields which causes disturbances in the normal surface temperature and increases methane emissions (Dong & Xiao 2016; Shrestha, Chapagain & Babel 2017). Therefore, it is crucial to monitor paddy fields both at global and regional scale, in terms of their spatial location, changes and drivers of the changes. Asia produces more than 90 percentage of rice in the world (Kuenzer & Knauer 2013), and at the same time almost 50 percentage of the global rice produce is consumed by Asian countries (Muthayya et al. 2014) as it can be seen from Figure 1. 1. Similar to the rest of Asia , rice is one of the major crops cultivated in Bhutan. It is the staple cereal and its per capita consumption is 172 kg per person annually (Ghimiray, Pandey & Velasco 2013).

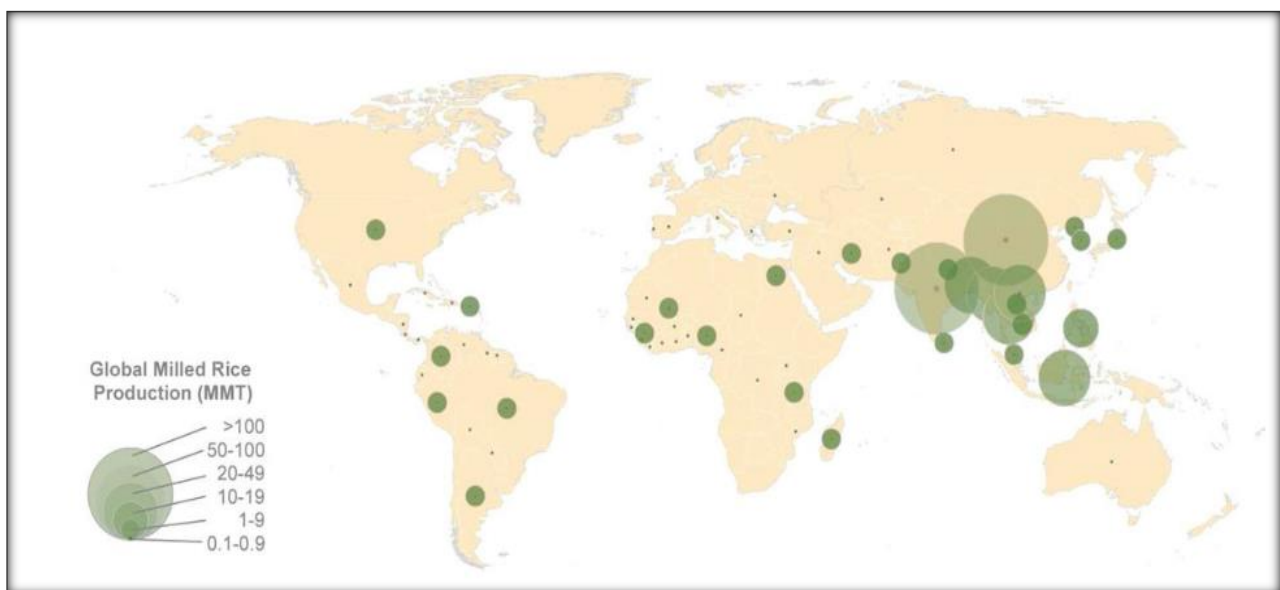


**Figure 1. 1 Global map of rice production in million metric tons**

Adapted from Muthayya et al. (2014)

## 1.3 Overview of Bhutan

### 1.3.1 Location and extent

Bhutan is a tiny mountainous country, located in the eastern Himalayas between China in the north and India in the west, south and east (Figure 1. 2). It has a total area of 38,394 sq. km. It extends between longitudes 89° E and 93° E, and latitudes 27° N and 29° N. Its longest east-west dimension

is about 300 km and from north-south extent is 170 km. It is heavily forested with 71 percent of area under forest cover; only around 3 percent is agricultural land (National Statistics Bureau 2017). The total population of Bhutan in 2017 was 727,145 with a population growth rate of 1.5% per annum (National Statistics Bureau 2018).

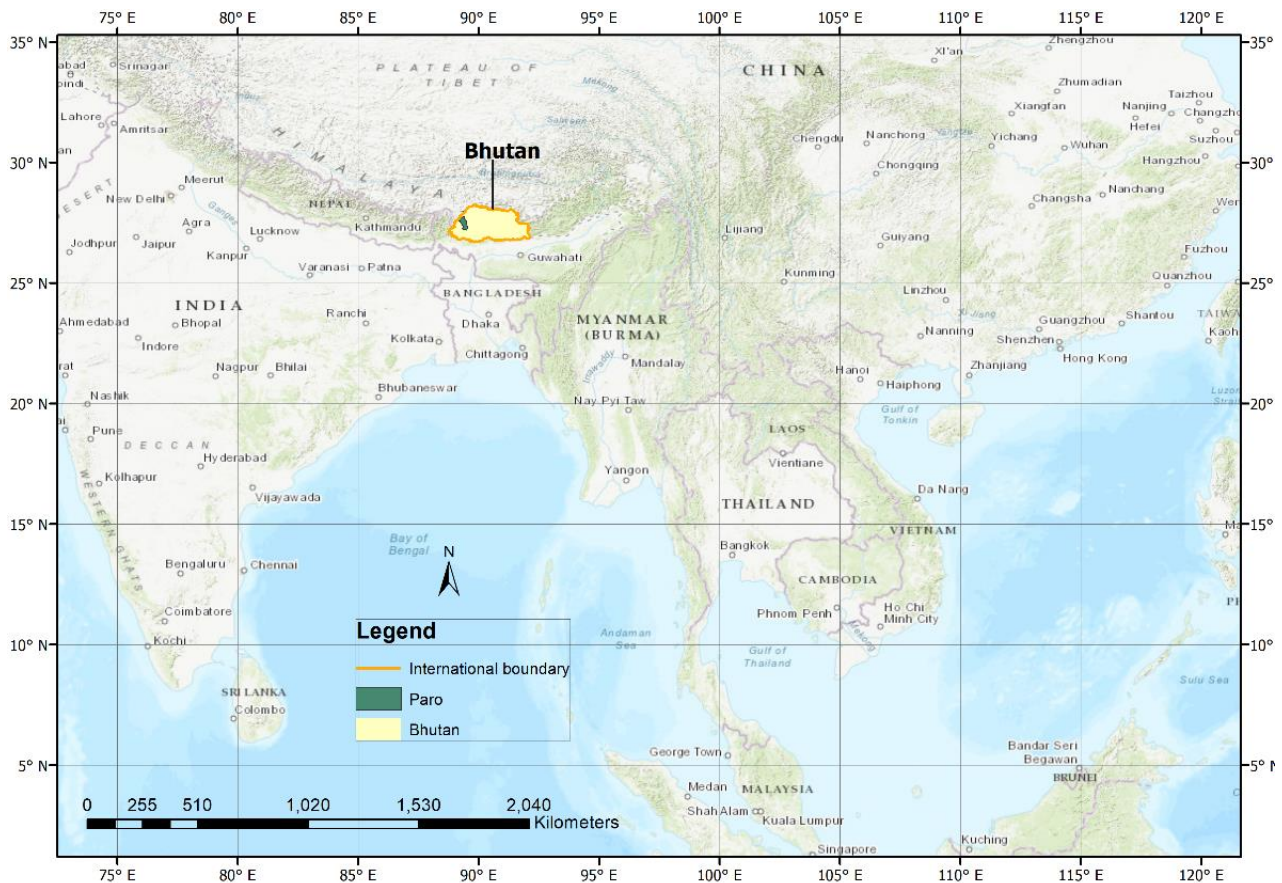


**Figure 1. 2 Location of Bhutan in the South East Asia region**

### 1.3.2 Topography

The lowest elevations are about 160 m above mean sea level in the Himalayan foothills of southern Bhutan, but as much of the country is mountainous it is unsurprising that the highest elevations exceed 7500 m in the Greater Himalayas in the north. Such extreme variations in altitude make it one of the most rugged and mountainous countries in the world. Four major river systems which flow southwards through Bhutan, join the Brahmaputra River before it drains into the Bay of Bengal. These rivers have immense ecological and economic significance to Bhutan.

### 1.3.3 Climate

Bhutan's climate is influenced by monsoon winds blowing from the Bay of Bengal and varies with elevation. The whole country can be broadly divided into three distinct climatic zones. In the northern part of Bhutan, the weather is extremely cold all-round the year and mountains are permanently covered with snow. Temperate central Bhutan experiences moderate temperature and rainfall.

Southern Bhutan remains hot and humid throughout the year, with temperatures ranging from 15-30°C. Figure 1. 3 shows a climate map of Bhutan with further subdivisions of three zones. In fact, the temperature invariably depends on the altitudes in Bhutan. Kubiszewski et al. (2013) observed that the temperatures decreased by 0.5 °C for every 100 m rise in elevation. Precipitation largely depends on latitude. Bhutan experiences four distinct seasons in a year: spring from March to May, summer from June to August, autumn from September to November and winter from December to February. Most crops are grown between spring to early autumn.

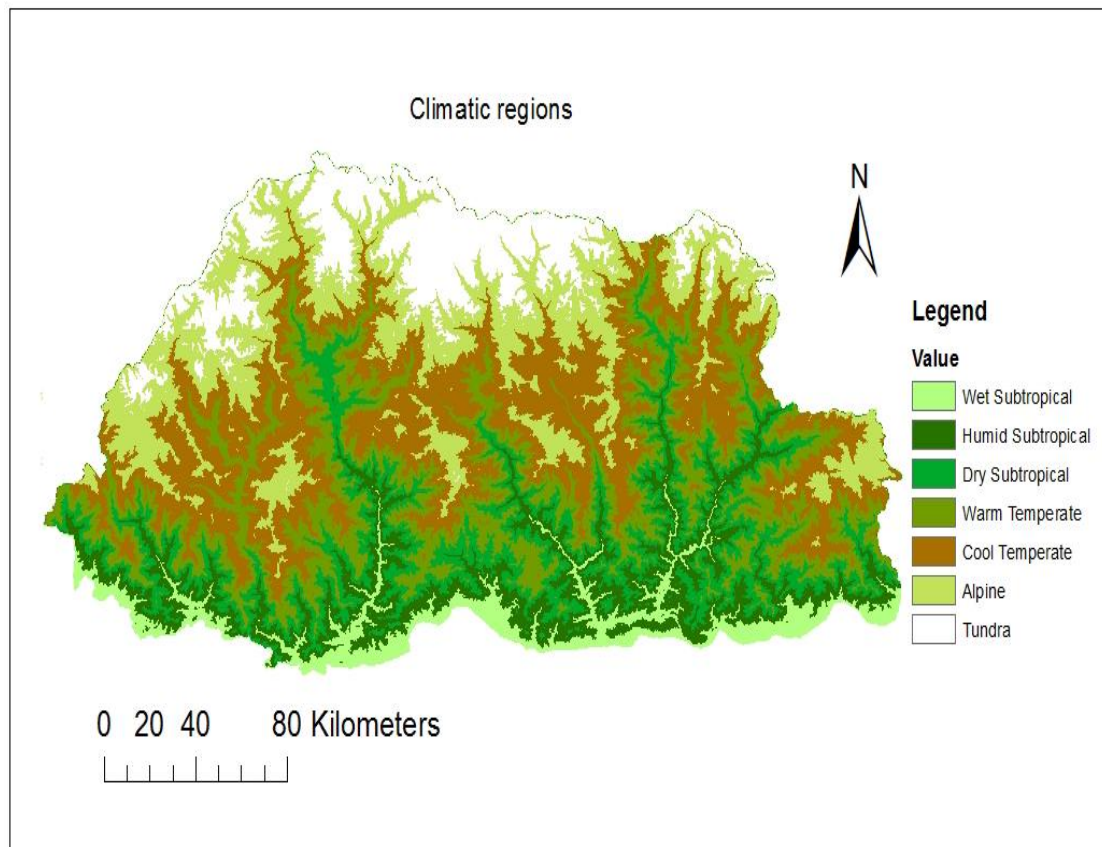


**Figure 1. 3 Bhutan: climatic zones**  
Source: (National Statistics Bureau 2017)

#### **1.3.4 Economy and agriculture**

Economically, Bhutan is an agrarian country with limited access to roads, electricity and modern infrastructure and has one of the world’s smallest and least-developed economies. However, Bhutan has begun its conscious progress towards modernizing its economic structure keeping in mind the sustainability of environment and culture for future generations; all under the umbrella of good governance. Agriculture is the main source of livelihood for about 62% of Bhutanese population and the staple crop is rice (National Statistics Bureau 2018). However, the country depends heavily on imported food items. The export of agricultural products is minimal and seasonal which widens the trade deficit.

The Government of Bhutan is working hard to achieve food self-sufficiency through different promotional activities and initiatives like regularizing government land to landless people, subsidies on hybrid seeds, farm mechanization, road connectivity and intensifying agricultural research (Chhogyel et al. 2015). Consequently, agriculture in Bhutan is making a transition from subsistence, small-scale farming to a large-scale farming despite many hindrances posed from the increasing wildlife population and construction activities.

The unbalanced levels of economic development between different districts in Bhutan is a leading cause of rural to urban migration. The development of infrastructure and the establishment of government institutions are concentrated in the major cities (Yangchen, Thinley & Wallentin 2015), of which Paro, the focus of this thesis, is one. Both urbanization and nature conservation are hindrances to achieving the national goal of food self-sufficiency.

In the light of tensions between different sectors, it is important to obtain accurate information on land use change related to rice cultivation, and its main causes for proper management of limited land resources. Using remote sensing (RS) and geographical information science (GIS) technologies, this study is of its first kind to locate and investigate accurate image dataset and methods to map LULC change in mountainous terrain and explore the main drivers of change in rice cultivation in Bhutan with reference to Paro Valley as the study area.

Remote sensing is a term used when the information of the object of interest is collected from a distance (remotely) and GIS is a set of methods and analytical tools that can store, manipulate, analyse and display geo-spatial data. The remotely acquired satellite images are processed to give information on LULC change. From LULC change map, numerous studies can be conducted, for instance to find out the factors causing the LULC change.

### **1.3.5 Environmental laws and policies**

Bhutan's development approach is based on the principle of Gross National Happiness (GNH). An excerpt from the Centre for GNH (2018) states:

GNH is a holistic and sustainable approach to development, which balances material and non-material values with the conviction that humans want to search for happiness. The objective of GNH is to achieve a balanced development in all the facets of life that are essential; for our happiness.

This can be achieved through the implementation of four pillars of GNH:

- i. Good governance;
- ii. Sustainable socio-economic development;
- iii. Preservation and promotion of culture;

- iv. Environmental conservation.

Guided by the principle of GNH, the constitution of Bhutan, 2008 mandates the government to maintain a minimum of 60 percent of country under forest cover for all times (Royal Government of Bhutan 2008). In line with the constitution, there are other laws, such as the Forest and nature conservation Act, 1995, which prohibit illegal cutting of trees and hunting.

### 1.4 Study area

Paro District, located in the north-western part of Bhutan (Figure 1. 4), is one of the fastest growing urban areas in Bhutan (Yangchen, Thinley & Wallentin 2015). It stretches from the confluence of two major rivers: one from the Thimphu valley and the other from Paro valley in the south to the Mount Jomolhari (7326 m) in the north on the border with the Tibetan Autonomous Region of China. It is the widest valley in the country with large extents of fertile rice fields located along the Pa Chhu, the local name for Paro River (Figure 1.6).

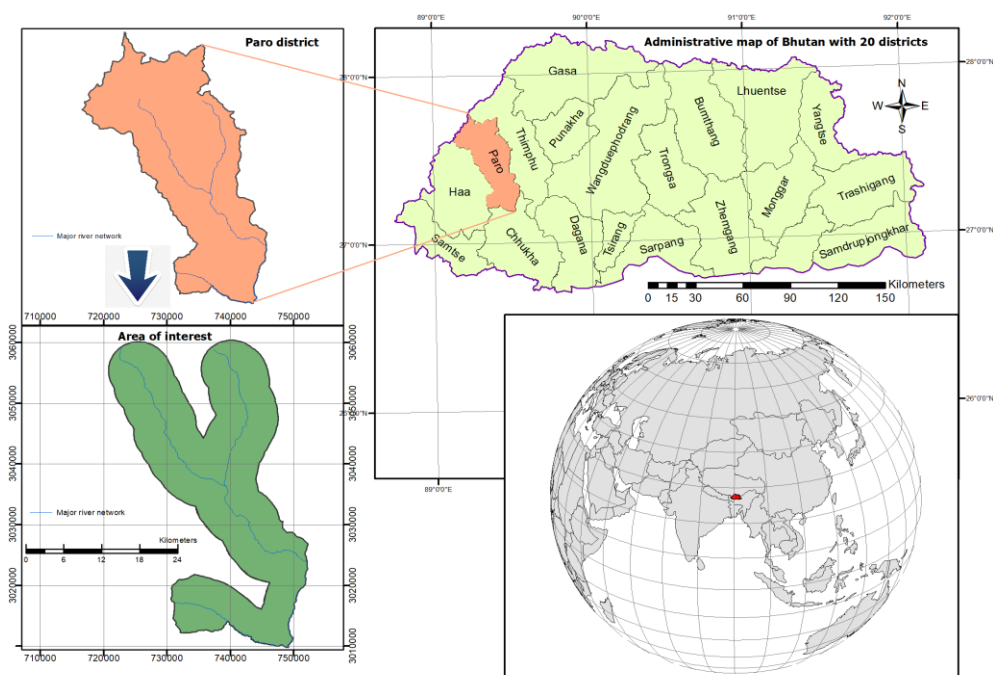


**Figure 1. 4 Location of Paro Valley and map of Bhutan with reference to world map.**

Paro is famous locally for its red rice (Yue-chhum in Dzongkha<sup>1</sup>) shown in Figure 1. 5, which is exported to developed countries like the USA and Canada. Due to the availability of a good communication system (an airport and roads) and the proximity to the capital city, Thimphu;

<sup>1</sup> Dzongkha is the national language of Bhutan.

continuous infrastructural development has been taking place in the area over the last two decades.



**Figure 1. 5 Red rice produced from Paro Valley.**

(Source: <https://i.pinimg.com/originals/82/85/ea/8285ead97ff578e4708ec1836c97b131.jpg>)

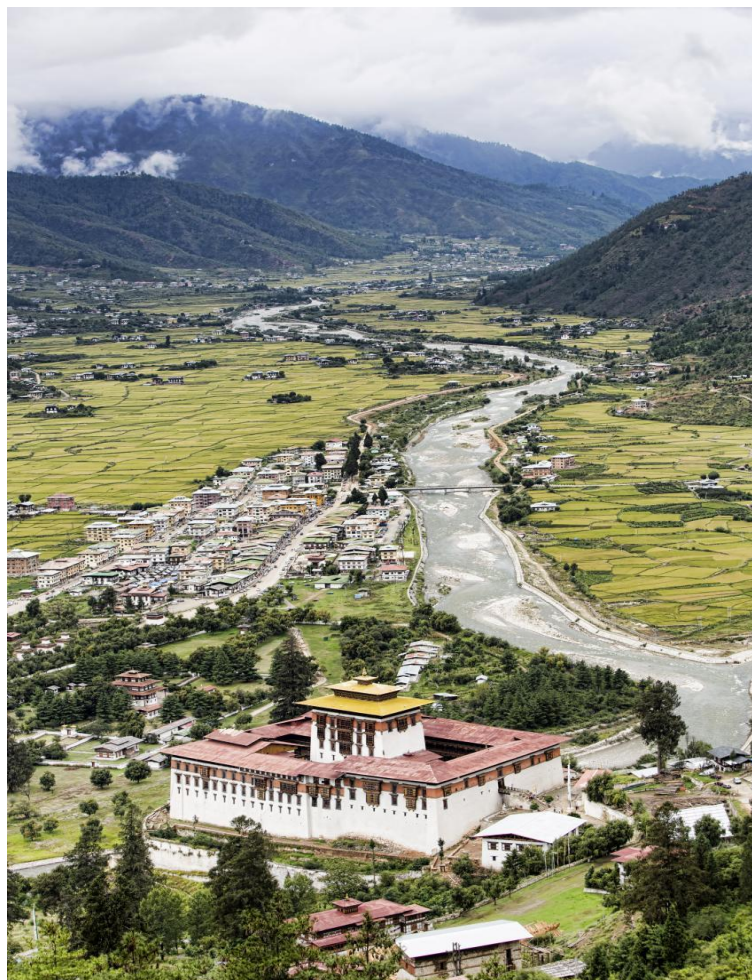


**Figure 1. 6 Paro valley showing Paro Dzong<sup>2</sup> in the front and Paro town in the background and rice field on left and right centre in light green/yellow tones.**

(Source: <https://upload.wikimedia.org>)

---

<sup>2</sup> Dzong is a typical type of fortress mainly serves as the district administrative headquarters, besides having religious and social purposes.

## **1.5 Aims and objectives**

This study aims to answer one major and one minor research question. The major question is:

Which dataset and image processing methods are most suitable for change detection of rice cultivation in Bhutan?

The minor question is:

What are the possible factors that have influenced rice land use change in the study area from 1995 to 2011?

The research objectives emanating from these two questions are:

1. Critically review and analyse different technologies used for LULC change detection studies.
2. Map the changes in rice fields using most appropriate method and analyse different drivers for this change in the selected area.

## **1.6 Thesis structure**

This thesis is presented in six chapters. Chapter One is an introductory chapter which gives a brief overview of land use and land cover change in the global context. It also provides an overview on the importance of rice and rice land use in Bhutan, and a background of Bhutan and the study area. The chapter ends with the statement of research questions in the form of aims and objectives. Chapter Two delves into the relevant literature and discusses drivers of LULC change and techniques to map LULC change in the context of both global research and the study area. Chapter Three elaborates the methodology that was adopted in this study to achieve the results. The results are presented in form of tables, charts, maps, graphs and descriptions in Chapter Four. The main findings of the research are then analysed and discussed in Chapter Five. Finally, Chapter Six states the important conclusions that have been drawn from the study and gives some recommendations for future research in similar environments.

# CHAPTER TWO

## 2 LITERATURE REVIEW

Since, more than 50 percent of global agricultural land use (LU) is under the paddy cultivation, the literature review in this chapter begins with a broad context of general land use land cover (LULC) change and drivers causing the LULC change both at global and regional scale. Then it reviews relevant literatures on the rice cultivation and finally concludes the chapter with brief review on the geospatial techniques used for mapping the change in LULC with special focus on mapping of rice.

### 2.1 Land use land cover change

Not so long ago, atlases and existing hard copy maps were the only available sources of information for land use land cover (Friedl et al. 2002). They exhibited reasonably good accuracy of land use but inherently failed to maintain the currency of data to study change of LULC. By the time a LULC map has been produced from the existing data sources, quite a lot of additional changes in the land cover would have occurred. Now remote sensing technology and different image processing algorithms have become the state-of-art tools for detecting changes in LULC which can be further used with other socio-economic data to find the causes of change (Chaplin-Kramer et al. 2015; Hamad, Balzter & Kolo 2017; Kumar & Rawat 2015; Vogelmann et al. 2012). Global LULC is an intrinsically non-static phenomenon (Hamad, Balzter & Kolo 2017) and requires most appropriate datasets in terms of spatial, spectral and temporal resolution to give an accurate information on change. This accurate information on the LULC change can be used to help proper management of land resources. Land is a scarce resource and many land uses compete for the limited available land (Lambin & Meyfroidt 2011). The modern approach to agricultural land use called "green revolution" which makes use of chemical fertilizers, improved cultivars, pesticides, mechanization and irrigation facilities, has helped immensely to increase the global grain yield with less amount of deforestation. But extensive use of fertilizers was found to pollute water and the soil gets more salinized from irrigation of rice fields (Foley et al. 2005).

Once viewed as a serious challenge in maintaining enough agricultural land to feed the increasing global population has been now overcome with the breakthrough of technological revolution and modern research in the agriculture field. The global food supply is much better with surplus storages but the persistence of fundamental issue on hunger is due to the lack of income to buy the food that abounds (Hazell & Wood 2008). The increase in global grain production was achieved, not by expanding agricultural land but it was due to the agricultural intensification. The new strategy of shifting from expansion of agricultural area to intensification has helped to reduce the demand for

billions of hectares of land conversion to agriculture (Cassman et al. 2005). However, sometimes, such global situation masks the real problem that most of the people face at national and local level. For instance, Bhutan's self-sufficiency for rice (the staple cereal) was lagging at 48% in 2010 and the deficit was met from imports (Japan International Cooperation Agency 2012).

## **2.2 General insights on sectoral causes of land use change**

As complex as the land use change is, so are the drivers of that change due to its spatial and temporal variation (Lambin, Geist & Lepers 2003). These drivers can exhibit high interdependence (Kleemann et al. 2017). Identifying the drivers of land use change involves the understanding of various factors influencing the decision on land use at individual, company, organisation and governmental levels. Various studies conducted at the local and regional level can help to understand the causes of LU change.

### **2.2.1 Natural factors**

The LULC change and climate change are closely interrelated. Climatic variations increase the demand for food and agro-based products from land and it can influence the LULC change either directly or through feedback mechanisms. Fluctuations of climate variables like temperature rise and erratic precipitation can negatively affect crop growths (Johnson & Hutton 2014; Ostwald, Wibeck & Stridbeck 2009). For instance, very little or no rain causes drought and excessive rain leads to soil erosion. Such forms of land degradation by variation in the climatic conditions triggers either abandonment of agricultural land or people go in search of better land which is achieved mostly through deforestation (Bewket & Abebe 2013; Lambin, Geist & Lepers 2003). Studies have shown that the temperature rise due to global warming has a negative impact on the yield of rice since the rising water level from snow melts inundates the low lying paddy fields (Kontgis, Schneider & Ozdogan 2015; Peng et al. 2004).

However, Kleemann et al. (2017) argue that it requires long term studies to detect and quantify the effects of climate change on land use. Apart from climate variability affecting land use, there is a range of other biophysical factors that are particularly considered as confounding constraints for cropland expansion (Lambin & Meyfroidt 2011). Conversely, several studies also revealed that the change in LULC influences the surface albedo of land (Liu et al. 2016). (Peng et al. 2004) argue that the LULC change is one of the main factors causing the global climate change. The global land use by anthropogenic activities alone contributes almost 35% of total CO<sub>2</sub> budget in the atmosphere (Foley et al. 2005). The climatic factors and change in agricultural land are interdependent and any disturbance in one can potentially produce a significant impact on the other.

### **2.2.2 Economic factors**

Globalization has helped to conduct international trade with different countries. Most developing countries face the consequences of economic globalization in the form of deforestation and increasing cropland (Lambin & Meyfroidt 2011). Although the import of food and wood products helps in conserving the natural environment for that nation, it displaces the demand for those products in other countries which ultimately increases deforestation (Lambin & Meyfroidt 2011). A plethora of economic variables like price, tax, irrigation, market, subsidies, transportation cost, demand, investment, technology, and manpower influence the land use land cover both at local and global scale (Lambin, Geist & Lepers 2003; Liu et al. 2014). For instance, the increasing demand for food products leads to expansion of agricultural land at the cost of losing forest. It is claimed that in the tropical regions of the world from 1980 to 2000, 55 percent of intact forest and 28 percent of disturbed forest were converted to agricultural land (Costa, Botta & Cardille 2003; Gibbs et al. 2010). But this can be counteracted through agriculture intensification and growing trees in the fallow land for timber (Lambin & Meyfroidt 2011). In their study, Hamad, Balzter and Kolo (2017) found that the agricultural land use can be heightened with the introduction of improved infrastructure and road connectivity to the farmers. The economic developments do not necessarily lead to the expansion of agricultural land area. This scenario is exemplified clearly in the case of Vietnam that the economic development forced to increase rice production by more than 25% between 2000 and 2011, but this was achieved through green revolution technique without having need to spatially expand the rice field (Kontgis, Schneider & Ozdogan 2015). But then the other aspect of economic development, which is in the form of rapid urbanization taking place almost in every country is a threat to the sustainability of cropland (Dong et al. 2015; Hazell & Wood 2008).

### **2.2.3 Demographic factors**

The mounting demand for food, fibre and fuel from the increasing population of the world leads to the expansion of agricultural and pastoral land at the cost of decreasing forest cover (Chaplin-Kramer et al. 2015; Lambin & Meyfroidt 2011). Research by Peng et al. (2004) has projected that with the increase in world population, rice production has to increase by 1% every year. This additional demand for rice can be either met from increasing the paddy field or intensifying rice agriculture. In fact, the non-static nature of population affects LULC. The out migration of population causes change in land use through labour shortage and inflow of remittances. The family members back home use this money for non-farm activities or diversify agriculture activities (Lambin & Meyfroidt 2011). Due to the increasing rural to urban migration of population, rapid urbanization has been taking place all over the world. This results in the growing conflict between the urbanization and the crop-land conservation (Liu et al. 2014). Although the urban land use covers only less than 0.5 percent of total land, it is predicted to lose annually 1.6-3.3 million hectare of fertile agricultural land to the growing

urban areas worldwide (Lambin & Meyfroidt 2011). The population drift to urban areas in most of the countries lead to agricultural land abandonment and the fallow land gradually turns into forest (Lambin et al. 2013).

#### **2.2.4 Institution factors**

Land is becoming a scarce resource and different land use will be competing for available land (Lambin & Meyfroidt 2011) , so proper laws, rules and guidelines should be implemented efficiently to utilize the limited land resource. In many countries, a balanced approach is adopted to intensify agriculture by introducing improved technologies, crop varieties and fertilizers. This enables the better use of the so-called wastelands (Lambin & Meyfroidt 2011) and apparently reduces pressure on forest cover while at the same time increases the food production. Some strict laws regarding conservation of environments helps to reduce the rate of deforestation in the conserved areas, but it increases the rate of forest disturbances outside the conservation area. A remarkable improvement in the preservation of forest was observed after most of the countries in Southeast Asia banned the practice of shifting cultivation (Lambin & Meyfroidt 2011). Most appropriate land use at local level improves the efficiency of land use at global level.

### **2.3 General causes of land use change in Bhutan**

A few studies on LULC change in Bhutan show varying results which is attributed to the varying spatial and temporal context of studies conducted. For instance, the forest cover in Bhutan has shown as decreased from 2000 to 2012 by Hansen et al. (2013) whereas in another study by Gilani et al. (2015), it was found to have increased by 3.6% in the period from 1990 to 2010. Similarly, Bruggeman, Meyfroidt and Lambin (2016) found a slight increase in the forest cover in Bhutan. However, there has not been any formal research carried out to map the change in rice cultivation area and understand the drivers of change in rice field in Bhutan.

#### **2.3.1 Natural factors**

Land cover in Bhutan is influenced by topography and climate (Johnson & Hutton 2014). Precipitation and temperature variability in Bhutan largely depends on the elevation, slope and aspect, which ultimately influences the type of land cover in a particular area (Dorji et al. 2016). Rice cultivation in Bhutan is dependent on monsoon rain and supplemented with irrigation channels. Any anomaly in the precipitation will cause either flood or drought which ultimately affects the rice cultivation (Ghimiray, Pandey & Velasco 2013). Bhutan is also known for rich biodiversity and conservation is given the priority. In the process of conserving wildlife, the human-wildlife conflict is a major issue which poses potential threat to conservation and economic development (Barua, Bhagwat & Jadhav 2013). In addition, many land covers in Bhutan are influenced by temperature and it is likely that

they will shift with climatic warming (Dorji et al. 2016)

### **2.3.2 Economic factors**

The construction of the first road from Phuentsholing (Indian border) to Thimphu (capital of Bhutan) and establishment of other infrastructure like telecommunication, transportation in 1961 marked the beginning of modern economy in Bhutan (Uddin, Taplin & Yu 2007). Since then Bhutan has made a rapid progress in the socio-economic development especially in the last two decades. The per capita GDP of Bhutan increased from USD 239 in 1980 to USD 2879 in 2016 (National Statistics Bureau 2017). Owing to the improved transportation facilities in the country, there is an increasing tendency to pursue cash crops like apples in the temperate regions; oranges, areca nut and cardamom in the subtropical in southern Bhutan. Other cash crops that are exported include ginger, chilies and vegetables (National Statistics Bureau 2017). However, Bhutan with a poverty rate of 8.2 percent is still one of the highest in the South East Asia.

### **2.3.3 Demographic factors**

The rural to urban migration rate of 6 percent in Bhutan is one the highest in South East Asia (Gosai & Sulewski 2014). This may be viewed as negative trend, but it contributes in reducing poverty and growth of economy. Internal migration occurs due to the uneven geographical distribution of labour and opportunities. There are two main reasons for rural to urban migration in Bhutan and they are: i) push factor is mainly due to lack of education facilities, lack of opportunities and small land holding and ii) pull factor of better employment opportunities in urban areas. The most developed districts are Thimphu, Chukha and Paro. Measures like rural electrification, transformation from subsistence economy to market economy were put in place to minimize the rural to urban migration but they failed to achieve this objective (Gosai & Sulewski 2014). Study by Gosai and Sulewski (2014) found that there was high rate of east to west migration of Bhutanese population. Farm mechanization in Bhutan is selectively feasible due to the landscape and terraced farming adopted to conserve soil degradation.

### **2.3.4 Institutional factors**

Bhutan is one of the developing countries which achieved a successful transition of land use simultaneously increasing food production and forest conservation this is mainly due to the good policies in place (Lambin & Meyfroidt 2011). Bhutan has a unique policy, i.e. i) to achieve self-reliance in cereals and essential oil; ii) increase rural income and iii) conserve the environment (National Statistics Bureau 2017). It is noble in intention but practically implementation is quite daunting when agriculture intensification and conservation of environment hardly go hand in hand (Lambin & Meyfroidt 2011). One of the major sources of revenue for Bhutan is the hydroelectricity which indirectly depends on the forest cover in the upstream to maintain the volume of water flow

from the catchment area (Bruggeman, Meyfroidt & Lambin 2016). Any disturbance in the hydrological cycle in the Himalayas has a direct impact on the economy (Saxena, Maikhuri & Rao 2005) of the people living downstream through the change in discharge (Costa, Botta & Cardille 2003). For this reason, the constitution of Bhutan mandates government to take extra initiative in maintaining its minimum forest coverage of 60% at all times (Royal Government of Bhutan 2008). A case study by Buffum, Gratzler and Tenzin (2009) suggests that due to better management of logging and grazing, the tree sapling densities in Yakpugang was found to be increasing. Slightly differing figures on the total forest cover by different researchers have been reported like 74.5% by Kubiszewski et al. (2013), 75% by Gilani et al. (2015), but these are well above the minimum requirement. This difference is due to the type of data used, methods and level of rigor.

Farmers have to bear the brunt of conservation in the form of losing their cattle and crops to the to wild animals (Sangay & Vernes 2008). A study carried out by Wang, Curtis and Lassoie (2006) found that the incidences of crop damage by wildlife increased drastically with the establishment of National parks and enactment of Forest and Nature Conservation act of Bhutan 1995 which specifically prohibits hunting and retaliatory killing of wild animals. Although the government with the help of external funding has commenced compensation to those owners whose livestock have been killed by tigers, leopards and bears (Sangay & Vernes 2008), it does not extend to the owners of damaged crops (Wang, Curtis & Lassoie 2006). This compensation scheme poses a serious question of sustainability because it depends on the external aids and the incidences of human-wildlife conflicts that are increasing every year. No formal studies have been carried out to find out how far the human-wildlife conflict contributes in land-use change in Bhutan, but obviously it does impact indirectly through the migration of population to urban areas in search of better opportunities.

Stringent conservation legislations and management practices are in place. This has achieved in maintaining 51 percent of total land cover as protected areas and biological corridors (Buffum, Gratzler & Tenzin 2009) but on the other hand, it has affected most Bhutanese population whose livelihood is directly dependent on agricultural and livestock farming which is the highest contributor of country's Gross Domestic Product (Johnson & Hutton 2014). Farmers deploy different means to ward off wild animals from damaging crops. One such measures is shown in Figure 2. 1 where a scarecrow of human shape is erected in the field of senescing rice in the study area.



**Figure 2. 1 Photograph of a scarecrow to prevent wild animals from entering the paddy field in the Paro valley**

(Photo credit: Kinley Jigyel Dorji, taken in October 2018)

## **2.4 Rice production system in Bhutan**

Due to the rugged terrain, rice in Bhutan is grown in terraced fields (Figure 2. 2) ranging from 160 m elevation in the south to as high as 2700 m (Ghimiray, Pandey & Velasco 2013). These authors classify the whole of Bhutan into three distinct rice agro-ecological zones based on the temperature and altitude which are described in the subsequent subsections.



**Figure 2. 2 Terraced rice farming in Bhutan.**

<https://grandcircle.scene7.com/is/image/GrandCircle/P9898/ScoopHero>

### **2.4.1 Wet subtropical (low altitude) zone**

The wet subtropical or low altitude zone for rice lies in the southern belt of Bhutan where its altitude ranges from 200 - 600 m above the mean sea level. Rice in this zone is cultivated using mainly rain fed water due to the lack of poor irrigation facilities. The warm temperature and other climatic conditions in this zone favour two cycles of rice plantation. However, due to relatively poor soil conditions (low nitrogen and potassium) and pests, the yield is reportedly less than other zones. This zone constitutes about 35% of total rice area in Bhutan.

### **2.4.2 Humid subtropical (mid altitude) zone**

The next higher altitude zone is the humid subtropical zone where its altitude ranges from 600-1500 m which is characterized by hilly slopes, lower rainfall, and temperature than the wet subtropical zone. The rice field in this zone is irrigated and yields are better due to the higher solar radiation and long ripening phase. It forms about 45% of total rice acreage.

### **2.4.3 Warm temperate (high altitude) zone**

The high-altitude zone ranges from elevation of 1500-2700 m with the current study area located in this zone. Rainfall in this zone is lowest among three zones (650-850mm annual) and rice fields are irrigated using canals and gravity feed. Only one cycle of rice is possible in a year and often the outbreak of rice blast disease is the main problem. It accounts to about 20% of total rice area.

## **2.5 Remote sensing data sources**

Due to the relatively recent advent of satellite remote sensing, change detection of LULC is possible for last 40-50 years only (Petit & Lambin 2001). Both at global and national levels of change detection in LULC, it is a common challenge that confuses many experts in the selection of appropriate satellite imagery, classification schema and methods (Gilani et al. 2015). One of the big issues here is the appropriateness of the datasets for the type of LULC change being detected. This is often the case of scale. For global scale LULC related mapping, different researchers have used satellite data from various sensors like Landsat data for Global Land Cover classification (De Fries et al. 1998); AVHRR for IGBP-DIS land dataset mapping; and MODIS for global land-use and land-use change (De Rosa et al. 2017). At regional level, probably due to its long history of data archival and being freely available, Landsat data are predominantly being used for LULC change mapping of different countries. For instance, the National Land Cover Database (NLCD-2006) for United States of America was developed using Landsat (Xian, Homer & Fry 2009). However, to spatially analyse the LULC change over long period of time requires a combination of more than one data source (Petit & Lambin 2001). Other countries and local level studies widely used Landsat images as the primary

source of data for LULC change studies (Oetter et al. 2001; Song et al. 2001; Vogelman et al. 2012). For example studies carried out by Singh, Singh and Tiwari (2013) in Arunachal Pradesh and Garrard et al. (2016) in Nepal testify that Landsat data can be used for LULC studies mountainous terrain like Bhutan.

## **2.6 Image processing techniques**

The LULC change analysis can be performed in diverse ways depending on the availability of data and purposes. There are numerous image classification algorithms developed since the 1980s for mapping of land use land cover. Most commonly used are pixel-based classification, sub-pixel-based classification and object-based classification (Li et al. 2014). The pixel-based classification treats each pixel to be spectrally pure and assumes it to represent a single land cover type (Xu et al. 2005). The pixel-based classification is further divided into unsupervised classification and supervised classification. In the unsupervised classification method, the computer automatically groups image pixels into different classes based on the digital number values of pixels without the need of human intervention (Puletti, Perria & Storchi 2014). The most commonly used algorithms of unsupervised classification are k-means (Blanzieri & Melgani 2008), Iterative Self-Organizing Data Analysis (ISODTA) (Dhodhi et al. 1999), Self-Organizing Map (SOM) and hierarchical clustering method (Goncalves et al. 2008). Although, unsupervised classification does not need signature sample and prior knowledge, it is computationally intense Vogelman et al. (2001) but less so in 2018.

In the supervised classification, analysts train the computer with sample sites from the known classes. Then every pixel in the image is compared with the training samples and classified into different classes depending on various decision rules. There are number of different classification algorithms like Maximum Likelihood Classifier (MLC), Minimum Distance-to-Means Classifier, Mahalanobis Distance Classifier and Parallelepiped. The supervised classification is most widely used method mainly due to simple in application, easy to understand and interpret (Radoux et al. 2014).

The third type of classification technique which considers geographical objects as the fundamental unit and classifies an image via image segmentation (Pal & Bhandari 1992). This approach is usually used in very high spatial resolution (VHR) images and it is proven to give better accuracy (Myint et al. 2011) than other types of classification. Due to the heterogeneity of nature, a single pixel from coarse resolution satellite images is likely to have a mixture of spectra from different land covers. The sub-pixel wise classification takes this fact into account and gives a better accuracy than pixel-based classification (Lu & Weng 2007). But this method has its own share of disadvantages which tends to be computationally intense, overfit data and rules are unknown (Gopal, Woodcock & Strahler 1999).

Civco et al. (2002) conducted a comparative study of different classification techniques and concluded that every method has their merit. Hence more than one approaches may have to be applied to achieve the desired results. However, Yangchen, Thinley and Wallentin (2015) did a LULC change study in Bhutan using Landsat image and MLC and their classification accuracy was fairly good. However, Gilani et al. (2015) used the object based image classification and reportedly achieved accuracy of 83% for a decadal study of LULC in Bhutan using Landsat image.

## **2.7 Change detection techniques**

Change detection is a process of quantifying temporal effects on an object by using multi-temporal satellite images (Singh 1989). Hall and Hay (2003) claimed that various change detection methods of varying robustness, complexity and refinement have been developed over last three decades. Different researchers have categorized the change detection methods into diverse groups based on their views. The most commonly used grouping categories as illustrated by El-Hattab (2016) are i) pixel-to-pixel approach, ii) post-classification change detection and iii) object-based change detection.

According to Hussain et al. (2013), the pixel-to-pixel change detection has several schemas like image differencing, image ratioing, regression analysis, vegetation indexing differencing, change vector analysis, principal component analysis (PCA), Tasseled cap transformation (TCT) and texture analysis. All the techniques have both advantages and limitations. For instance, the image differencing and ratioing are simple and easy to interpret but they do not provide a complete matrix of change information (Coppin & Bauer 1996). They are traditionally designed to work with quantitative raster than qualitative input data and produce an index or magnitude of change between dates, which can only then be recoded into binary change or no change results using specified thresholds. This method is criticised for the non-normal distribution of change which it is originally based (Singh 1989). A similar problem of a lack of a complete change matrix is associated with PCA and TCT.

Post-classification change detection technique analyses the outputs of independently classified images of different dates (El-Hattab 2016). This approach has two stages: digital image processing to generate a thematic map of land cover and the change detection analysis using the two thematic outputs. The post-classification change detection approach is widely used because when the images are independently classified, the atmospheric and sensor effects are reduced and a complete matrix of change information is generated (Hussain et al. 2013). However, the final accuracy is a function of accuracy of individual classification (Coppin et al. 2004).

Machine learning can be performed using three approaches: i) Artificial Neural Network (ANN), ii)

Support Vector Machine (SVM) and iii) Decision tree. They are non-parametric supervised algorithms used to estimate data properties based on training data (Hussain et al. 2013). The main drawback for ANN is its functions are not available in most image processing software like ERDAS Imagine. Whereas SVM is computationally expensive and difficulty in selecting the best kernel function. Decision tree model cannot be replicated to other date images (Hussain et al. 2013).

The most advanced method is the object-based image comparison. In this approach, the objects that are extracted from first image are searched from the second image (Hussain et al. 2013). It is relatively easy to implement but difficult to search spatially corresponding objects in the second date image. This approach of change detection does not provide 'from-to' change.

## **2.8 Integration of remote sensing data with other spatial data**

Since, the advent of satellite remote sensing technology in later half of the twentieth century, it has proven to be a robust tool for studying the LULC dynamics (Chowdhury 2006). The combination of remote sensing data with spatially referenced ancillary data such as bio-physical, economic, demography and social data is increasingly used to study the drivers of LULC change (Gilani et al. 2015; Weng 2002). The outcome of the LULC classification generated by image processing software like ERDAS Imagine; IDRISI (Baban & Wan Yusof 2001) and ENVI are used with other secondary spatial data in the GIS software for further analysis, update and retrieval (Rawat & Kumar 2015).

# CHAPTER THREE

## 3 METHODS

The project focussed on the usage of remote sensing (RS) and Geographical Information Science (GIS) tools to map the land use land cover (LULC) change and explore some of the major drivers of the change in rice land use in the Paro Valley of Bhutan. This chapter outlines the description of different processes performed to achieve the result.

### 3.1 Data collection

Hosts of remote sensing satellites are being launched in space, and users have been provided with a wide range of choice of imagery from optical to RADAR and LiDAR of different spatial, spectral, temporal, and radiometric resolutions depending on the applications. The requirement of historical imagery beginning from 1995 for the current study has narrowed the choice to only a few sensors. Landsat, Système Pour l'Observation de la Terre (SPOT) and Indian Remote Sensing Satellite (IRS) sensors were operational during the study period from 1995 to 2011. SPOT-1 was launched on 22 February 1986 and IRS-1A was launched on 17 March 1988. Initially, both the SPOT and the IRS series had 4 spectral bands and 20 m spatial resolution for SPOT-1 and 36 m for IRS-1. Procuring data from them for this study was not feasible due to the monetary cost charged for SPOT and quite lengthy procedure associated with IRS imagery download and moreover, the resolution of IRS-1A is not better than the Landsat Thematic Mapper imagery that is supplied freely. Hence, due to the historical, continuous and free of cost images, the Landsat series is only viable choice and they are widely used in change detection study (Abd El-Kawy et al. 2011; Banskota et al. 2014).

Originally, the study was aimed at mapping rice cultivation for 1995, 2005 and 2015 but due to the available field reference data dating back to 2011, the 2015 date image had to be changed to 2011..

Multiple datasets of both raster and vector formats were used in the study. The entire data were acquired from two sources. They are i) United States Geological Survey (USGS) database and ii) government agencies in Bhutan.

#### 3.1.1 Brief background on the Landsat series

The open and free access to the Landsat archive since 2008 by USGS has revolutionized the usage of Landsat data (White et al. 2014) especially in the change detection from the Landsat Time Series (LTS) data (Banskota et al. 2014; El-Kawy et al. 2011). The LTS mission from Landsat-1 to Landsat-5 acquired data of approximately 80 m spatial resolution in 4 spectral bands using Multispectral

Scanner System (MSS) from 1972 to late 1990 and briefly in 2012. The Landsat-3 sensor had a fifth band in Thermal Infrared (TIR) region. Apart from the MSS, the Landsat-4 and 5 sensors had a Thematic Mapper (TM) sensor which collected data in 7 spectral bands (Table 3. 1). The spatial resolution of the four bands in visible and Near Infrared (NIR) and two bands in Short Wave Infrared (SWIR) spectrum is 30 m and 120 m for one TIR band. The Landsat-7 was launched on 15 April 1999 with the Enhanced Thematic Mapper Plus (ETM+) sensor and has comparable properties with TM except with the improvement of spatial resolution of TIR to 60 m and an additional panchromatic band of 15 m spatial resolution was included. As a part of the Landsat Data Continuity Mission (LDCM), the Landsat-8 was launched on 11 February 2013 with Operational Land Imager (OLI) and Thermal Infrared Sensor (TIRS). Likewise, Landsat-9 is planned to launch by December 2020 with higher imaging capacity than the previous series which will add more valuable data to the Landsat image archive. The operational dates for the Landsat series are summarized in Figure 3. 1.

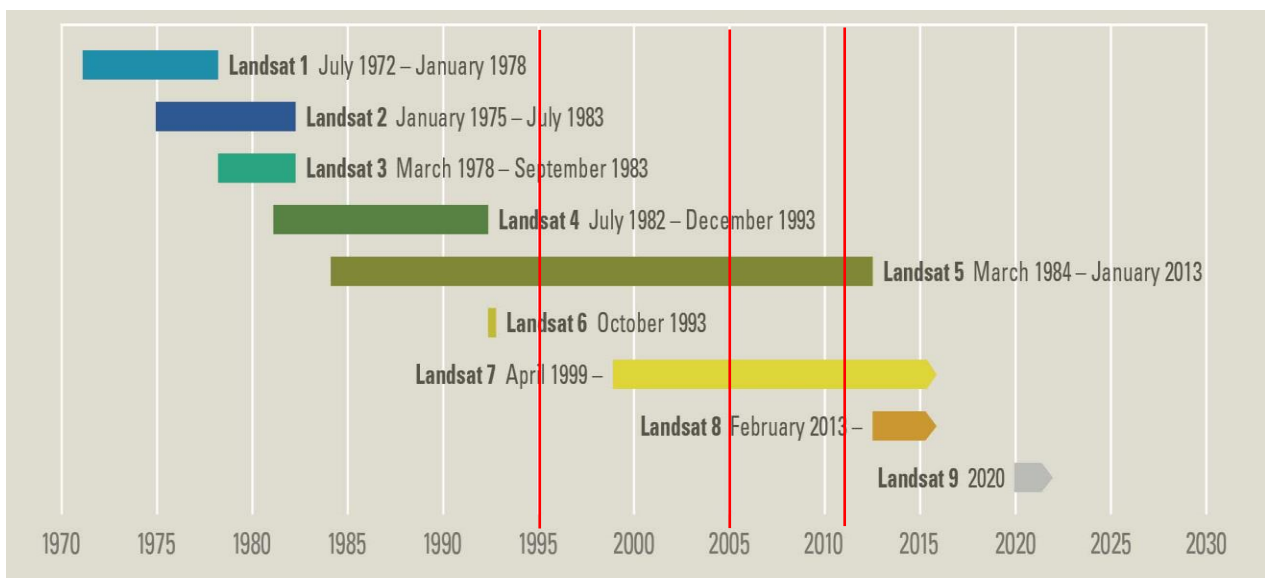


**Figure 3. 1 Landsat Time Series. The red lines indicate the year of images used for the current study**

Adopted and modified from: <https://landsat.usgs.gov/landsat-missions-timeline>

The OLI has higher quantization of 12 bits while the previous Landsat series of MSS have 6 bits and TM and ETM+ have 8 bits. The USGS through rigorous calibration has kept a consistency in sensor and image characteristic from Landsat-4 to 8. Hence the satellite images from TM, ETM+, and OLI are compatible with time series studies (Powell et al. 2010).

**Table 3. 1 Outline of Landsat-5 TM bands and their corresponding spatial resolution**

<b>Bands</b>	<b>Wavelength (<math>\mu\text{m}</math>)</b>	<b>Spatial resolution (m)</b>
Band 1 – Visible Blue	0.45-0.52	30
Band 2 – Visible Green	0.52-0.60	30
Band 3 – Visible Red	0.63-0.69	30
Band 4 - Near Infrared (NIR)	0.76-0.90	30
Band 5 – Near Infrared (SWIR1)	1.55-1.75	30
Band 6 - Thermal	10.40-12.50	120* (30)
Band 7 – Mid-Infrared (SWIR2)	2.08-2.35	30

Source: <https://eos.com/landsat-5-tm/>

As it can be seen from the crop calendar attached in Appendix A, the rice growing months in Paro valley are from June to September, so this window of timeframe was used to search cloud-free images of 1995, 2005 and 2011 in the USGS archive. After selecting the appropriate images for the study area, a special order for Level 2 processed imagery was placed through the USGS web portal Earth Explorer (<https://earthexplorer.usgs.gov/>). The specialized software developed by NASA called Landsat Ecosystem Disturbance Adaptive Processing System (LEDAPS) is used to derive surface reflectance data products. The software uses Second Simulation of a Satellite Signal in the Solar Spectrum (6S) radiative transfer model along with ancillary data to the level-1 processed Landsat TM images (USGS 2018b). 6S is a computer code which can accurately simulate the interaction of electromagnetic radiation with the atmosphere to estimate the digital number-to-radiance coefficients by exact atmospheric parameterization calculation (Yeom et al. 2017). The USGS is a scientific agency of US government whose primary role is to study the natural resources and hazards that pose threat to the USA. Table 3. 2 shows the different date images downloaded from the website.

\* 120 m spatial resolution of thermal band resampled to 30 m.

**Table 3. 2 List of Landsat scenes used for the study (Path 138, Row 41)**

Landsat-5 TM Scene ID	Sun	Sun	Date of acquisition	Time of acquisition (GMT)	Local Time (GMT+6)	Cloud Cover
	Azimuth	Elevation				
LT51380411995268BKT00	123.69°	45.93°	25-09-1995	03:31:15	09:31:15	34%
LT51380412005215BKT01	105.88°	62.99°	03-08-2005	04:17:45	10:17:45	64%
LT51380412011232KHC00	115.85°	61.23°	20-08-2011	04:18:36	10:18:36	24%

### 3.1.2 Data from Bhutan Government

The cadastral data with land use information was acquired from the National Land Commission Secretariat (NLCS) of Bhutan. A nationwide cadastral survey using high precision Differential Global Positioning System (DGPS) and total station instrument was carried out from 2008 to 2013. From the meta-data, the field cadastral data in Paro district (study area) was collected during the summer of 2011. Besides, plot boundary information, the cadastral survey had collected land use information. This cadastral field data was used as ground truth to assess the accuracy of image classification of 2011 image. Other ancillary data as shown in Table 3. 3 were also obtained from different government agencies in Bhutan.

**Table 3. 3 List of ancillary data from the government of Bhutan**

Data	Data Type	Year
PRISM-DSM	Raster	2014
Land cover	Raster	2010
Land use	Vector	2012
Temperature and Rainfall	Vector	1995 -2011
Demographic data	Numeric	1995-2011

### 3.2 Software used

Among several digital image processing and GIS software, Earth Resources Data Analysis System (ERDAS) Imagine 2018 and ArcGIS Version 10.6 were used to process and analyze different data used for this study. These software are widely used in the field of geospatial science and are available in the Flinders University, where this research was carried out.

### 3.3 Image pre-processing

In the mountainous terrain like the current study area where the agriculture fields are small and heterogeneous, the mapping of land use with 30 m spatial resolution of Landsat image is increasingly difficult and less accurate. In such cases, using the combination of derivatives of original data and ancillary data like Digital Elevation Model (DEM) has been shown to improve the accuracy of image classification (Feng et al. 2018). Particularly, the combination of first principal component (PC1), NDVI and DEM data has produced the highest image classification accuracy in the similar study conducted by Bahadur K.C. (2009) in Nepal and Eiumnoh and Shrestha (2000) in Thailand. Most of the agriculture fields are in the valley floor and extend up to approximately 300 m of relative elevation from the valley floor as it can be seen from Figure 3. 2. The author made use of this condition by integrating a relative DEM as the fourth band in the image composite which was used for further classification.

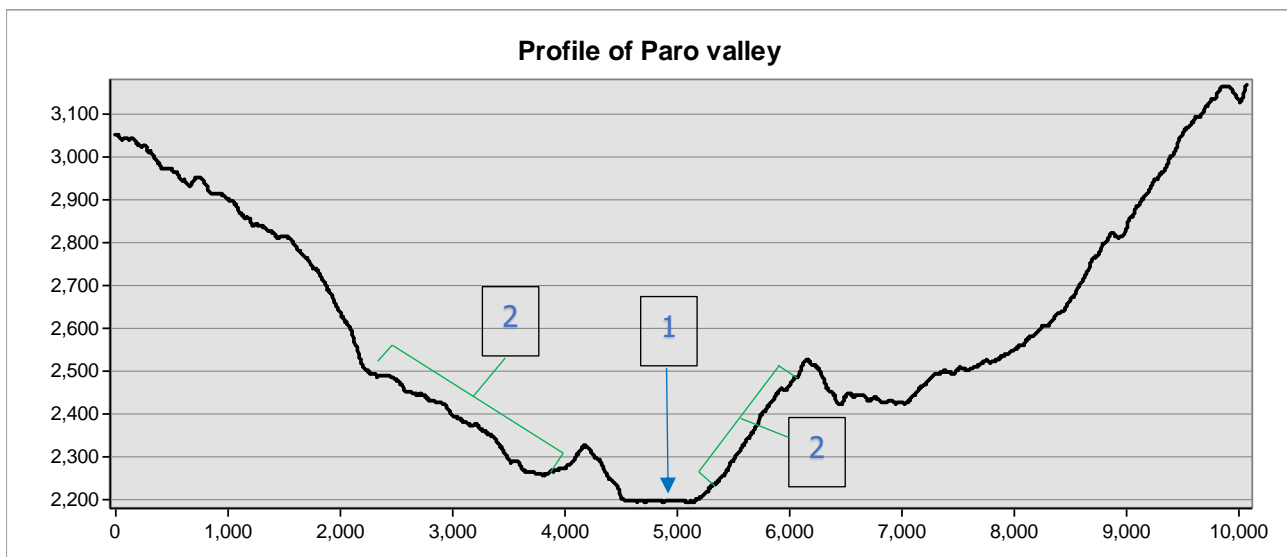


**Figure 3. 2 Cross section profile of Paro valley**

Where 1 is the river bed, 2's are locations of agriculture in the Paro valley

#### 3.3.1 Geometric correction

The combined effects of various geometric distortions which are caused by scan skew, non-linear scan, altitude and attitude of sensor, earth's rotation and curvature make the co-registration of two images (either from two different sensors or two different dates from the same sensor) extremely difficult (Netanyahu, Le Moigne & Masek 2004). It is essential to have an accurate per-pixel registration of multi-temporal satellite data since any registration error can potentially affect the accuracy of the change detection study (Dai & Khorram 1998; Shalaby & Tateishi 2007; Singh 1989). The Level 2 Precision Terrain corrected (L2PT) product of Landsat data were already geometrically and radiometrically corrected and georeferenced to the World Geodetic System 84 (WGS84).

However, to verify geometric registration of 2011 image, it was verified against readout coordinates from Google Earth of ten well defined features. Then the Landsat images of 1995, 2005 and ancillary data were compared against the 2011 image to confirm image-to-image geometric registration. Using the swipe tool in the ERDAS Imagine, 1995 and 2005 images were swiped over the 2011 image and observed for any shift in features like road, river, town etc.

### **3.3.2 Projection**

Satellite images that were downloaded from the USGS website were in Geographic Coordinate System (GCS) and World Geodetic System 1984 (WGS84) datum. Whereas the ancillary data delivered from the government of Bhutan were in Universal Transverse Mercator (UTM) projection and Drukref 2003 datum. Drukref 2003 is a National Grid for Bhutan which uses geocentric Coordinate Reference System as its base and the Transverse Mercator as its projection. The origin of latitude is at  $0^{\circ}$  and the central meridian is  $90^{\circ}$ E. The false easting is 250,000 m and false northing is 0 m with a scale factor of 0.9996 and unit of measurement is in meter. In order to have a common system of projection and datum, all the image and ancillary data were transformed and reprojected to UTM grid and WGS84 datum using software encoded transformation algorithms. The errors in this process were far smaller than the pixels size (30m) being dealt with in this research. . The study area falls under the UTM grid zone 45 N.

### **3.3.3 Clipping study area**

As the focus of this study was mainly on rice fields and its adjoining land cover and more over the rice fields are mostly located in the major river valleys; a buffer of 5 km around the major rivers in Paro district was defined to form the bounding limit for my study area. This study area was used to subset all the data used in this study.

### **3.3.4 Cloud masking**

The summer in the Himalayas are characterized by heavy cloud coverage which is one of the major problems with optical remote sensing. It was a big challenge to obtain cloud-free summer images in the study area. The spatial distribution of clouds and their thickness were different for different date images. The cloud quality assessment (QA) band is a single band image encoded with pixel values for different attributes. Table 3. 4 shows the pixel values for different attributes of cloud quality assessment band. Landsat Ecosystem Disturbance Adaptive Processing System's (LEDAPS) quality conditions are expressed either as true or false and are stored as binary digit. Different attributes of cloud QA band are assigned pixel values which can be used for setting threshold to remove certain attributes.

**Table 3. 4 Surface reflectance values of cloud quality assessment (sr\_cloud\_qa) band.**

<b>Attribute</b>	<b>Pixel Value</b>
Dark Dense Vegetation	1, 9
Cloud	2, 34
Cloud Shadow	4, 12, 20, 36, 52
Adjacent to cloud	8, 12, 24, 40, 56
Snow	16, 20, 24, 48, 52, 56
Water	32, 34, 36, 40, 48, 52, 56

Adopted from: <https://landsat.usgs.gov/landsat-surface-reflectance-quality-assessment>

The threshold values of greater than or equal to 2 except 9 were used in the model (Figure 3. 3). In fact, it masked out cloud; cloud shadow; adjacent to cloud; snow and water in the image – although there was no snow cover in the study area. In order to have same spatial extent of output image from the cloud masking model, the combined cloud quality assessment band was used for all the three-date images. Obviously, some part of the cloud-free image was lost in some images due to the inclusion of cloud areas of the other two images. Similarly, ancillary data like cadastral field data, PRISM DEM, and land cover maps were masked using the combined cloud file.

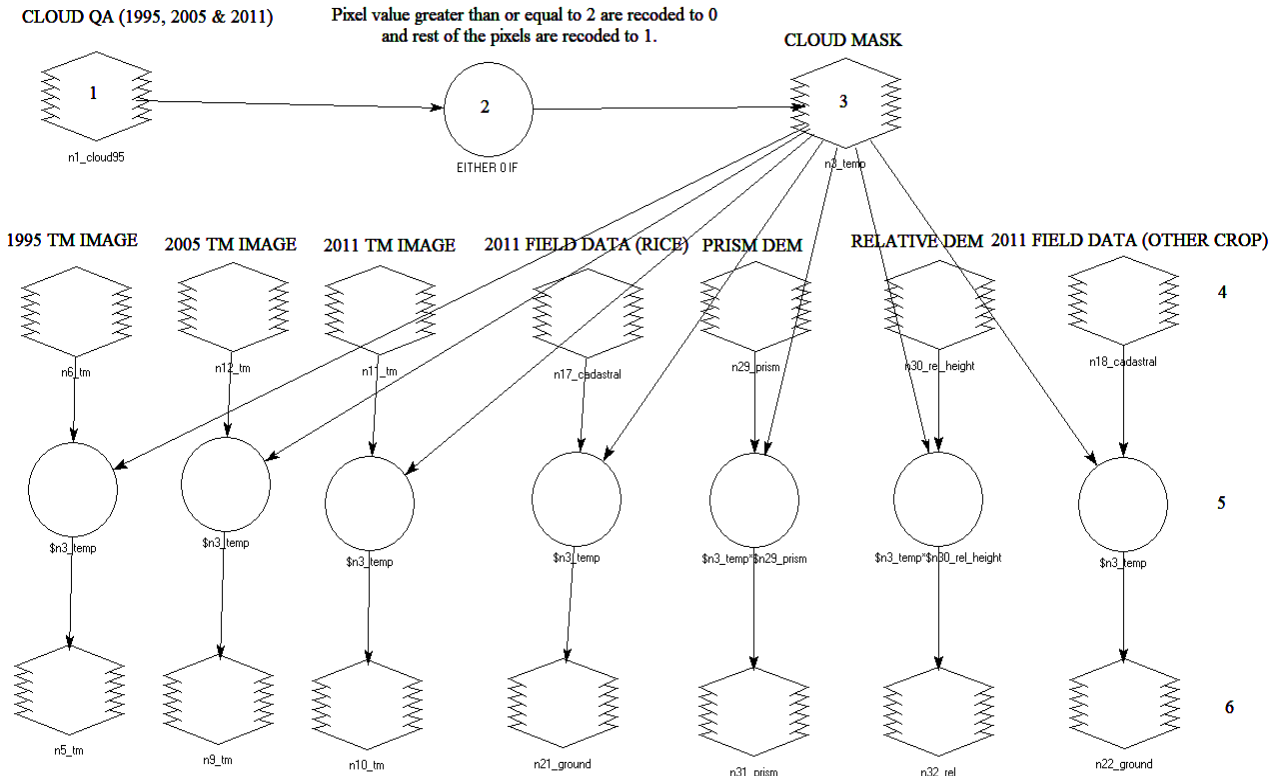


**Figure 3. 3 Cloud masking model**

In the Figure 3. 3, 1 is combined cloud QA band; 2 is a function to recode cloud QA pixels into 1 and 0 based on the threshold value of 2; 3 is recoded cloud mask rasters; 4 are input raster files to be masked; 5 is function that multiplies all individual input rasters with the mask raster (4X3). The encapsulated postscript for this spatial model is given in Appendix B.

### 3.3.5 Topographic normalization

In addition to the natural variability of reflectance responses from the same land cover class, the topographic effect that is introduced by the different slope and aspect in undulating terrain further contributes to the spectral variance even within a uniform land cover type. Such artifacts in the image can confound the image classification and analysis (Riaño et al. 2003). Hence, it is considered as possible pre-processing step in the multispectral and multi-temporal digital image analysis. The topographic normalization or topographic correction is a technique to compensate for the difference in solar illumination caused by irregular terrains. There are varieties of methods proposed in the literature, however, there has not been a standard and universally accepted method so far. The topographic normalization in ERDAS initially assumes that the surface is non-Lambertian. The model is based on the semi-empirical method used by Minnaert (1941) to measure the roughness of the moon's surface. It uses a set of constants called Minnaert coefficients which depend on the

wavelength of electromagnetic radiation and land cover type. It needs a co-registered digital elevation model (DEM), elevation and azimuth of the sun on the day of image acquisition. This approach according to Civco (1989) was useful in minimizing the spectral variance by almost 69 percent. However, the Minnaert coefficients for individual band can be determined by performing ordinary linear regression on the linearized Minnaert equation (Equation 1) which is beyond the scope of this study.

$$\ln(\rho_T) = \ln(\rho_H) + K_k \ln\left(\frac{IL}{\cos\theta_z}\right) \quad \text{Equation 1}$$

Where  $\rho_T$  is the reflectance of inclined surface,  $\rho_H$  is the reflectance of horizontal surface,  $K_k$  is the Minnaert constant for band  $k$ ,  $\theta_z$  is the solar zenith angle and  $IL$  is the illumination condition given by:

$$IL = \cos\gamma_i = \cos\theta_p \cos\theta_z + \sin\theta_p \sin\theta_z \cos(\phi_a - \phi_o) \quad \text{Equation 2}$$

Where  $\gamma_i$  is the incident angle,  $\theta_p$  is the slope angle,  $\phi_a$  is the solar azimuth angle and  $\phi_o$  is the aspect angle.

However, a considerable number of attempts were made to find from literature the Minnaert constants for Landsat-5 TM that were calculated for similar conditions of terrain and vegetation. Minnaert constants shown in Table 3. 5 which were obtained by Colby (1991) for Rocky Mountain National Park in Colorado were used in this study. The Panchromatic Remote-sensing Instrument for Stereo Mapping (PRISM) Digital Elevation Model (DEM) of 8.9 m horizontal resolution was used for determining slope and aspect angles. The solar angle and sun azimuth were obtained from the meta-data of the image.

**Table 3. 5 Minnaert constant**

<b>Landsat-5 TM bands</b>	<b>Minnaert constant</b>
Band 1	0.09
Band 2	0.19
Band 3	0.31
Band 4	0.43
Band 5	0.96
Band 7	0.14

### 3.3.6 Generation of the river network

Standard tools in the ArcGIS: fill, flow direction, flow accumulation and stream order were used to

delineate major stream network from the PRISM DEM.

### 3.3.7 Extraction of relative digital elevation model (DEM)

All pixels of the raster streams that were generated in section 3.3.6 were converted into points and assigned elevation values from the PRISM DEM. Simultaneously, masking of DEM by the study area and conversion of DEM raster to points were done. The Near tool identified the nearest river point from each DEM points. A new field which can store the relative heights above the nearest point on the river was added to the DEM point file. The DEM points data and river point data were combined into one table through join tool. The difference of heights between the DEM points and the nearest stream point were stored into the new field as relative heights of those points from the major rivers. Finally, all the points of DEM were converted back to raster based on the relative height data. This modified DEM was named as relative DEM. The entire process was executed in a model built using the toolbox in the ArcMap (Figure 3. 4).

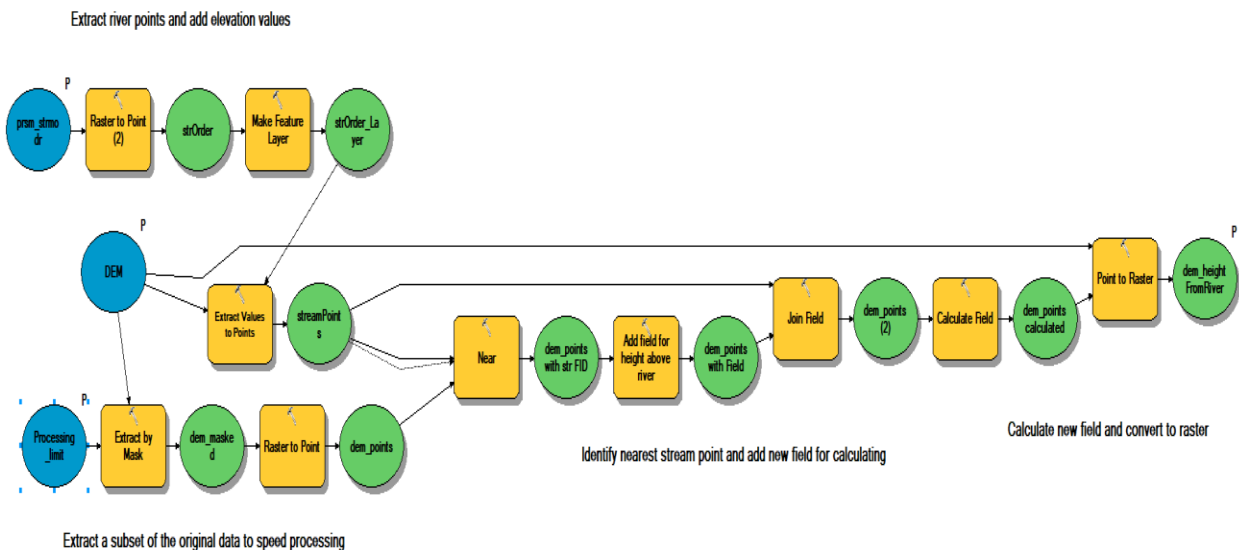


**Figure 3. 4 Model in the ArcTool box to extract relative DEM. The Python script for this model is given in the Appendix B.**

### 3.3.8 Principal Component Analysis (PCA)

The inbuilt PCA tool in ERDAS Imagine was utilised to derive principal components. PC1 and PC2 were extracted from the Landsat-5 TM image of 2011 which was further used for image classification.

Principal Component Analysis (PCA) is a mathematical transformation that is used to reduce the dimensionality of interrelated variables of a dataset into a smaller number of uncorrelated and independent variables called principal components (Jolliffe 2011). The first principal component

(PC1) accounts for the maximum variability in the data and each succeeding principal component contains as much of the remaining variability as possible. In remote sensing context, individual image bands are the variables. The PCA transformation effectively looks for any redundant information in the different bands and transforms into a set of uncorrelated principal axes based on equation 3. Another application of PCA is by considering the bands with least variance enables to detect subtle details which normally consists of regular noise in the image.

$$P_e = \sum_{k=i}^n d_k E_{ke} \quad \text{Equation 3}$$

Where  $P_e$  is the output PC value of PC axis e,  $d_k$  is an input digital number of band k,  $E_{ke}$  is the eigen vector matrix with k rows and e columns.

Mathematically, it starts by forcing all the principal components to have zero variance/co-variance in the eigenmatrix with non-zero eigenvalues such that  $v_1 > v_2 > v_3 > \dots > v_n$  of PCA to get the best transformation function.

$$V = E_{ke} \cdot Cov E_{ke}^T = 0 \quad \text{Equation 4}$$

Where  $Cov E_{ke}^T$  is the covariance of transposed eigen matrix  $E_{ke}$  and  $V$  is the diagonal matrix of eigen values represented by:

$$V = \begin{bmatrix} v_1 & 0 & 0 & \dots & 0 \\ 0 & v_2 & 0 & \dots & 0 \\ 0 & 0 & v_3 & \dots & 0 \\ \vdots & \vdots & \vdots & \ddots & \vdots \\ 0 & 0 & 0 & \dots & v_n \end{bmatrix} \quad \text{Equation 5}$$

### 3.3.9 Normalized Difference Vegetation Index (NDVI)

The unique characteristics of leaves to absorb red light by chlorophyll and reflect near-infrared (NIR) radiation by mesophyll cells have helped scientists to formulate several vegetation indices to study the abundance and vigor of vegetation. One such index is the Normalized Difference Vegetation Index (NDVI). It is a non-linear ratio of the difference between near-infrared and visible red to the sum of visible red and near-infrared as represented by equation 6. According to Jensen (2009), it is known to reduce many effects of multiplicative noises, for instance like varying solar illumination effects, shadow effects, and topographic variation and atmospheric attenuation. It enables to differentiate subtle differences in classes which cannot be seen in original image. NDVI values range from -1 to +1. Pixels with higher values of NDVI appear brighter which is an indication of higher biomass and healthier vegetation.

$$NDVI = \frac{\rho_{NIR} - \rho_{Red}}{\rho_{NIR} + \rho_{Red}} \quad \text{Equation 6}$$

Where,  $\rho_{NIR}$  corresponds to band 4 and  $\rho_{Red}$  corresponds to band 3 in Landsat-5 TM image.

There is an inbuilt function in the ERDAS Imagine software to calculate NDVI, but a model was developed to multiply the NDVI by a factor of 1000 to make its data range from -1000 to +1000, so that it fits with the data range of other layers like PC-1 and DEM.

### 3.3.10 Layer Stack

The layer stack tool in the ERDAS Imagine was used to combine different layers of data to generate the following composite datasets:

- i. PC1-NDVI-DEM
- ii. PC1-PC2-NDVI-DEM
- iii. PC1-PC2-NDVI-Relative DEM
- iv. PC1-PC2-NDVI-DEM-Relative DEM

While doing this, proper care was observed to choose the right number of bits and data type for the output data so that it accommodated different data types and range of input layers. For instance, PC1, in this case, was unsigned integer, PC2 was signed integer, NDVI was in signed integer, DEM was in unsigned and relative DEM was in an unsigned integer.

## 3.4 Digital image processing

Since there was no ground truth data for 1995 and 2005, a detailed exploration of different datasets and methods was carried out for the 2011 Landsat data. Supervised and unsupervised classification for four different datasets prepared in section 3.3.10 and the original Landsat-5 TM image were performed. Accuracies for each dataset of both supervised and unsupervised classification were assessed using the cadastral field survey data of 2011. Classification accuracies from both supervised and unsupervised classifications of five datasets were compared. The maximum likelihood classifier (MLC) of supervised classification on the original 2011 TM image resulted the highest accuracy. The MLC classification algorithm was used to map the LULC from the original 1995 and 2005 TM images assuming they give similar classification accuracy. From the thematic LULC map of 1995, 2005 and 2011, changes in rice land use were mapped and analysed statistically. From the change detection data and other socio-economic and meteorological data, further analyses were done to find out some major drivers that have brought change in the area of rice cultivation. The flow chart in the Figure 3. 5 shows the major processes undertaken in this study.

The main purpose of image classification is to derive different classes of land cover or themes by

automatically grouping all pixels of an image based certain spatial, spectral, and temporal patterns. The study used both the forms of pixel-based image classification which are described in the following sections.

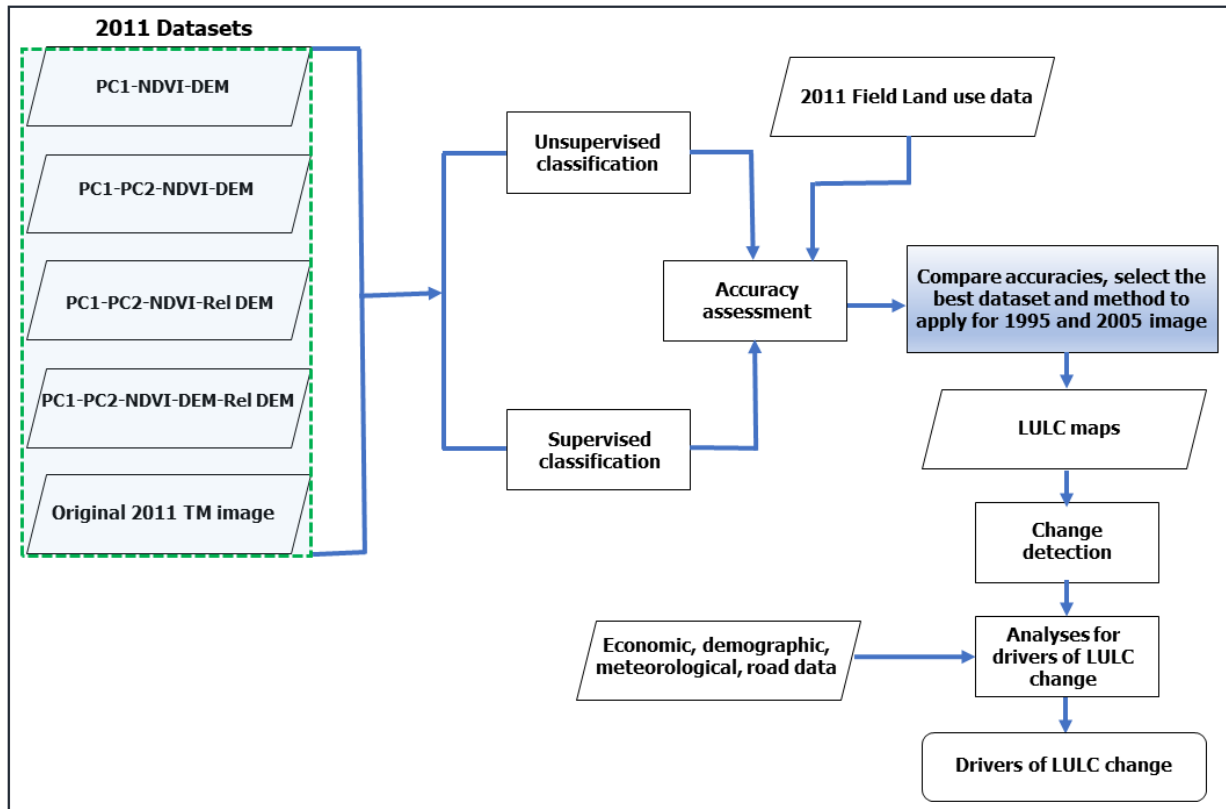


**Figure 3. 5 Flow diagram of main processes**

### 3.4.1 Unsupervised classification

Unsupervised classification is one form of pixel-based image classification which effectively partitions multispectral feature space into natural clusters of pixels purely based on their spectral characteristics (Lillesand, Kiefer & Chipman 2004). This approach aggregates the pixels into spectrally distinct classes and the user has to identify the clusters for real world information with the help of priori knowledge or some other forms of references (large scale map or imagery). It needs minimal initial input from the analysts like number of classes, maximum iterations and convergence threshold. Among several algorithms for unsupervised classification, one of the most popular forms of clustering algorithm is the Iterative Self-Organizing Data Analysis Technique (ISODATA) that was used for the classification of the image in this study. Based on the user's specification of number of classes, the algorithm arbitrarily allocates seed clusters in the data space. Then each pixel is assigned to the nearest cluster. In the process, clusters are either merged, split or deleted depending on the statistics of clusters. If the clusters are closer than the specified minimum distance, they are merged

into single class. On the other hand, if the standard deviation of a cluster is larger than the user specified value, then that cluster is split into two. Clusters with the number of pixels fewer than the predefined minimum number are deleted. In the subsequent iterations, the mean vectors are recomputed and based on the new mean vectors, pixels are reclassified. This process iterates till there is no significant change in the cluster statistics or reaches maximum number of iterations. In this study, the author specified the maximum clusters of 200, maximum iteration of 30 and 0.95 convergence threshold. Other options of clustering like minimum size was set to 0.01%, maximum standard deviation to 5 and minimum distance as 4. Finally, with the help of high resolution Google Earth image of 2012, 200 classes were assigned to one of the four LULC classes; viz. 1. Forest, 2) Rice field, 3) Other crops and 4) Built up. The same approach was used to classify five different datasets of derived from Landsat-5 TM 2011 image.

### **3.4.2 Supervised classification**

Supervised classification is another type of pixel-based image classification where it makes use of known classes of pixels to classify unknown pixels in the image and those pixels of known identity are called as training samples (Campbell & Wynne 2011). The supervised classification begins with the training stage where the analyst gathers a set of statistics of spectral responses called signatures from the samples of known and homogeneous areas in the image to train the classification algorithm. To get a better classification result, the training sample must be complete and representative.

In ERDAS Imagine, training polygons were delineated using a seed pixel. The inquire cursor was used to choose a single pixel within the prospective training area. Then with the help of Region Growing Properties, spectral Euclidian distance was adjusted such that adequate number of spectrally similar pixels and contiguous to the seed pixel were selected by a polygon. Spectral signature from these selected pixels was added in the signature editor as a training sample for that known class. For a parametric classifier to be used, a least number of pixels in a training sample must be theoretically,  $n + 1$  where  $n$  is the number of spectral bands in the image for accurate computation of variance and covariance (Lillesand, Kiefer & Chipman 2004). In the case of level 2 processed Landsat-5 TM image, there are 6 spectral bands and the minimum training sample must have at least 7 pixels. Practically, it can range from  $10n$  to  $100n$  pixels. This process was repeated for all other classes of land use and ensured that the samples represented the entire pixels to be classified. The next step is the training set refinement. By viewing the image alarm of selected signatures gives a preview of how well the training samples can classify the other pixels by parallelepiped classifier. Accordingly, additional training samples can be collected, or redundant samples can be removed. Another crucial step in refining the signature is to evaluate the separability of spectral signatures of candidate training classes. There are four different measures of distance in ERDAS to check the spectral similarity between the training classes. They are i) Spectral Euclidian

Distance (SED), ii) Divergence distance, iii) Transformed Divergence distance and iv) Jefferies-Matusita (JM) distance. In this study, the measure of JM distance was used to test the separability of different signatures. Mathematically, the JM distance is calculated as in Equation 7.

$$JM = \sqrt{2(1 - e^\alpha)} \quad \text{Equation 7}$$

However, the ERDAS Imagine software uses

$$JM = 1000x\sqrt{2(1 - e^\alpha)} \quad \text{Equation 8}$$

Where

$$\alpha = \frac{1}{8}(\mu_i - \mu_j)^T \left(\frac{C_i + C_j}{2}\right)^{-1} (\mu_i - \mu_j) + \frac{1}{2} \ln \left( \frac{|C_i + C_j|/2}{\sqrt{|C_i| |C_j|}} \right) \quad \text{Equation 9}$$

Where  $\mu_i$  and  $\mu_j$  are the mean vectors of samples  $i$  and  $j$  respectively.  $C_i$  and  $C_j$  are covariances of sample  $i$  and  $j$  respectively.

The JM distance in ERDAS Imagine varies between 0 to 1414; where 0 indicates the two classes are exactly same and 1414 means two classes are completely separate (ERDAS Field Guide 2003). The signature evaluation ensured that necessary deletion, merging or addition of signatures were done before carrying out classification. The Maximum Likelihood Classifier (MLC) which is based on the parametric decision rule calculates the variance and covariance of the pixels in the training classes and assumes that every pixel has equal probability of being in a certain class. This assumption mandates the distribution of training samples to be Gaussian (Jensen 2014). Using a probability density function, probabilities of an unknown pixel being in different training classes are calculated and the pixel is assigned to the class with highest probability value or it can be classified as unknown when the probability is less than the threshold value specified by the analyst. In ERDAS Imagine, while using the MLC, there is an option to save the distance file which is a single band continuous raster file representing the Chi-squared distance between the mean of the training class and the candidate pixel (ERDAS Field Guide 2003). The brighter pixels are spectrally farther from the training class and they are possibly misclassified, and darker pixels mean more accurately classified.

Using the Chi-squared distance file, the threshold in the distance histogram can be set either manually dragging or entering the statistical parameters, so that it automatically sets in the histogram (Figure 3. 6). This process basically screens out the incorrectly classified pixels and assigns the class to unclassified.

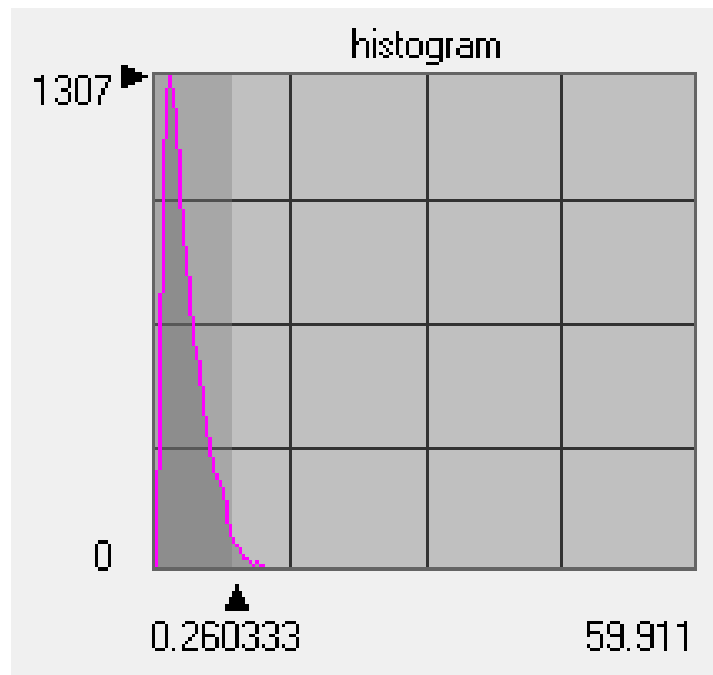


**Figure 3. 6 Histogram of distance file in MLC for rice class; threshold set at 39.972**

### **3.4.3 Post-classification smoothing processes**

#### **Recode**

The post-classification processes of unsupervised classification become more labour intensive. All 200 spectral classes discriminated by the ISODATA were assigned meaningful land use classes by using the author's priori knowledge of the study area and the high-resolution Google Earth image of 2012. Due to the significantly large number of classes, even the slightest spectral variations in the objects was accounted by assigning separate class. With the help of the recode function in the ERDAS Imagine, all the 200 classes from the unsupervised classification were finally recoded to four land cover classes.

#### **Neighbourhood function**

Due to the spectral variability, it is natural and inevitable that any pixel-based spectral classifier is likely to produce an output with mixed classes. This is termed as salt-and-pepper effect (Lillesand, Kiefer & Chipman 2004). The classification result does not make much sense if this effect is not removed. One of the means to smoothen the thematic output of classification is majority filter. The majority filter operates based on the logical operation if the centre pixel in the moving window is not the majority class, the centre pixel is changed to the neighbouring majority class and it is major, the identity remains unchanged. In this study, a 3x3 majority filter was consistently applied in all the output image of classification.

#### **Clump and Sieve**

Other forms of smoothing functions like clump, sieve and eliminate tools were used. Clump function identifies the contiguous clumps of pixels and groups into single thematic class. The clump tool was applied to the output from the majority filter operation. The sieve removes the clumps that are smaller than the minimum size and they are recoded as unclassified. After sieve operation, another round of recode was carried out. Eliminate function works similar to sieve except it fills up the eliminated pixel by taking mean of neighbour pixels.

#### **3.4.4 Accuracy assessment**

The outcome of any classification method can produce visually attractive land cover maps but that is not complete unless there are some mechanisms to quantify the accuracy of the image classification (Lillesand, Kiefer & Chipman 2004). According to Campbell and Wynne (2011), accuracy is defined as the measure of agreement between the reference data which is accepted/assumed as correct and the classified image. Obviously, it is important to have as accurate reference data as possible to minimize the error in the measure of accuracy. The other important aspect of accuracy assessment is that both the reference data and image must ideally be of same date. However, it is not always possible to get both the data on the same date, so they must be as close as possible in terms of date of acquisition. The non-site-specific accuracy assessment and the site-specific accuracy assessment are two forms of classification accuracy assessment. In the non-site-specific assessment, it does not account for the agreement between the specific sites within the two maps, but it only considers the overall agreement. In other words, it ignores the compensating errors occurring in various locations within the overall maps (Congalton & Green 2008). The second type of assessment is the detailed comparison between the specific locations in both reference data and the classified map. This is known as the site-specific accuracy assessment and it is a more reliable form of accuracy assessment.

In this study, site-specific accuracy assessment was performed by comparing each pixel of rice in the entire map. For that, a co-registered reference data, which in this case was a rasterized field cadastral survey data of 2011 of same cell size (30 m) was used.. A spatial model was developed in ERDAS Imagine (Figure 3. 7) to subtract classified rice raster file from the field raster file of rice.

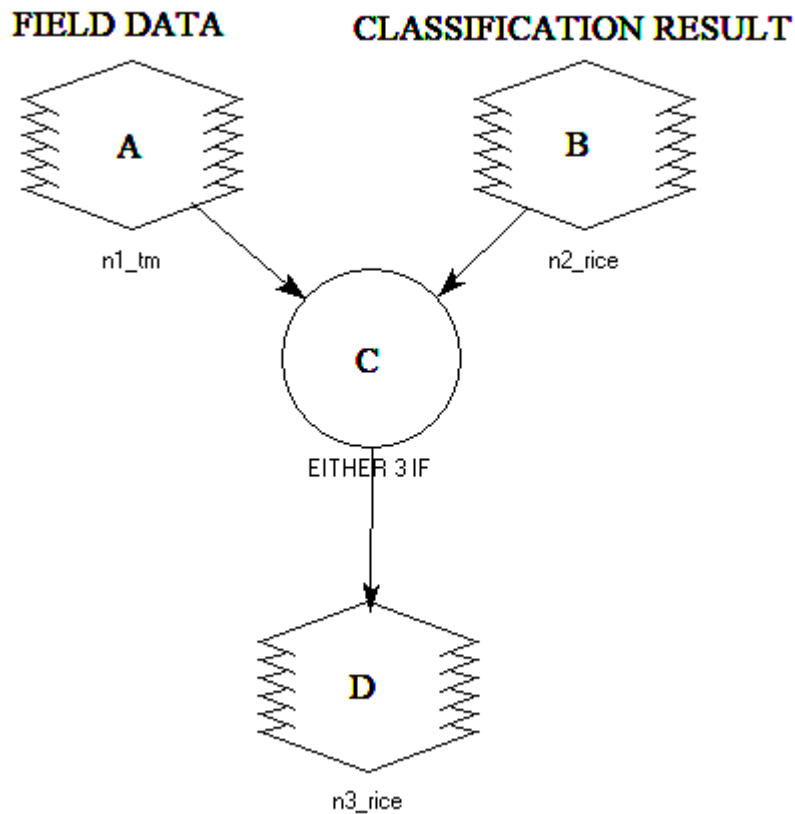


**Figure 3. 7 Spatial model to subtract two thematic images used for accuracy assessment**

The logic that was used in the function C says that if both pixel values in A and B are 0, then the output pixel value in D is assigned 3 which was later recoded as no data; if A-B is -1, then the output pixel in D is assigned the value 2 which is the error of commission; if A-B is 0, then these pixels are accurately classified and if A-B is +1, it is an error of omission.

The model yielded a thematic map showing the spatial distribution of commission error, omission error and accurately classified pixels of rice. The statistical parameters like number of pixels, percentage and area were generated by running the Summary function in the ERDAS Imagine.

### **3.4.5 Land use land cover mapping**

The best method and dataset that produced highest accuracy in 2011 image was applied to the images of other two dates of 1995 and 2005. The high-resolution Google Earth image and the author's knowledge of the area were used to train the signatures. In some occasions, the same AOI that was used in 2011 image was used to extract the sample signature. Due to the absence of field data, accuracy check could not be done for 1995 and 2005 image classification.

### **3.5 Change detection**

Among the several change detection algorithms available, due to its intuitiveness and simplicity, the post-classification change comparison method (also called delta classification) is a most widely used quantitative change detection method (Colditz et al. 2012; Jensen 2005). Remotely sensed images of different date are rectified and classified separately. Then the two thematic maps are compared pixel-by-pixel to extract the change map. This method gives the information on the 'from-to' change in land classes. However, its accuracy is solely dependent on the accuracies of individual classification (Coppin et al. 2004; FAO 2016).

The same spatial model developed for the accuracy assessment (Figure 3. 7) was used to obtain the difference of two thematic images. The output image consists of the spatial information on increase, decrease and no change in rice. For more statistical information on the changes, author used Matrix Union and Summary function under the Raster GIS in ERDAS Imagine. Changes in rice field from 1995 to 2005, 2005 to 2011 and 1995 to 2011 were determined using the above approaches.

### **3.6 Geospatial analyses for drivers of rice-land**

One of the aims of the study was to discover some major drivers for change in rice cultivation in the study area. The causes were investigated by analysing socio-economic, meteorological and demographic data and reviewing relevant government policies. Observations of rainfall and temperature at a lone meteorological station which is in the study area were analysed by using Microsoft Excel for any anomalies that might have contributed to the change in land use. In the similar manner, population data and socio-economic data were analysed to establish any correlation with the change in rice field in the Paro valley. Some relevant government policies were also analysed to find if they have had any impact on the change in the rice field.

# CHAPTER FOUR

## 4 RESULTS

This chapter presents the results obtained from different steps of image processing performed in the preceding chapter. It is structured into six main sections: 1. Image pre-processing; 2. Digital image processing; 3. Accuracy assessment; 4. Change detection; 5. Accuracy of post-classification change detection; and 6. Drivers of change in rice cultivation.

### 4.1 Image pre-processing

#### 4.1.1 Geometric verification

The radiometric and geometric corrections for the precision and terrain corrected (L1TP) data were carried out by the USGS and their level of accuracy depends on the number of Ground Control Point (GCP) available and quality of image. The root mean squared error (RMSE) of geometric correction reported by the USGS was compiled from the image metadata file (Table 4. 1).

**Table 4. 1 The Root Mean Square Error (RMSE in pixels) of geo-rectification of three date images done by USGS**

TM Image	RMSE (pixels)				Overall
	QUAD_UL	QUAD_UR	QUAD_LL	QUAD_LR	
1995	0.301	0.247	0.234	0.230	0.301
2005	0.384	0.381	0.354	0.692	0.388
2011	0.407	0.362	0.495	0.340	0.393

QUAD\_UL: Upper left corner of the image scene; QUAD\_UR: Upper right corner of the image scene; QUAD\_LL: Lower left corner of the image scene; QUAD\_LR: Lower right corner of the image scene.

Further verification was applied using the Google Earth coordinates for 10 well defined features in the study area. The overall error in the distance was observed to be  $\pm 5.32$  m which is about one-sixth of a Landsat-5 TM pixel. The result for this verification is shown in the Table 4. 2.

**Table 4. 2 Results of geo-registration of Landsat-5 TM 2011 image with Google Earth 2012**

Ground Point	Google Earth		Landsat 5 (2011)		Error (m)
	Easting (m)	Northing (m)	Easting (m)	Northing (m)	
GP1	752087.65	3023841.57	752092.76	3023844.28	5.78
GP2	762906.63	3038478.94	762910.49	3038473.11	6.99
GP3	760804.23	3045391.03	760803.73	3045395.44	4.44
GP4	739163.88	3034414.55	739166.98	3034420.92	7.08
GP5	739241.47	3036361.89	739238.92	3036367.69	6.34
GP6	734667.15	3051932.86	734668.21	3051934.07	1.61
GP7	734991.65	3081715.9	734990.66	3081721.57	5.76
GP8	745485.51	3025588.91	745490.85	3025591.17	5.80
GP9	737752.7	3015398.51	737749.95	3015401.36	3.96
GP10	771020.65	3040445.08	771017.63	3040449.6	5.44
RMSE					±5.32

Visual checking by swiping 1995, 2005 images, PRISM DEM and field cadastral data over 2011 image also found that they were all well co-registered.

#### 4.1.2 Cloud masking

Cloud quality assessment (QA) band contains the information of different attributes of cloud. Figure 4. 1 show different patterns and location of clouds and their shadows in three-date Landsat-5 TM images. The varying tone of grey colour indicates different attributes of the cloud quality assessment band. The model masked cloud shadows, adjacent to cloud which appears too dark to identify any object beneath it, snow and water vapour.

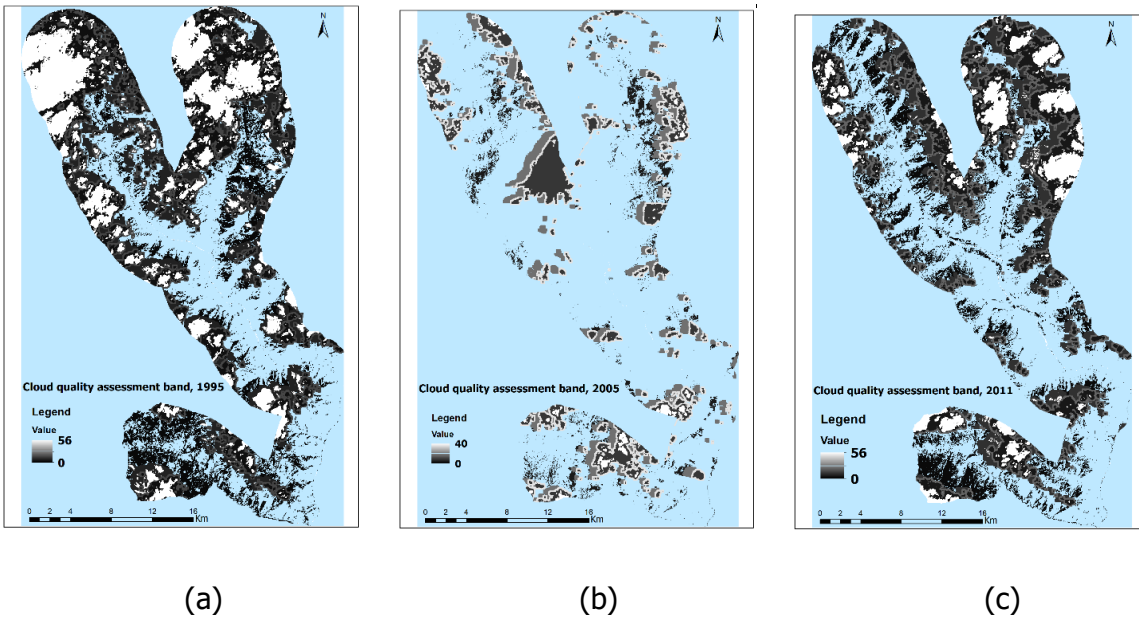


**Figure 4. 1 Cloud quality bands (subsets) for (a) 1995, (b) 2005 and (c) 2011 Landsat TM images**

For the change detection study, multi-temporal images need to have same spatial extents. To obtain same cloud free spatial area of interest, the combined cloud quality assessment band masked the images of 1995, 2005 and 2011. Same spatial extents for other data like DEM and field data were also achieved using the same cloud QA band. As it can be seen from Figure 4.2 (c), about 33% of the study area was masked out and these areas were mostly under forest cover. But this has not affected much for the rice field. It was found that about 7% of rice field was removed from the study area due to cloud masking.

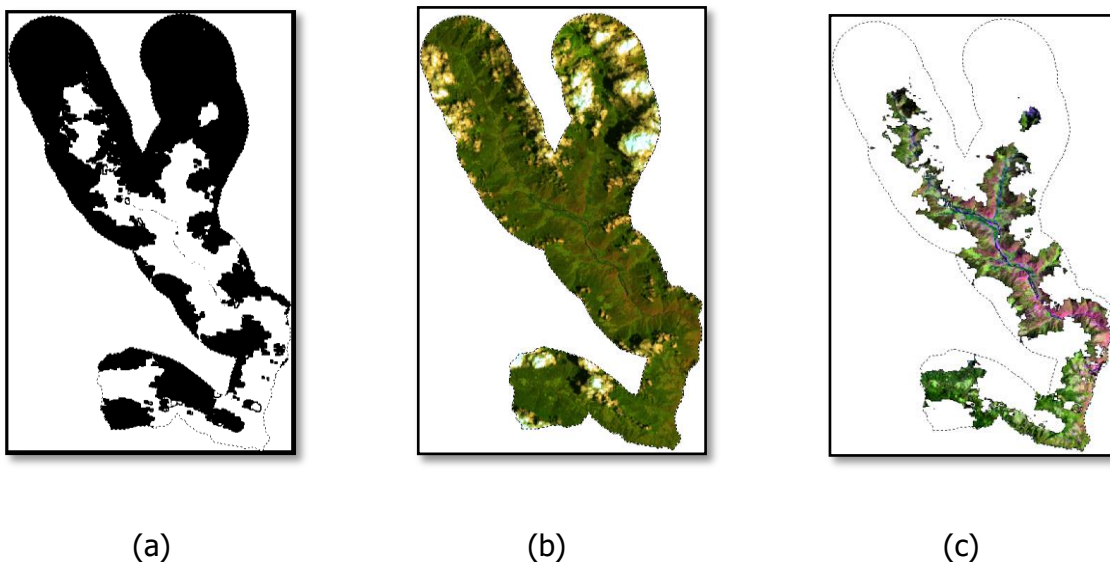


**Figure 4. 2 Image of (a) combined cloud QA band, (b) 2011 TM image with cloud cover (BGR=543) and (c) output of cloud masking (BGR=543)**

### 4.1.3 Topographic normalization

Topographic normalization minimized uneven sun illumination but there were parallel lines generated in the topographically normalised output image. Both visually and statistically, the brightness values of south facing slopes were reduced in topographically-normalised images, while north facing slopes became brighter (Figure 4.3).

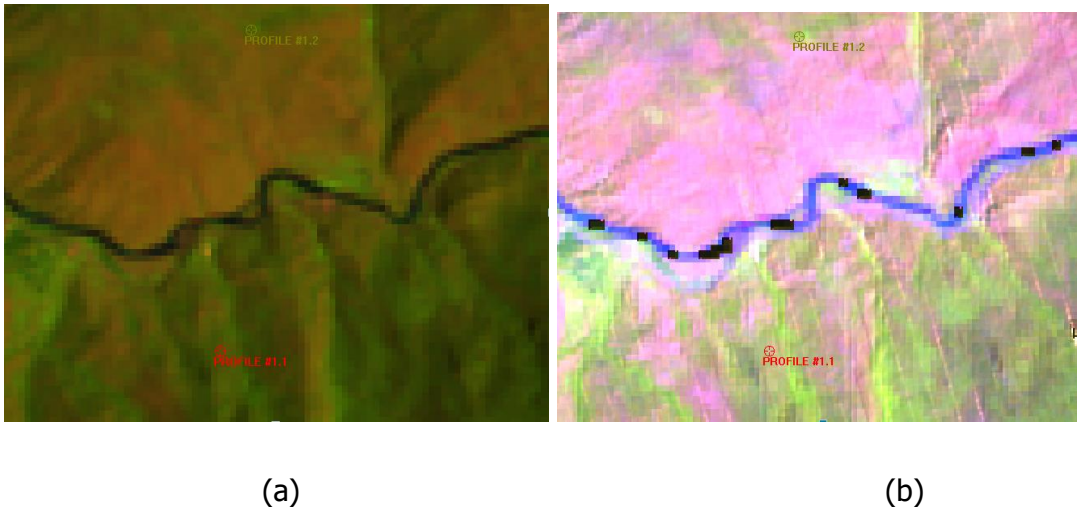
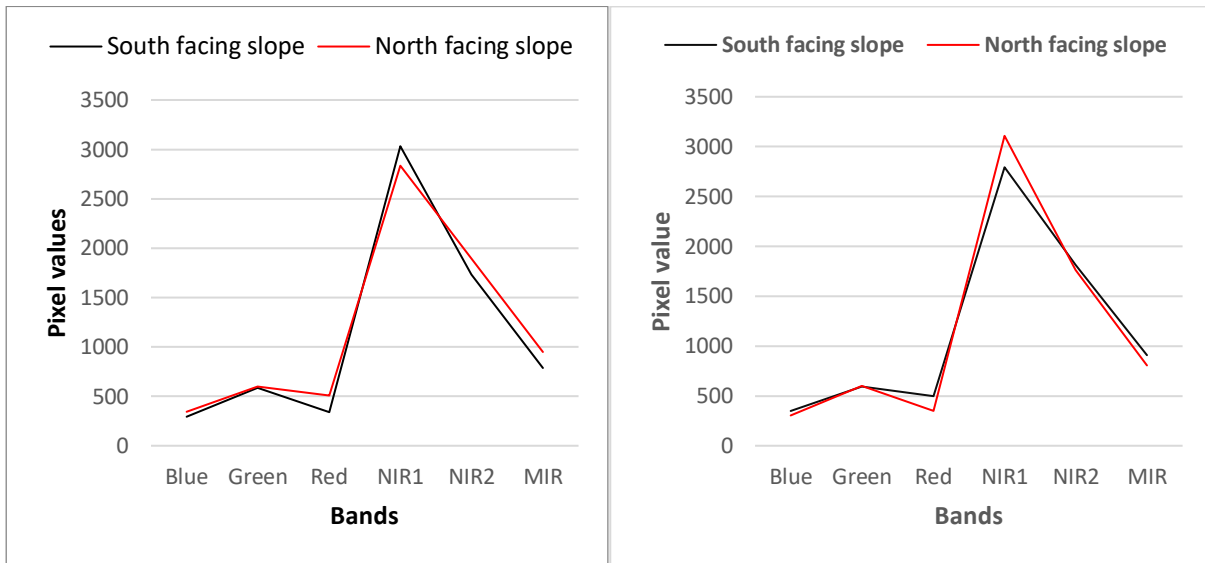


**Figure 4.3 (a) 2011 TM image before topographic normalization and (b) 2011 TM image after topographic normalization; band combination 5,4,3 RGB.**

The pixel values of two locations (Figure 4.3) with different aspects but the same land cover type were compared before and after performing topographic normalization. Statistics for these two locations are shown in Table 4. 3 and Figure 4. 4. Reflectance values of band 2 to 6 increased after topographic normalization for a pixel sample located on the north facing slope. Reflectance values in all six bands for a sample pixel from the south facing slope decreased, thereby making darker.

**Table 4. 3 Comparison of pixel values for two locations for original and topographic normalization image**

Bands	Surface reflectance value at Profile 1.1 (North Facing Slope)		Surface reflectance value at Profile 1.2 (South Facing Slope)	
	Original	Topo Normalized	Original	Topo Normalized
1	349	344	304	294
2	595	602	600	585
3	497	506	352	343
4	2793	2835	3108	3032
5	1814	1898	1765	1735
6	907	947	803	789



(a)

(b)

**Figure 4. 4 Spectral profiles of two locations for (a) original 2011 TM image (b) Topo normalized image.**

The black line is a spectral profile graph of a south facing pixel which shows higher reflectance for the original image than the topographical normalized image. The red line is a spectral profile graph of a north facing pixel which indicates the increased in the reflectance values in the topographic normalization. This shows that the topographic normalization has made the illumination even.

#### 4.1.4 Generation of river network

Application of hydrology tools in ArcGIS produced a network of major rivers in the study area and using the rivers as reference, a 5-km buffer was created which was used as the bounding limit of the study area.

#### 4.1.5 Extraction of relative digital elevation model

The python script of the model described in section 3.3.7 is attached in the Appendix C. This model generated a modified DEM whose values were relative heights from the nearest river points. The data range of relative DEM is from -44 m to 2011 m. The relative DEM is shown in Figure 4. 5. After the cloud masking was applied to the relative DEM, its data range changed from -44 m to 1705 m.

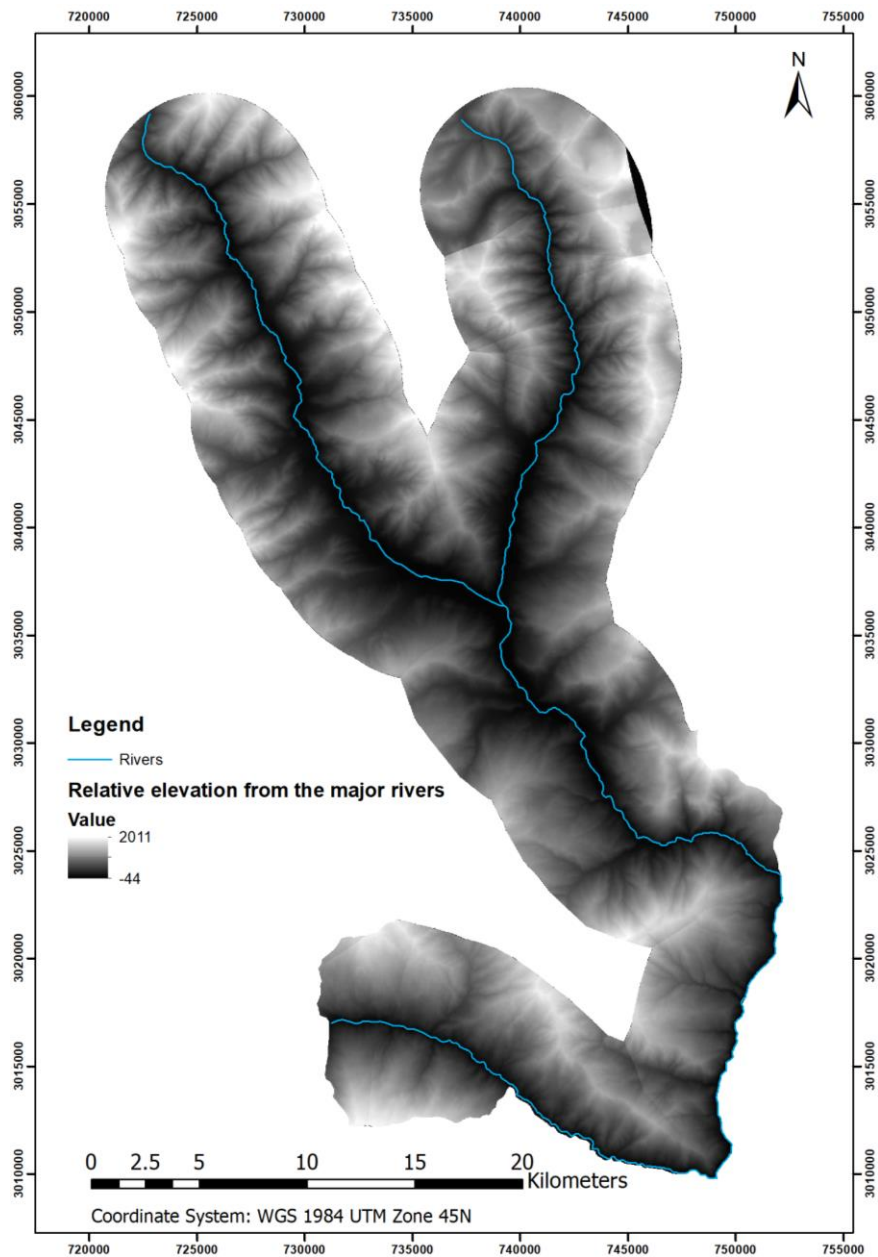


**Figure 4. 5 Relative DEM with values of relative height from the nearest river points**

#### **4.1.6 Principal Component Analysis**

The analysis of eigenvalues from principal component analysis (PCA) showed that the first and the second PCs combined contained 95 percent of the image information by variance. The remaining four PCs had very small portion of information, which could be attributed to noise. Table 4. 4 and Figure 4. 6 show the eigenvalues for the different PCs which are related to the amount of information contained in each PC. Based on this, PC1 and PC2 were extracted as separate bands to be used with other derivatives for classification.

**Table 4. 4 Amount of information in different PCs expressed in terms of eigenvalues and percentages.**

PC	Eigen values	Percentage	Cumulative %
PC1	607526	73	73
PC2	184236	22	95
PC3	31535	4	99
PC4	3325	0	99
PC5	1711	0	99
PC6	952	0	99

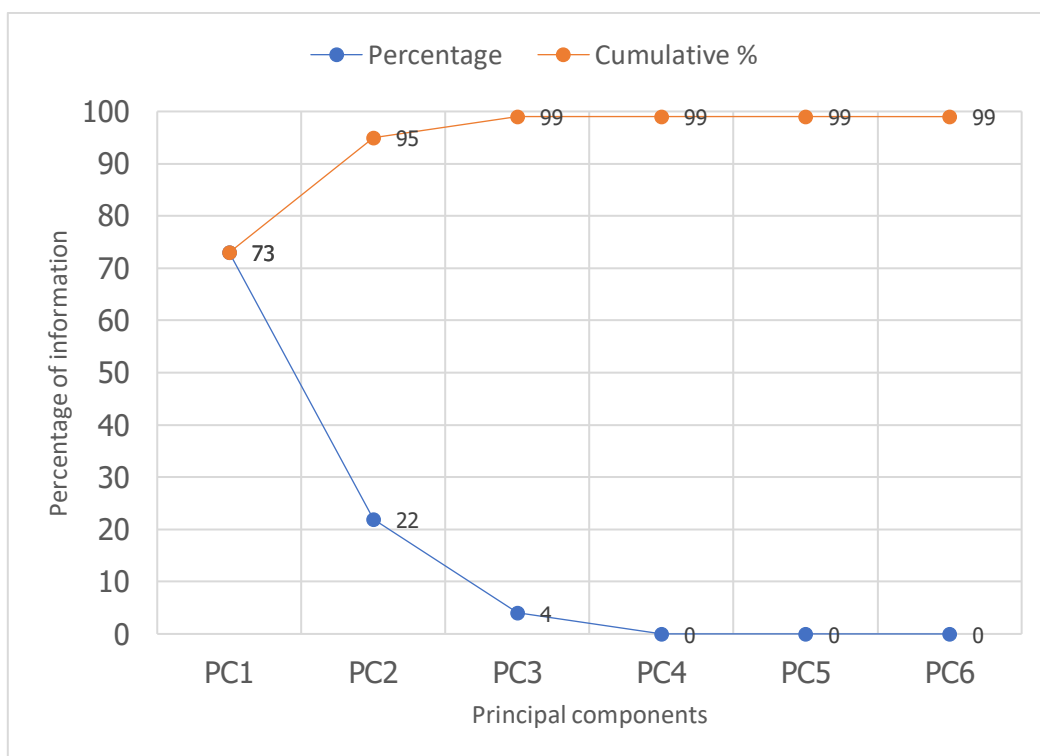


**Figure 4. 6 Percentage of information content in different PCs**

#### 4.1.7 Normalized Difference Vegetation Index

The actual values of NDVI which lie between -1 and +1 were rescaled by a factor of 1000 to create a compatible data range with PC1, PC2, DEM and relative DEM values. Ranges of values for each image are given in Table 4. 5. The lowest value of all data layers was -2982 for PC2 and the highest was 10717 for the PC1.

#### 4.1.8 Layer stack

Different derivatives of data had different ranges of values as shown in the Table 4. 5.

**Table 4. 5 Ranges of values in different datasets**

<b>Datasets</b>	<b>Type</b>	<b>Minimum</b>	<b>Maximum</b>
PC1	Integer	0	10717
PC2	Float	-1982	3731
NDVI x1000	Integer	0.05	887
DEM	Integer	1905	4130
Relative DEM	Integer	-44	1705

In order to accommodate all the values from different layers into single image, the data type of output was suitably selected. For example, in the composite image of PC1-NDVI-DEM, both the lowest and the highest data values were from PC1 (0 and 10717 respectively). All the values for NDVI and DEM fall within this range. Since all values were positive and the 16 bits data can have maximum of 65535 ( $2^{16}-1$ ), so the output data type for this combination was chosen as unsigned 16 bits (U16) from the available options in ERDAS Imagine. For rest of the composite images, the list is given in Table 4. 6.

**Table 4. 6 Different data type selected while combining different layers of datasets**

<b>Composite datasets</b>	<b>Bit depth</b>	<b>Range of values that a cell can contain</b>
PC1-NDVI-DEM	Unsigned 16 bit	0 to 65535
PC1-PC2-NDVI-DEM	Signed 16 bits	-32768 to 32767
PC1-PC2_NDVI-Rel DEM	Signed 16 bits	-32768 to 32767
PC1-PC2-NDVI-DEM-Rel DEM	Signed 16 bits	-32768 to 32767

## 4.2 Digital image processing

### 4.2.1 Supervised classification

After evaluating the separability of training signatures of different training classes of the same land class, signatures whose Jefferies-Matusita distance was less than 1370 were merged to reduce the number of training classes. The 96 training samples collected throughout the image were reduced to 43 signatures after separability testing. The MLC classified all the pixels of the image based on the posterior probability. It even classified those pixels which did not belong to any particular land class. So, the threshold tool in the ERDAS Imagine reassigned those pixels whose Chi-squared distance exceeded a threshold value to unclassified class.

### 4.2.2 Post-classification processes

All the outputs from recode function of unsupervised classification and threshold function of supervised classification were processed with post-classification smoothing operations like majority filtering, clump, sieve and eliminate. This series of processes rendered neat output images as shown in the Figure 4. 7 (d) which can be better analysed and interpreted.

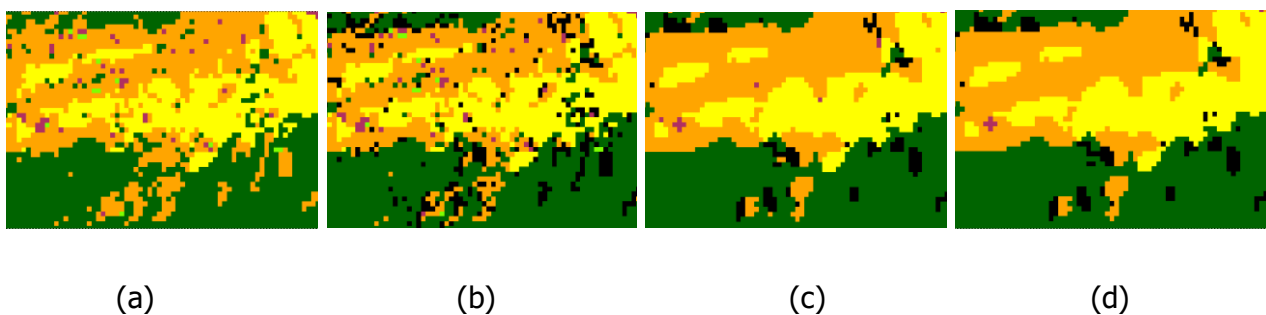


**Figure 4. 7 Classification output images after (a) MLC, (b) Threshold, (c) Majority filter and (d) Clump and Eliminate**

### 4.2.3 Accuracy assessment

Accuracy of the classification outputs for rice and other crop was assessed by comparing the classified pixels of rice and other crops in of 2011 image with the 2011 cadastral field survey data which also had land use information. Due to the absence of ground truth data for forest and built up areas in 2011, their accuracies could not be assessed. For the purposes of calculation, it was assumed that the accuracy of the other two classification would be similar to the accuracy of 2011 image (81.4%) because the images were from the same sensor (Landsat-5 TM), their acquisition months were close to each other and the same methodology was applied to all the image classification.

### 4.2.4 Accuracy assessment for unsupervised classification

The comprehensive accuracy assessments of rice and other crops for five different datasets are

tabulated in Table 4. 7. Due to the lack of reference data for forest and built up land cover classes, their classification accuracy could not be evaluated and the presentation of accuracy assessment in the form of error matrix was not feasible. Of 24743 pixels of rice in the reference data, the unsupervised classification of the original Landsat TM image of 2011 classified 19909 pixels correctly, which accounts for 80.5% accuracy. The accuracies for other datasets remained very low ranging from 55.1% with 44.9% of omission error for PC1-PC2-NDVI-DEM-ReIDEM dataset to 60.5% for PC1-PC2-NDVI-DEM.

**Table 4. 7 Comparison of classification accuracy of rice (unsupervised) among different datasets**

Datasets	PC1-NDVI-DEM		PC1-PC2-NDVI-DEM		PC1-PC2-NDVI-ReIDEM		PC1-PC2-NDVI-DEM-ReIDEM		Original Image	
	No. of pixels	%	No. of pixels	%	No. of pixels	%	No. of pixels	%	No. of pixels	%
Commission Error	1862	7.5	2063	8.3	2152	8.7	3274	13.2	1420	5.7
Accurate classification	14526	58.7	14965	60.5	13864	56.0	13627	55.1	19909	80.5
Omission Error	10145	41.9	9897	39.5	10887	44.0	11134	44.9	4949	19.5

Similarly, the accuracies of unsupervised classification of other crops were very low in all the datasets. The original TM image yielded relatively better accuracy of 64.4 percentage. That is 41862 pixels out of 65006 other crop pixels were correctly classified. The details of errors are compared in the Table 4. 8.

**Table 4. 8 Comparison of classification accuracy of other crop (unsupervised) among different datasets**

Datasets	PC1-NDVI-DEM		PC1-PC2-NDVI-DEM		PC1-PC2-NDVI-ReIDEM		PC1-PC2-NDVI-DEM-ReIDEM		Original Image	
	No. of pixels	%	No. of pixels	%	No. of pixels	%	No. of pixels	%	No. of pixels	%
Commission Error	11051	17.2	9751	14.8	8451	13.3	10401	16.4	4461	6.9
Accurate classification	38354	59.1	37703	57.6	35753	55.3	40304	61.9	41862	64.4
Omission Error	26652	40.9	27303	42.4	29253	41.8	24702	38.2	23402	35.6

#### 4.2.5 Accuracy assessment for supervised classification

The supervised classification on different composite data yielded no better accuracy than the unsupervised classification. However, the accuracy of MLC from the original image was slightly better than the unsupervised classification. 81.4 percent of pixels of rice were accurately classified with minimal error of commission (5.4%) and 18.6% omission error. Likewise, the accuracy for other crops also improved marginally in the supervised classification of original image. Table 4. 9 and Table 4. 10 show the details of accuracy assessment for the supervised classification for rice and other crops. Hence, dataset and method that produced highest accuracy were adopted for other two dates. Consequently, the MLC of supervised classification on the original Landsat-5 TM image was performed for 1995 and 2005 images. Since, there was no ground reference data corresponding to these dates, there was no basis to test the accuracies of classification of these two images.

**Table 4. 9 Comparison of classification accuracy of rice (supervised) among different datasets**

Datasets	PC1-NDVI-DEM		PC1-PC2-NDVI-DEM		PC1-PC2-NDVI-ReIDEM		PC1-PC2-NDVI-DEM-ReIDEM		Original Image	
	No. of pixels	%	No. of pixels	%	No. of pixels	%	No. of pixels	%	No. of pixels	%
Commission Error	2145	8.7	1862	7.5	3208	13.0	4974	20.1	1346	5.4
Accurate classification	14769	60.0	14436	58.3	12864	52.0	13114	52.8	20138	81.4
Omission Error	9897	40.0	10392	41.7	11877	48.1	11629	47.2	4604	18.6

**Table 4. 10 Comparison of classification accuracy of other crop (supervised) among different datasets**

Datasets	PC1-NDVI-DEM		PC1-PC2-NDVI-DEM		PC1-PC2-NDVI-ReIDEM		PC1-PC2-NDVI-DEM-ReIDEM		Original Image	
	No. of pixels	%	No. of pixels	%	No. of pixels	%	No. of pixels	%	No. of pixels	%
Commission Error	13001	20.4	11701	18.3	9101	13.7	9751	15.5	4203	6.5
Accurate classification	39004	60.8	39654	61.5	37053	57.1	37839	58.1	42675	66.6
Omission Error	26002	39.2	25352	38.5	27953	42.9	27167	41.9	22331	33.4

A raster image was generated from the accuracy assessment model. Accurately classified pixels are shown in yellow for rice and orange for other crops. The error of commission, or the pixels which were not rice in the reference data but were classified as rice in the image are in red. The omission error or the pixels which were excluded from the class in the classification image are in purple. This error map gives the visual clue on the spatial distribution of classification errors. As it can be seen from the error maps shown in Figure 4. 8 and Figure 4. 9, most of the errors occur at the edges of cultivated zone in the valley floor.

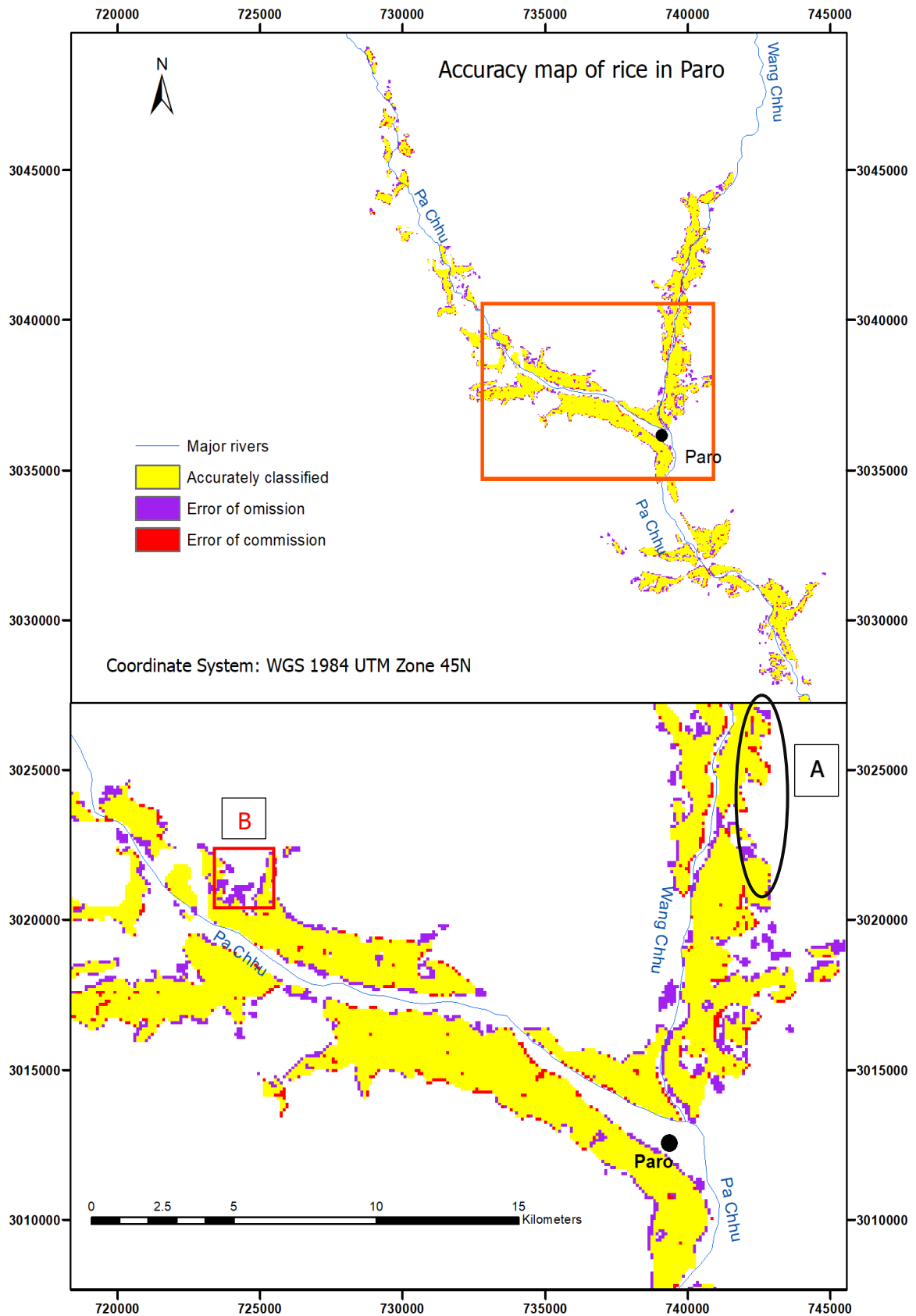


**Figure 4. 8 Error map of rice classification on 2011 TM image using supervised classification. Most of the errors were seen to occur along the edges of LU as marked by A and rarely in larger clumps as labelled by B.**

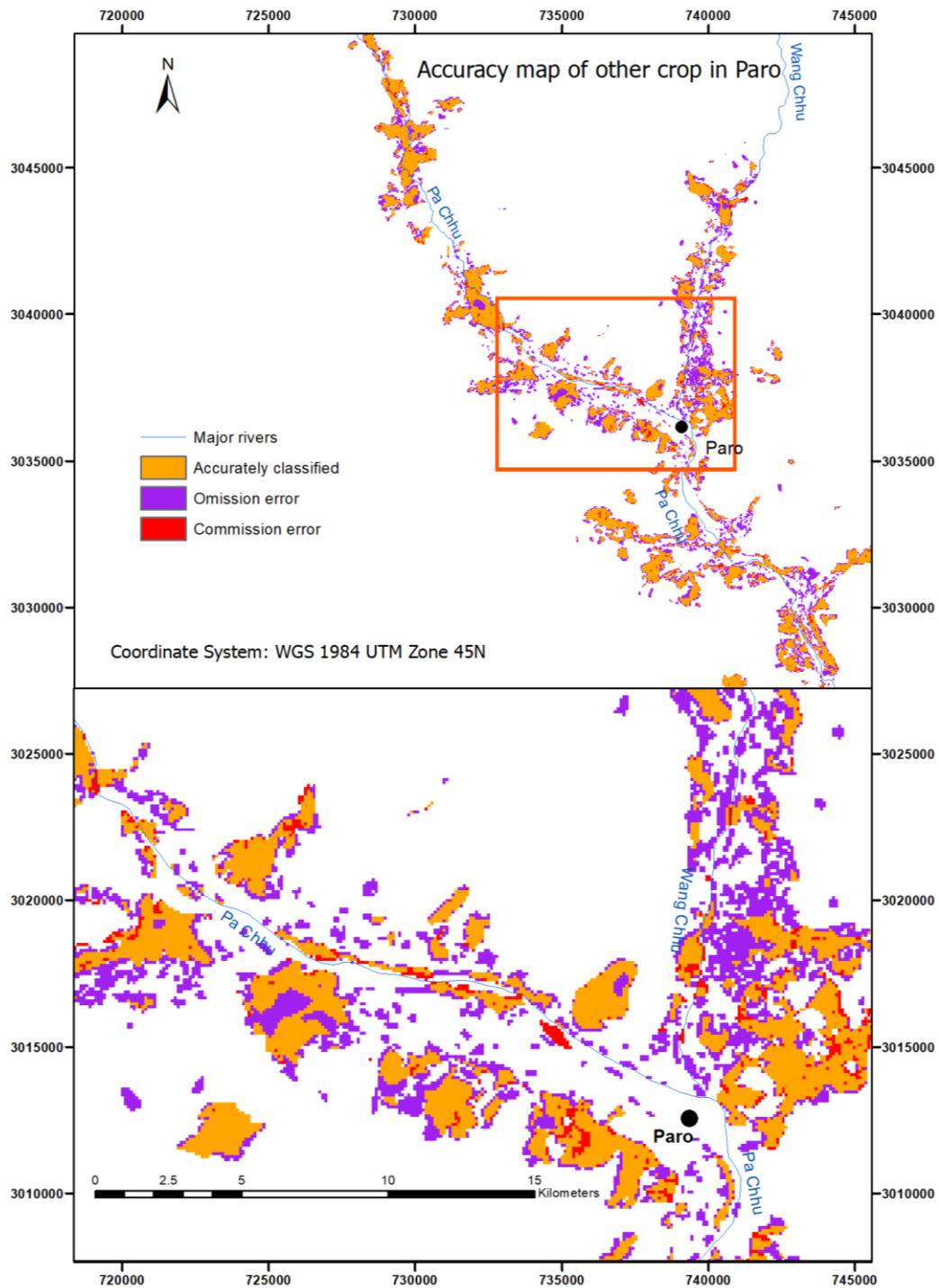


**Figure 4. 9 Error map of other crops classification on 2011 TM image using supervised classification**

#### **4.2.6 Land use land cover mapping**

The supervised classification with MLC yielded three LULC maps (Figure 4. 10, Figure 4. 11 & Figure 4. 12). For the purpose of clarity, final maps have only four major land classes (Forest, Rice, Other crop and Built up).

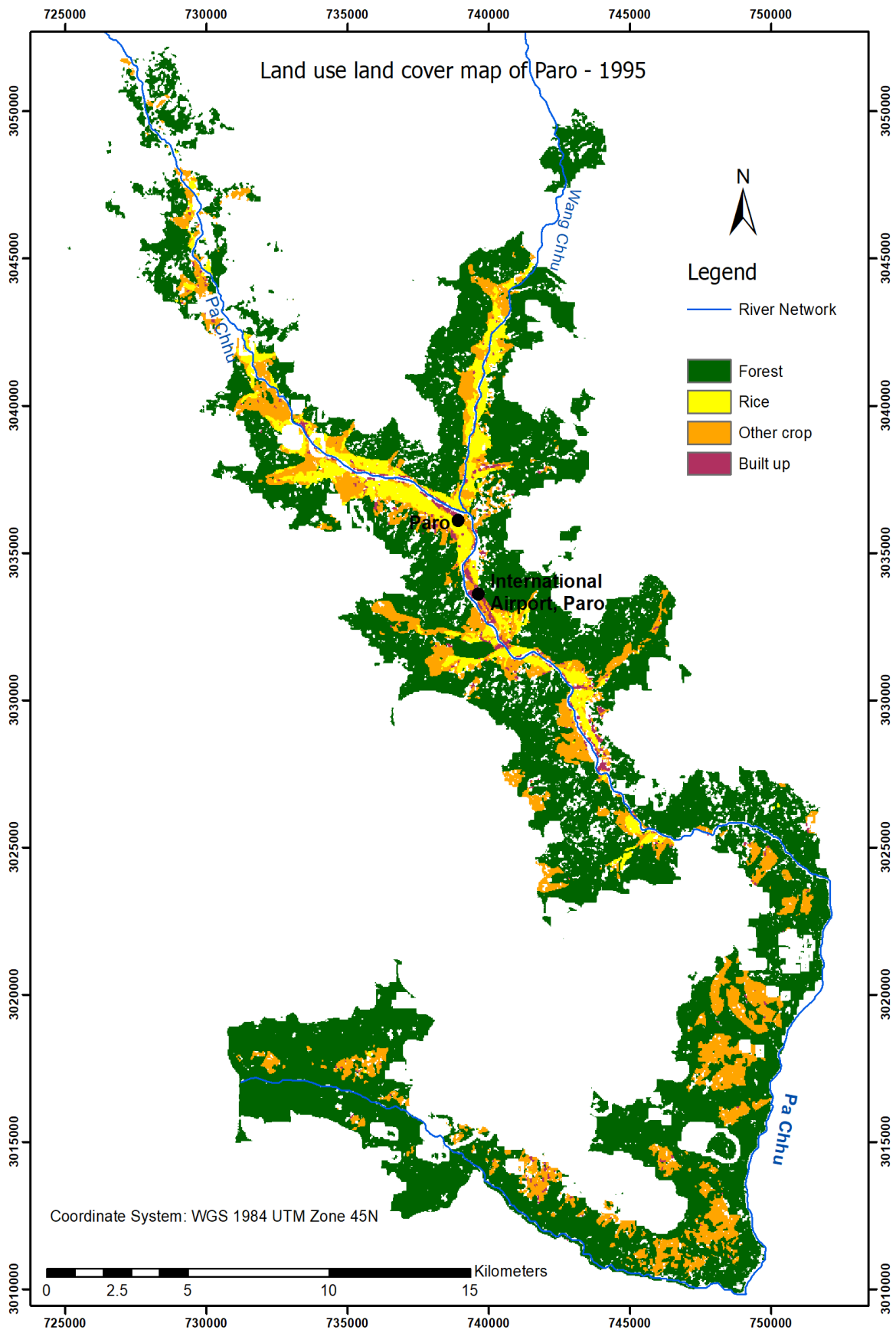


**Figure 4. 10 Land use land cover map of Paro Valley, 1995**

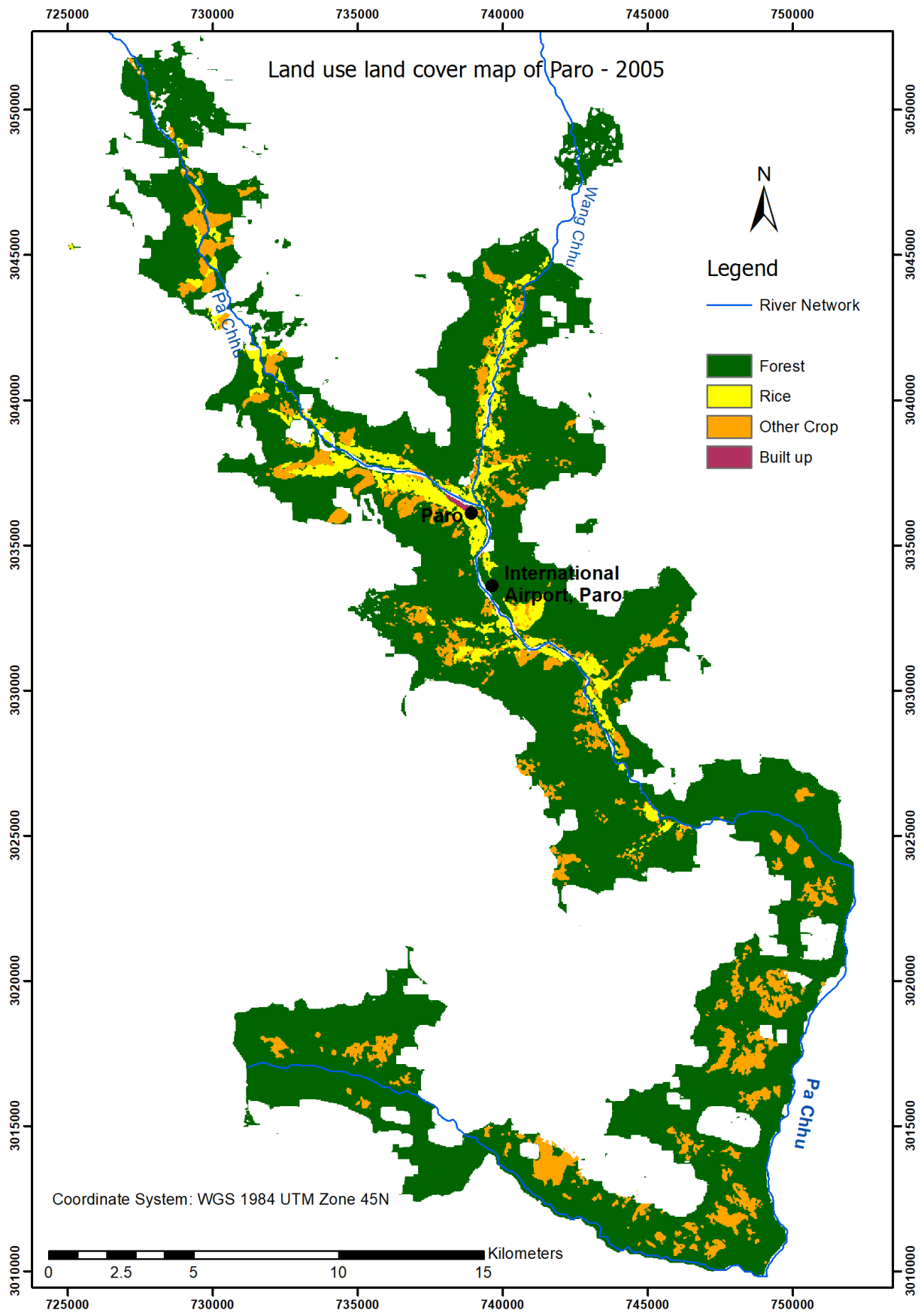


**Figure 4. 11 Land use land cover map of Paro Valley, 2005**

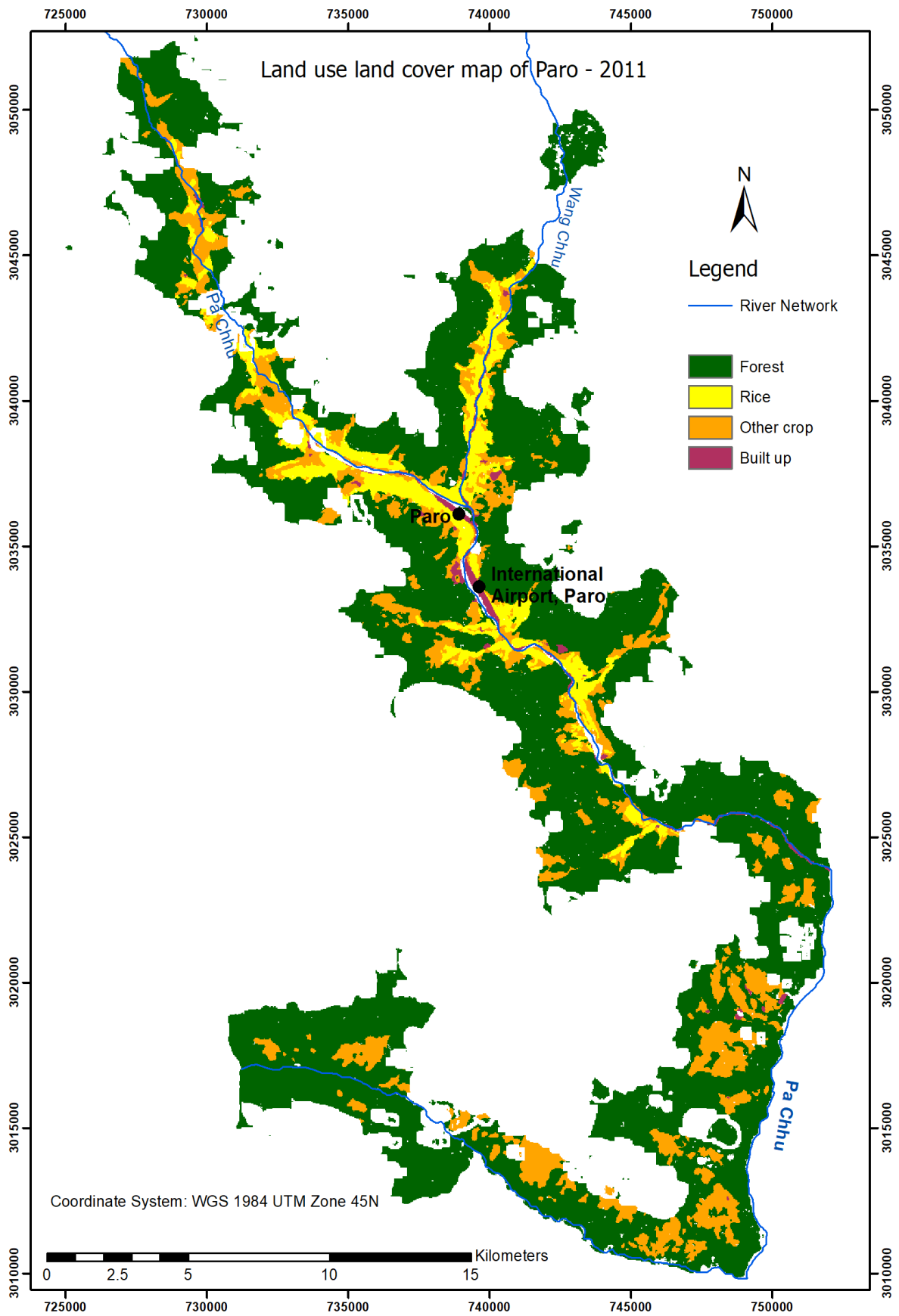


**Figure 4. 12 Land use land cover map Paro Valley, 2011.**

### 4.3 Change detection

The Figure 4. 13 shows the net change in the areas of rice cultivation between the different years. There was an overall decrease of 102 hectares in rice from 1995 to 2005 but the area then showed a considerable increase of 584 hectares from 2005 to 2011.

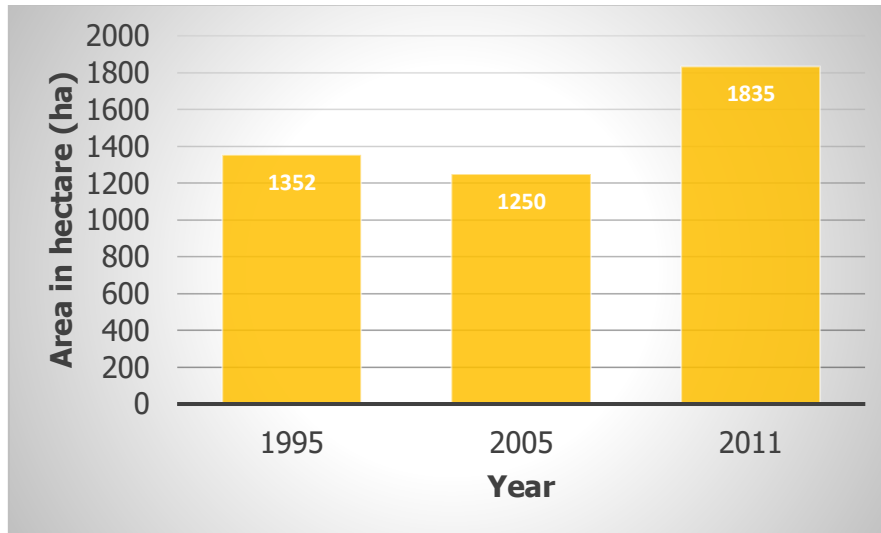


**Figure 4. 13 Total area of rice in study area for 1995, 2005 and 2011**

#### 4.3.1 Change from 1995 to 2005

By over laying two thematic maps, a change matrix was generated (Table 4. 11). It can be seen that the diagonal elements: 17186, 1069, 1792 and 11 are area in hectare of Forest, Rice, Other crops and Built up respectively that remained unchanged from 1995 and 2005.

**Table 4. 11 Change matrix of land cover from 1995-2005**

		From 1995			
		Area in hectare	Forest	Rice	Other Crops
To 2005	Forest	17186	203	1461	144
	Rice	42	1070	113	18
	Other crops	432	69	1792	79
	Built up	0.3	3	3	11

There was an overall decrease in rice fields of 275 hectares between 1995 and 2005. About 203 hectares of the 275 hectares of rice were classified to forest and 69 hectares were converted to other crops. A small area consisting of approximately 3 hectares became built up. On the other hand, out of the 172 hectares increase in rice fields in the same period, the highest gain was from the other crops which amounted to 113 hectares, followed by forest (42 hectares) and built up (18 hectares). The net decrease of 102 hectares was observed from 1995 to 2005. The geographical locations of these changes are shown in Appendix E.

#### 4.3.2 Change from 2005 to 2011

From 2005 to 2011, forest and other crops exhibited the largest change. A total of 2587 hectare of forest was classified into other land classes. Out of this 1893 hectares became other crops, 478 hectares became rice and 216 hectares was classified as built up. However, the forest class only increased by 307 hectares, with 275 hectares of other crops and 32 hectares of rice becoming forest. The rice area in the 2011 image increased by 692 hectares and there was a small overall decrease in the rice fields of 107 hectares. The gain (1949 hectares) of other crops was more than the loss (512 hectares) from the 2005 to 2011 change detection output. The complete change matrix is shown in the Table 4.13 and the spatial distribution of these changes on Appendix F.

**Table 4. 12 Change matrix of land cover from 2005-2011**

		From 2005			
		Area in hectare	Forest	Rice	Other Crops
To 2011	Forest	18940	32	275	0
	Rice	478	1221	213	1
	Other crops	1893	56	2140	0
	Built up	217	19	24	16

#### 4.3.3 Change from 1995 to 2011

On analysing the changes in LULC from 1995 to 2011, it can be seen that 1053 hectares of forest was lost to other land cover types but only 442 hectares of other land cover became forest. As a result, there was a net loss of about 600 hectares of forest during this 16-year period. However,

there was a significant increase of 530 hectare in rice fields against an 86-hectare decrease, giving a net increase of rice of 484 hectares. The maximum contribution in the increase of rice field came from the other crop class. Similarly, there was an overall loss of 847 hectares of other crop which can be set against a 1077-hectare gain which led to a net increase of 230 hectares from 1995 to 2011. The spatial distribution of changes is presented in Appendix G.

**Table 4. 13 Change matrix of land covers from 1995-2011**

		From 1995				
		Area in hectare	Forest	Rice	Other Crops	Built up
To 2011	Forest	16752	14	404	30	
	Rice	108	1261	383	39	
	Other crops	883	61	2560	133	
	Built up	62	11	60	53	

The spatial distribution of changes in rice cultivation from 1995-2005, 2005-2011 and 1995-2011 are given in the Figure 4. 14.

Change detection of rice field in Paro

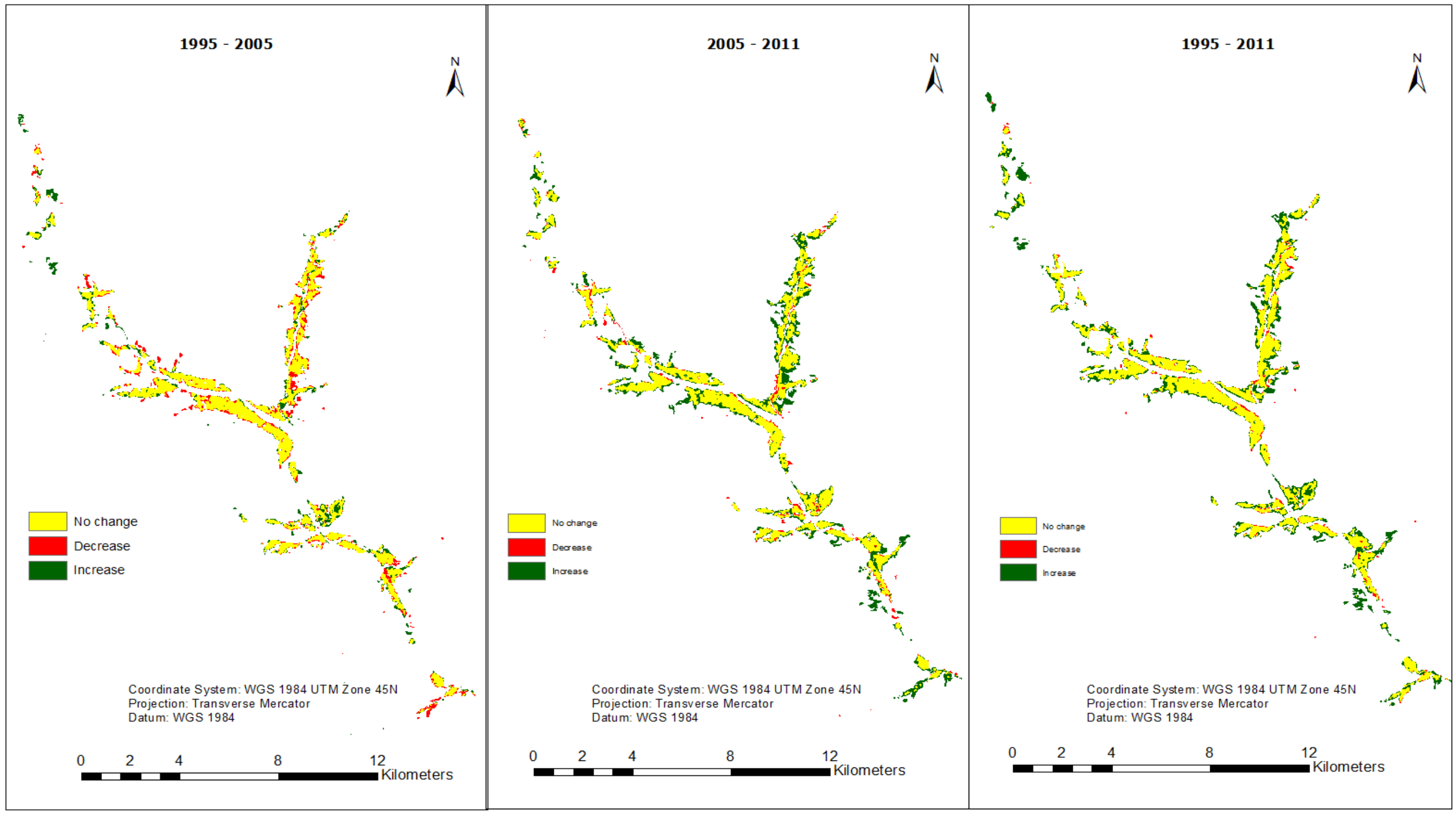


Figure 4. 14 Maps showing change in rice cultivation between different years

## 4.4 Accuracy of post-classification change detection

### 4.4.1 Statistical method

Since there was no ground reference data to independently assess the classification accuracies of 1995 and 2005 images, the same methodologies were applied to classify these images and for the computational purposes as 2011 image classification. It was assumed that their classification accuracies to be similar at 81.4 percentage each. Based on this assumption, two forms of change detection accuracies can be calculated:

- i. Product of individual classification accuracies.

$$\begin{aligned}\text{Change detection accuracy} &= 0.814 \times 0.814 \\ &= 0.662954 \approx 66\%\end{aligned}$$

- ii. If the errors are completely random and assuming classification error can be equated to standard deviation.

$$\begin{aligned}\text{Change detection accuracy} &= 1 - \sqrt{0.19^2 + 0.19^2} \\ &= 1 - 0.2687 \approx 73\%\end{aligned}$$

If a mean is taken from these two forms of accuracies, then the post-classification change detection accuracy comes about 70%.

### 4.4.2 Visual assessment of change detection accuracy

Visual verification of the change detection maps was accomplished with reference to the historical images in the Google Earth that were closest to the TM acquisition dates. The green area within a light blue border in Figure 4. 15 shows a change in rice cultivation from 1995 to 2005. In other words, the land use was not rice in 1995 but it shown as rice in 2005 classified image. On verifying with a Google Earth image of 2012, the area was found to be under rice cultivation. This change result seems to be correct. However, a 2006 Google Earth image, which was closest to the 2005 TM image, seems to have some issues with geometric registration and could not be used for the verification.

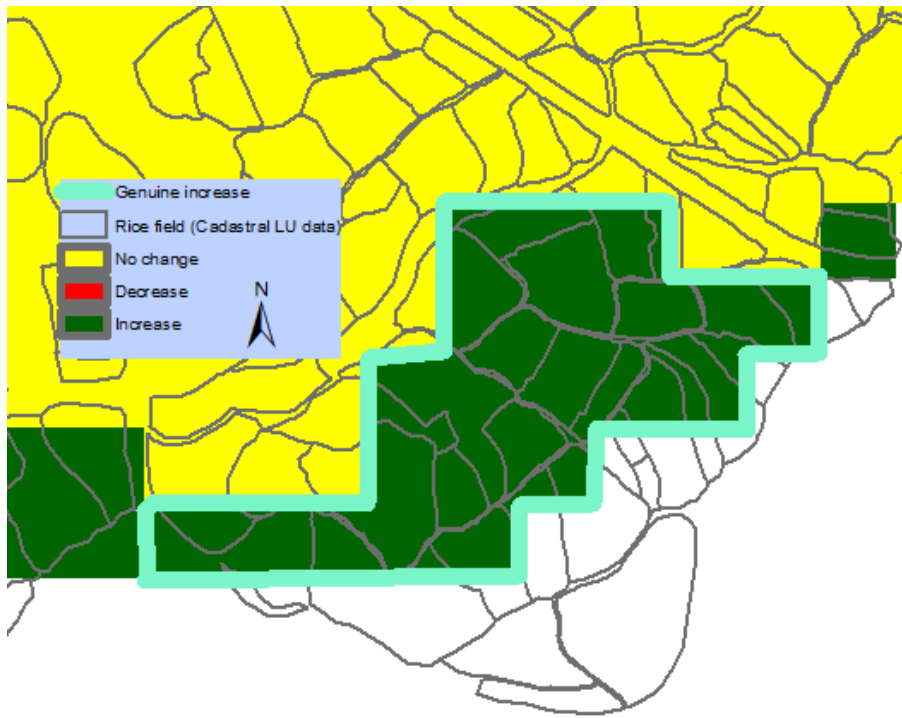


**Figure 4. 15 The increment of rice from 1995 – 2005 from change detection analysis**

The classification result of 2005 was quite generalized with rice in the polygon marked with a red boundary in Figure 4. 16. It was an error in classification that has misrepresented the area as increase in the rice but on careful verification with Google Earth imagery, settlement areas and non-rice fields were also classified as rice in 2005 image.

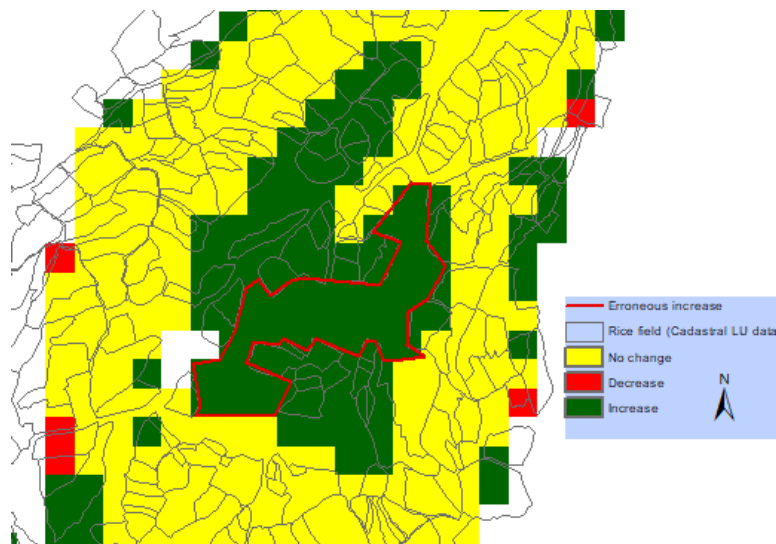


**Figure 4. 16 The red boundary line shows the increase in rice from the classification maps**

There were other cases, where a decrease in rice was detected in the image classification but it did not happen on the ground. That is a clear indication of omission error in the image classification. For example, the red area under the dark bold polygon (Figure 4. 17) is shown as decrease in rice field in 2005 classified image but from the Google earth image, rice field had not decreased.

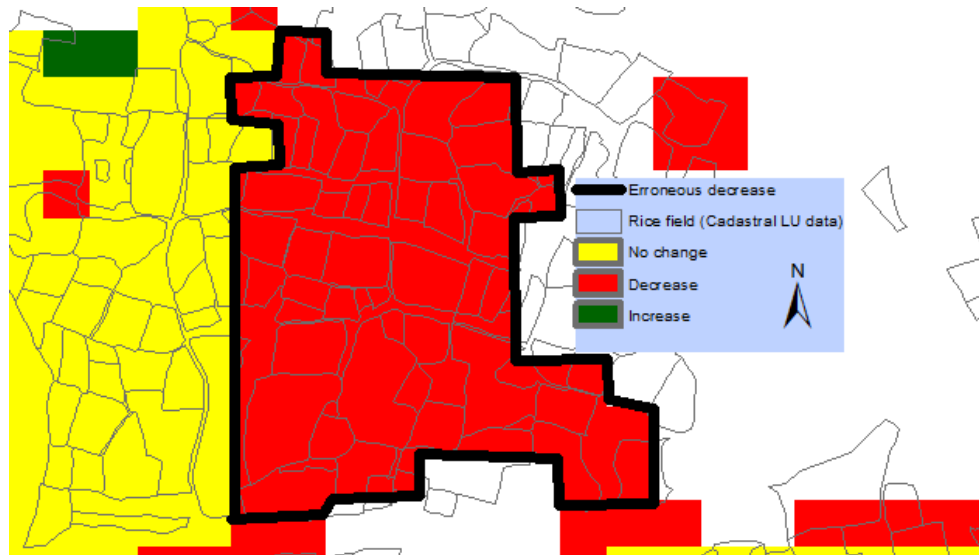


**Figure 4. 17 The area marked by black polygon is shown as decrease in rice from 1995 to 2005 due to the error of omission in the 2005 image classification.**

From the above illustrations, it is clear that some of the changes in rice fields are due to the errors in image classification.

## 4.5 Drivers of LULC change

The change detection analysis revealed that there was a marginal increase in the area of rice cultivation during the study period and the change detection accuracy was relatively low. In spite of uncertainties due to the errors in change detection, the author attempted to find out some of the major causes that might have led to increase in the rice farming in the Paro valley by analysing socio-economic data, meteorological data, demographic data and policies of the country.

### 4.5.1 Natural factors

A supplemental irrigation system is practised in the Paro valley. It is essentially supplementing rain-fed crops with water from the irrigation channels whenever there is a shortfall of rain during the cropping season (Oweis 1997). Such a supplemental approach helps in managing natural resources and stabilizes crop yields. The daily rainfall measurements recorded in the study area from 1991 to 2011 were aggregated to monthly and annual rainfall data. Figure 4. 18 is a bar chart representing the annual rainfall data from 1995 to 2011.

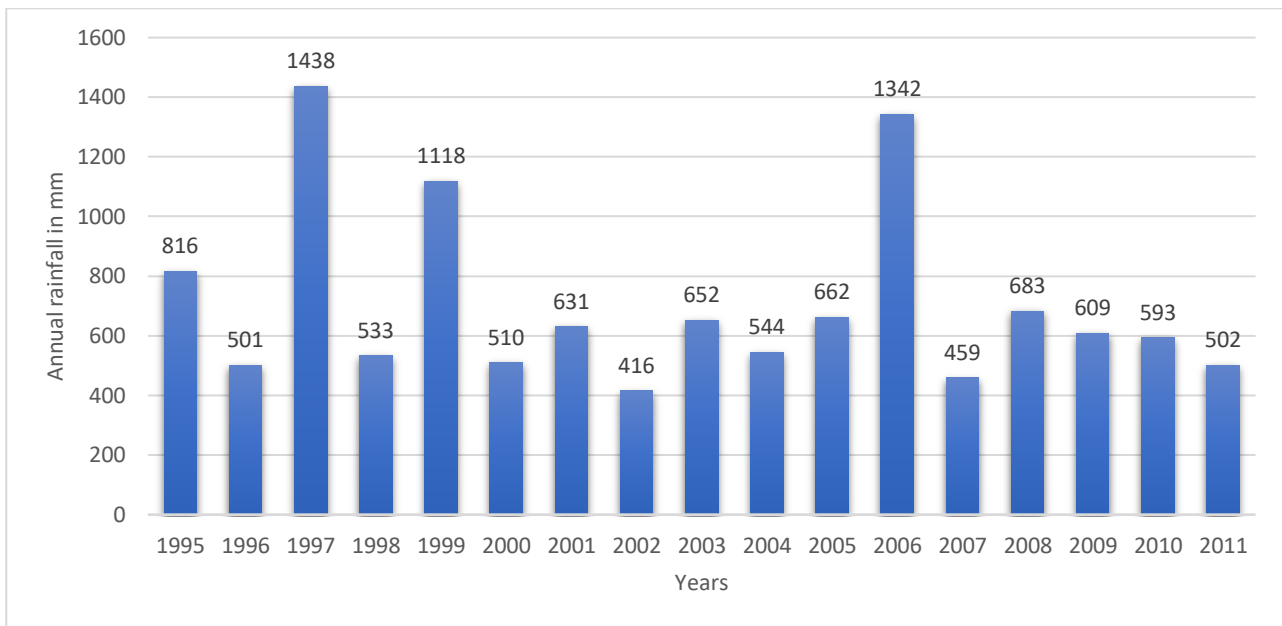


**Figure 4. 18 Annual rainfall from 1995 to 2011 in the study area**

A closer analysis of rainfall data during the rice growing season in Paro (June-September) which is depicted in Figure 4. 19, shows a similar trend like that of the annual rainfall. The irrigation facilities had possibly played an important role in supplementing the shortage of water during the dry days. Therefore, the minor fluctuations in the rainfall pattern during the rice season do not seem to have had significant effects in the change in the area of rice cultivation during the study period.

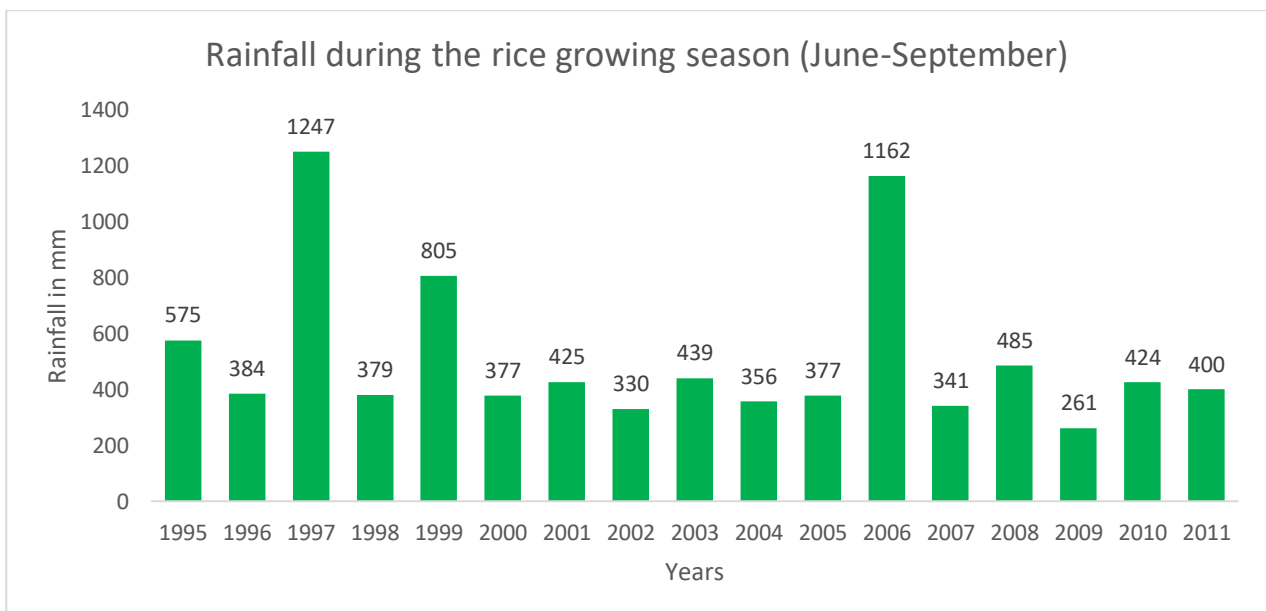


**Figure 4. 19 Rainfall during the rice growing months (June-September) from 1995 -2011**

Graphs of monthly mean temperature data of three study years in Paro (Figure 4. 20) show that the average temperature from May to December for 1995 was much lower than the other two years.

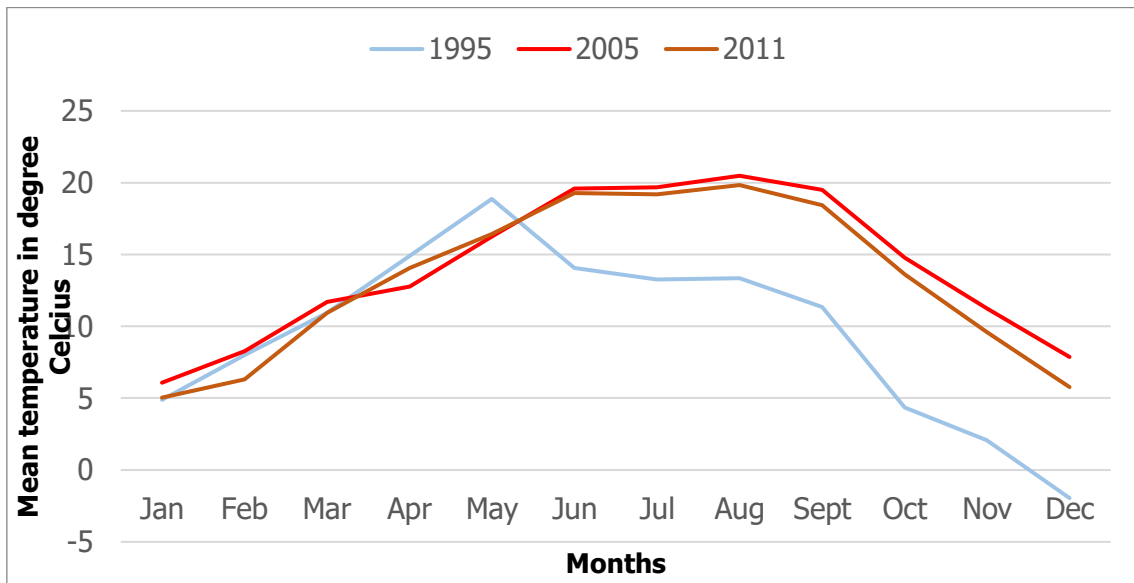


**Figure 4. 20 Mean monthly temperatures for 1995, 2005 and 2011 in the Paro valley**

Figure 4. 21 shows the mean temperature graph during the rice growing season. The average temperature of 2005 is slightly higher than 2011. According to (Sánchez, Rasmussen and Porter (2014), the optimum range of temperature for rice to grow is 13.5 °C to 27.5 °C. From the mean temperature data, the temperature in the study area during the period from 1995 to 2016 remained within this range. Therefore, temperature does not seem to have affected the rice production in Paro valley.

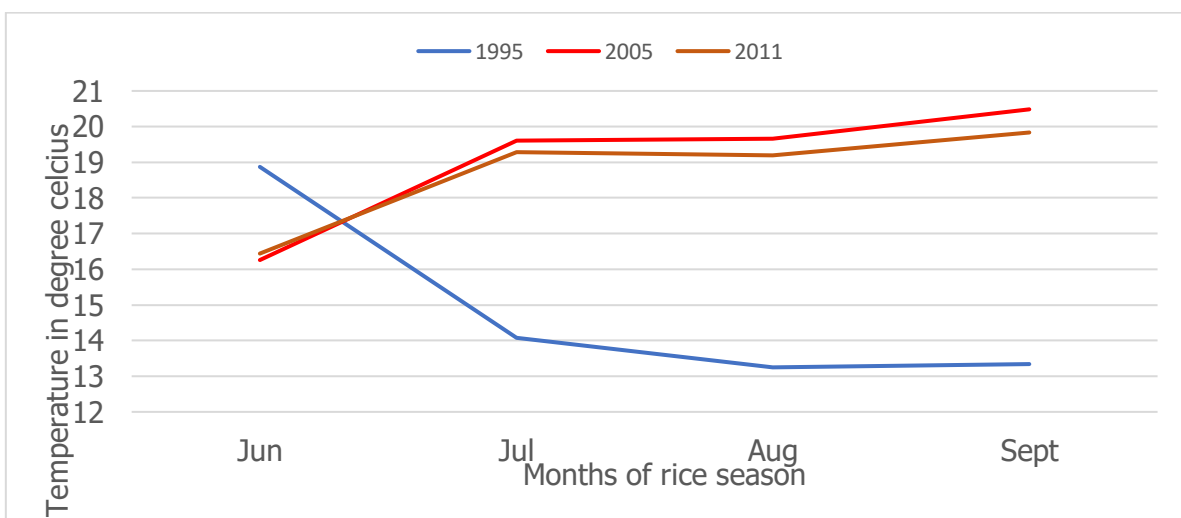


**Figure 4. 21 Mean temperatures of rice growing months (June-September) of 1995, 2005 and 2011**

### 4.5.2 Economic factors

Gross Domestic Product (GDP) is an indicator of the overall economic health of a nation. The economy of Bhutan in 1995 was relatively low (6% of GDP growth rate) compared with 2005 (6.7 % GDP growth rate) (Figure 4. 22). There was a slight rise of 0.7% in the GDP from 1995 to 2005. The decline in rice cultivation in the study area during the same period did not seem to have brought significant impact in the overall GDP. However, the GDP growth rate increased to 9.7% in 2011. Since, agriculture is the main sector that contributes most to the nation’s GDP, the trend of change in the area under rice in Paro from 1995 to 2011 correlates with growth in GDP.

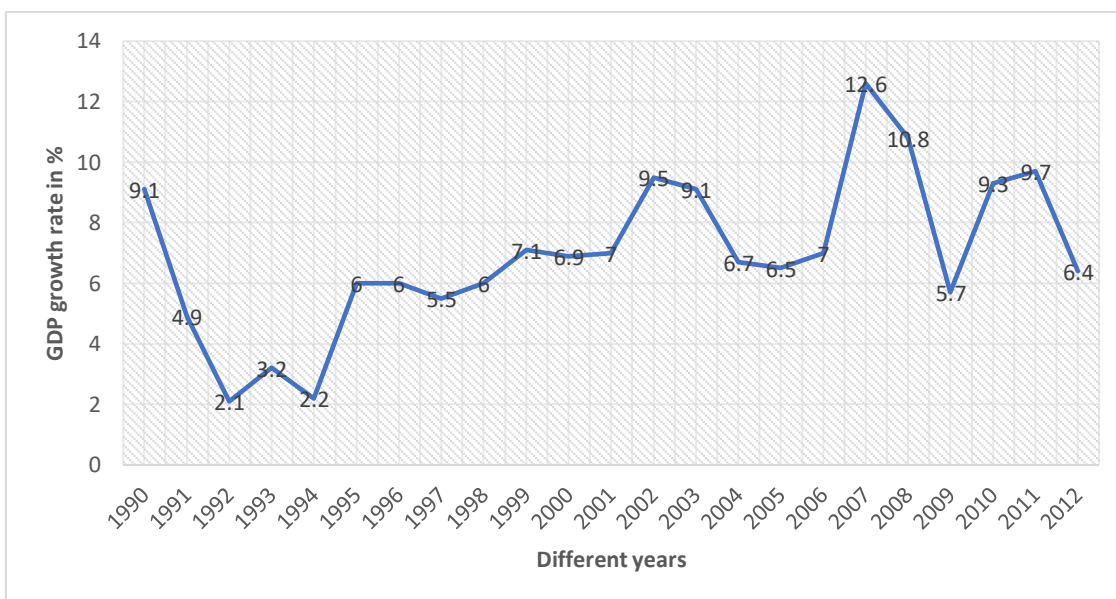


**Figure 4. 22 Growth in GDP for Bhutan, 1990 to 2012**

### 4.5.3 Demographic factors

Referring to Figure 4. 23, there was an increase in the population of Bhutan of about 53,000 persons from 1995 to 2005, or approximately 5,300 persons per year. In the second segment of the period studied (2005-2011), the total increase was 73,283 persons or an annual population increment of approximately 12,200 persons. During the relatively slower population growth from 1995 to 2005, the area of rice cultivation decreased by small margin. However, when the population growth rate increased by more than two-fold between 2005 and 2011, there was a substantial increase in the area of rice fields. This suggests that the increase in population in Bhutan had led to increase the rice cultivation in the Paro valley.

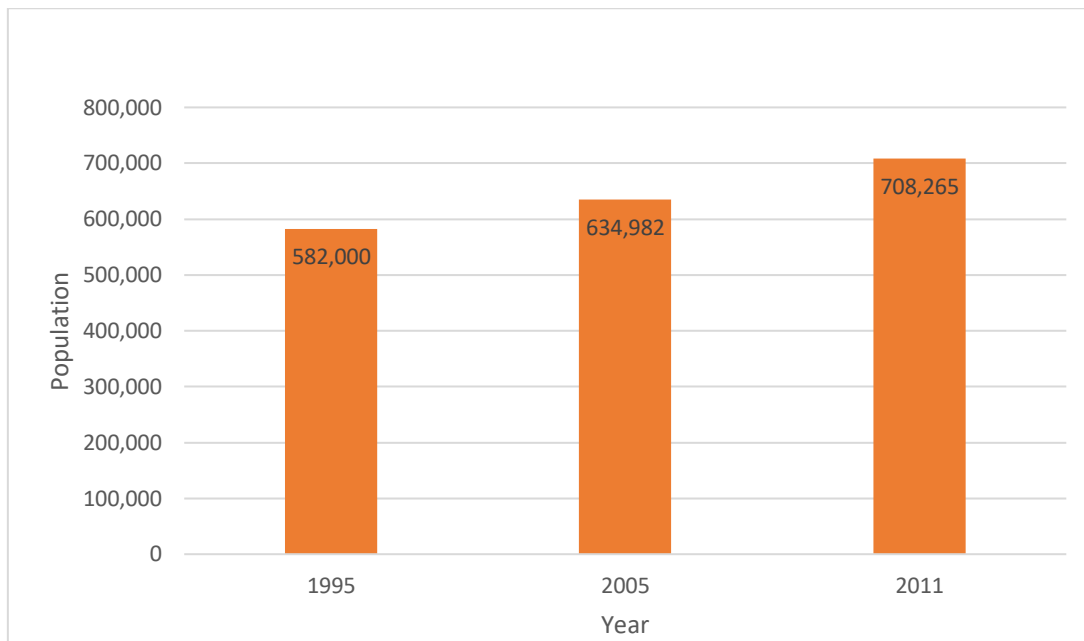


**Figure 4. 23 Total population of Bhutan in 1995, 2005 and 2011**

#### **4.5.4 Policy factors**

Clauses (iii) and (vii) of section 10 (a) of the Forest and Nature Conservation Act of Bhutan 1995, prohibit:

- iii. felling, girdling, lopping, tapping, uprooting, or injuring any tree and removing any timber or other forest produce (including stones, boulders, and sand) or quarrying
- vii. hunting, fishing, taking, removing, destroying, poisoning or injuring any wildlife, or setting traps or snares;

The impacts of laws would have been gradual in manifesting on the rice cultivation in Paro valley. Many other factors are simultaneously responsible to observe the final impact on the change in the acreage of rice cultivation. The law on the conservation of forest and nature came into effect from 1<sup>st</sup> September 1995. It suggests that a decrease in rice fields from 1995 to 2005 could be possibly due to the increase forest coverage indicated in the change detection matrix. It can also be inferred from the population data and above policy, that when the population growth was low, the law was more effective than when the population growth was higher in the later part of the study period.

As a part of stepping up the food production, the Land Act, 2007 empowers government to identify genuinely landless people and people living in the ecologically risky areas and grant them government land for rehabilitation. In order to compile this data, a nationwide high precision cadastral survey was held from 2008 to 2013. These programs could have contributed in the steady increase in rice cultivation by 585 hectares in the study area from 2005 to 2011.

# CHAPTER FIVE

## 5 ANALYSIS AND DISCUSSION

### 5.1 Image pre-processing

#### 5.1.1 Geometric verification

The Landsat images acquired from the USGS archive were geometrically already corrected by USGS using Ground Control Points (GCP) and a global digital elevation model. The accuracy of a geometric correction depends on the quality of image, and the number and distribution of GCPs (USGS 2018a). The root mean square error (RMSE) of each scene geometrically corrected by USGS is documented in the image metadata files. Depending on the nature of application, the RMSE value can be used as a filter to select images with the desired levels of geometric precision. But the choice of images in this study was solely decided by the minimum cloud coverage and the cropping season. The RMSEs of the images used were 0.301, 0.388 and 0.393 pixel for 1995, 2005 and 2011 respectively. Further work on the geometric registration of 2011 image by the author using high resolution Google Earth imagery resulted in a root mean square deviation in the position of  $\pm 5.32$  m or approximately one-sixth of a Landsat TM pixel. For the change detection, the conventional requirement is that the RMSE must be within 0.5 pixel (Lunetta & Elvidge 1999; Shalaby & Tateishi 2007). The images in this study were below this threshold. Co-registration amongst different datasets were checked visually with the help of the swipe tool in ERDAS Imagine and all data had good geometric integrity which gave the author confidence in subsequent image analyses.

#### 5.1.2 Generation of river network

The Panchromatic Remote-sensing Instrument for Stereo Mapping (PRISM) digital elevation model with an 8.9 m cell size when used with hydrology tools in the ArcGIS generated a detail network of rivers and streams. Since the study was only interested in major rivers, a threshold of 150000 pixels was used in the flow accumulation raster to reject the shorter rivers and streams. The major rivers generated from the digital elevation model were overlaid on the Landsat image. Visually these showed a good level of agreement with the main rivers in the imagery.

#### 5.1.3 Extraction of relative Digital Elevation Model

The major rivers were then used as reference to calculate the relative heights of all DEM cells from the nearest river bank; which were then stored as new values for the corresponding cells. It was thought that the inclusion of these data with other data layers might help to better discriminate rice from other crops because most of the rice cultivation in the study area is found within a relative height of approximately zero and 300 m from the closest major river. Due to the high resolution of

the DEM, the computation took quite long time of approximately 36-38 hours. The processing time would have reduced if the DEM raster was resampled to an equal cell size of a Landsat TM cell. There were few pixels in the DEM raster with negative values for relative heights. This happened when considering the shortest horizontal distance between the river and the DEM cells. There might have been some cells in the DEM raster whose elevation values were less than the elevations of nearest river cells.

#### **5.1.4 Normalized Difference Vegetation Index**

The Normalized Difference Vegetation Index (NDVI) is a unit less index whose values range from -1 to +1. The higher chlorophyll content in healthy vegetation absorbs more visible red light and reflects more near-infrared radiation. This gives rise to high, positive NDVI for healthy vegetation. Conversely, lower values of NDVI indicate stressed vegetation (same vegetation type) or a different vegetation type with less photosynthetic activity. The NDVI also depends on the leaf area or plant cover (Turvey & Mclaurin 2012). The NDVI for the seasonal crops like rice increases from the time of planting to the fully mature stage, and then decreases during leaf senescence. In this study, the NDVI values for rice, other crops and forest fall in almost same range from around 0.60 to 0.75. This must be the reason for misclassifying rice as forest and vice-versa.

## **5.2 Digital image processing**

### **5.2.1 Unsupervised classification**

The ISODATA algorithm generated 200 clusters of spectrally distinct classes of pixels. Unsupervised classification, being relatively computer automated, it is faster than supervised classification and requires less human input. However, the interpretation and labelling of clusters with corresponding real-world land class description can be quite labour intensive. High resolution Google Earth imagery, the author's knowledge of the area and land use data from the 2011 cadastral survey helped in assigning meaningful class names to the clusters. In doing so, several spectrally distinct classes were combined to single land class. For instance, the ISODATA algorithm discriminated a rice class into more than one spectral classes but they are labelled as rice during the post-classification processes.

### **5.2.2 Supervised classification**

With the help of the highest resolution Google Earth images, an exhaustive list of spectral signatures from different sample classes was collected before supervised classification was attempted (Cingolani et al. 2004). Based on the evaluation of signature separability using the Jeffries-Matusita (JM) distance, the threshold distance was set to  $\geq 1390$  for a pair signatures to be separable. This commonly used threshold value corresponds approximately to 97% of the upper bound (i.e., 2) of the JM distance (Adam & Mutanga 2009; Das et al. 2018). The Maximum Likelihood Classifier (MLC)

is the most widely used supervised classifier in land use and land cover change research due to its simplicity and high efficiency (Eiumnoh & Shrestha 2000; El-Kawy et al. 2011; Gilani et al. 2015; Yangchen, Thinley & Wallentin 2015). Moreover, the supervised classification resulted in a better accuracy in the 2011 image than the unsupervised classification, so the same method was used in the other two images as well. There was an example of same land cover class depicted different spectral signature even in the rice class. The Rice2 and other crop showed similarity in the spectral signature Figure 5. 1.

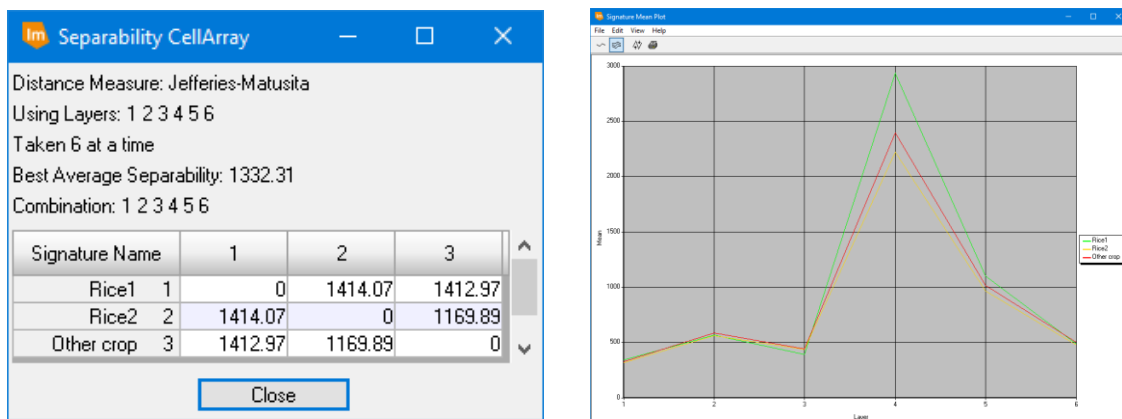


**Figure 5. 1 Sample spectral signature showing two spectrally different rice class and rice class overlapping with other crop.**

### 5.2.3 Accuracy assessment

Accuracy assessment in the context of image classification is an integral part of producing a final output map. The accuracy label attached to a map informs users about the level of confidence that they can place on the map while making decisions. Besides, it provides a basis to compare, analyse and interpret different datasets (Congalton & Green 2008). Accuracy assessment of the 2011 image classification was done using cadastral field survey data. The reference field data which was collected in 2011 had land use information that was limited to "rice" and "other crops". Hence, the accuracy of image classification was assessed selectively for these two classes of land use. However, the accuracy assessment used in this study was comprehensive because the entire population of rice and other crop pixels was used to assess the classification accuracy. Each individual pixel of rice or other crop from the reference dataset was compared to the corresponding classification outputs for rice and other crops. This type of approach for accuracy assessment transcends the issues introduced by sampling biases and its associated statistical computations (Clarke 1994; Congalton & Green 2008). Another advantage of this method is that the spatial distribution of errors can be viewed in the form of map as Figure 4. 8 and Figure 4. 9. As indicated in this map, accurately classified pixels are coloured yellow, omission errors are in purple and commission errors in red. The spatial model given in Figure 3. 7 takes the difference between the two input raster files and generates a raster file with three types of pixel values. If both the pixels were rice, the output pixel value was 0,

which means that the particular pixel was correctly classified (yellow). If the reference pixel was rice (pixel value 1) and the classification pixel is non-rice (pixel value 0), the output pixel value becomes 1; and thus, that pixel is an error of omission (purple). On the other hand, when the reference pixel is 0 and the classified pixel value is 1, the difference is -1, which means that pixel is a commission error (red) category. A special condition was specified in the model that when both the pixels were 0. In this case, their difference will also be 0, which obviously overlaps with accurately classified rice pixels. So, when both the pixels were 0, their difference was assigned a unique value (3 in this case) and later recoded as an unclassified value. A problem was encountered in ArcGIS of its inability to handle negative pixel values. Therefore, pixels with negative values were recoded to +2.

#### **5.2.4 Accuracy of PC1-NDVI-DEM composite data**

Eiumnoh and Shrestha (2000) and Bahadur (2009) found that the inclusion of DEM data with Landsat TM imagery improved the accuracy of image classification in Thailand and Nepal respectively. The best accuracies resulted from the band combination of PC1-NDVI-DEM. However, both supervised and unsupervised classification of PC1-NDVI-DEM in this study produced poor accuracies of around 60%. On analysing the Eigenvalues from the PCA, the first principal component contained 73% of total image information. It was anticipated that the low accuracy could be because of the rejection of the other PCs which constituted 27% of the information. Subsequently, PC2, which had 22% of the information, was included as an additional band to form a new composite image: PC1-PC2-NDVI-DEM. Though the first two principal components accounted to 95% of the image information based on variance, overall accuracy dropped further to 58% in both supervised and unsupervised classification of this dataset. As an exploratory attempt, a modified DEM band whose values were the relative heights above the nearest river bank (referred to as the relative DEM) was used with other bands. Two additional datasets were produced, one was a combination of PC1-PC2-Relative DEM and the other PC1-PC2-NDVI-DEM-Relative DEM. The accuracy from both the classification method of these datasets did not show any improvement on the other datasets discussed above.

It was realized that some spectral characteristics of the image were being lost after performing PCA and calculating NDVI. PC-1 contains maximum of overall scene albedo and PC2 contains the next inter band variations (ERDAS Field Guide 2003). The NDVI layer contains information on the vigour and greenness of vegetation (Xue & Su 2017). The Relative DEM layer has height information. The combination of these different data layers lost the original spectral uniqueness of the image. This led to the inability to discriminate between otherwise spectrally different objects. For instance, Figure 5. 2 shows the data profiles of forest and rice in the PC1-NDVI-DEM composite image. The ISODATA unsupervised classification algorithm classified them as the same class, even though they could be discriminated spectrally in the original TM image.

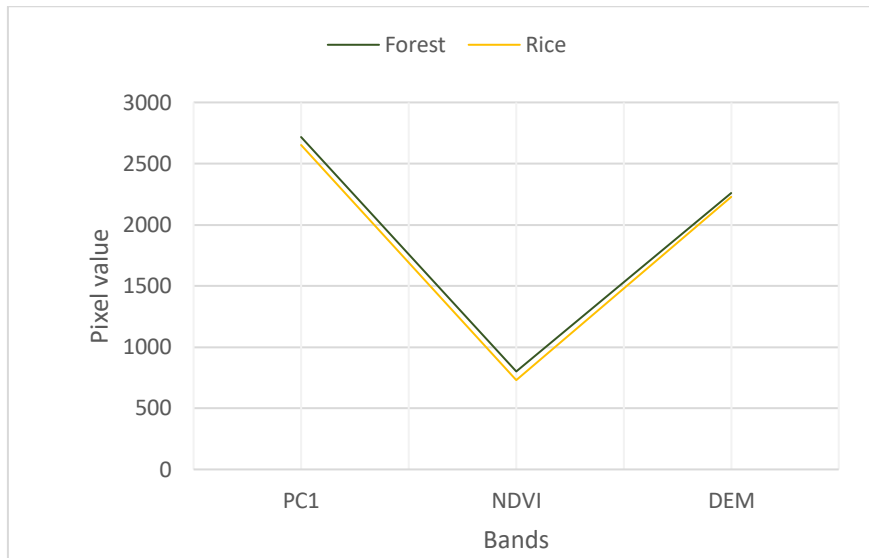


**Figure 5. 2 Mean values of forest and rice classes in the PC1-NDVI-DEM composite image.**

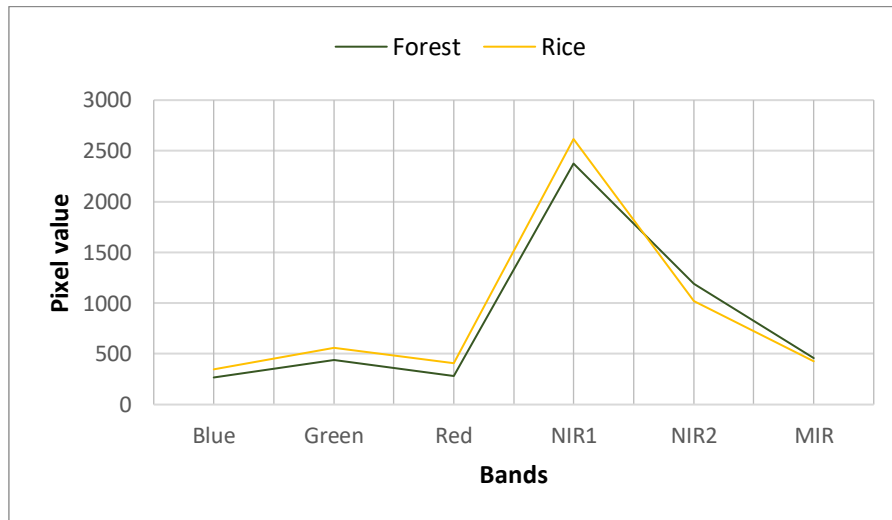


**Figure 5. 3 Spectral signatures of forest and rice in the original Landsat image for the same pixels used to calculate mean values in Figure 5. 2.**

### 5.2.5 Accuracy of original TM image

The original Landsat image was used for image classification due to the poor results from classifications of the different composite images. Accuracies for both methods of classification in the original Landsat TM images were much better than for datasets discussed above. The MLC supervised classification resulted in a slightly better accuracy (81.4%) than unsupervised classification (80.5%) but still they were just below the threshold of 85% specified by Anderson, Hardy and Roach (1972) for land use and land cover studies. It was observed that most classification errors occurred along the edges of rice fields. The area marked A in Figure 4. 8 shows an array of

pixels along the edges of rice fields. One of the causes of edge effect was conversion of polygon field data into raster yielded patches of more area as shown in the Figure 5. 4. Despite the overall accuracy of rice falling below 85%, its confidence level is high because entire population (n=24743) was used for accuracy assessment.

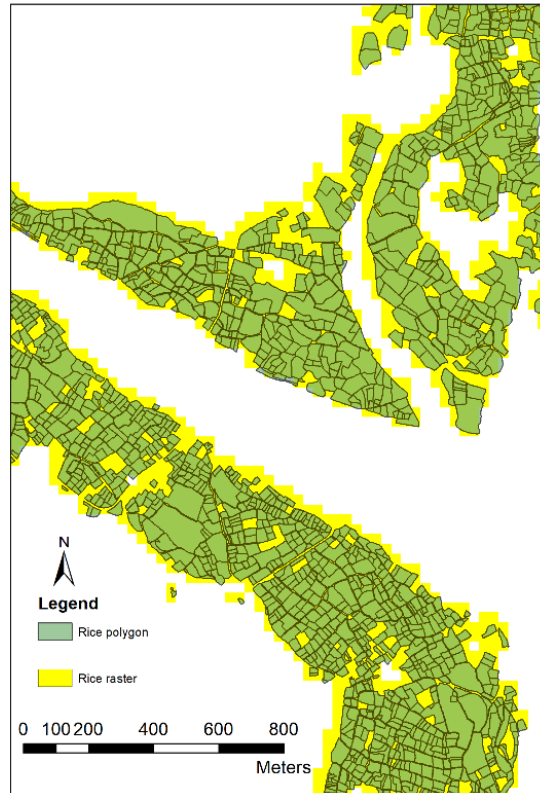


**Figure 5. 4 Mismatch of edges between the rice raster and the polygon rice**

Another pertinent issue was the difficulty in getting a spectrally homogeneous data for the training classes. Therefore, sample classes were kept as small as possible to avoid mixed pixels. However, spectral heterogeneity was contributed by the nature of size of individual plots of rice fields. Figure 5. 5 clearly shows that the maximum number of plots in the study area is less than a pixel (30 m x 30m) and the next highest of number of plots lies in the one-two pixel size class, i.e., 31-60m.

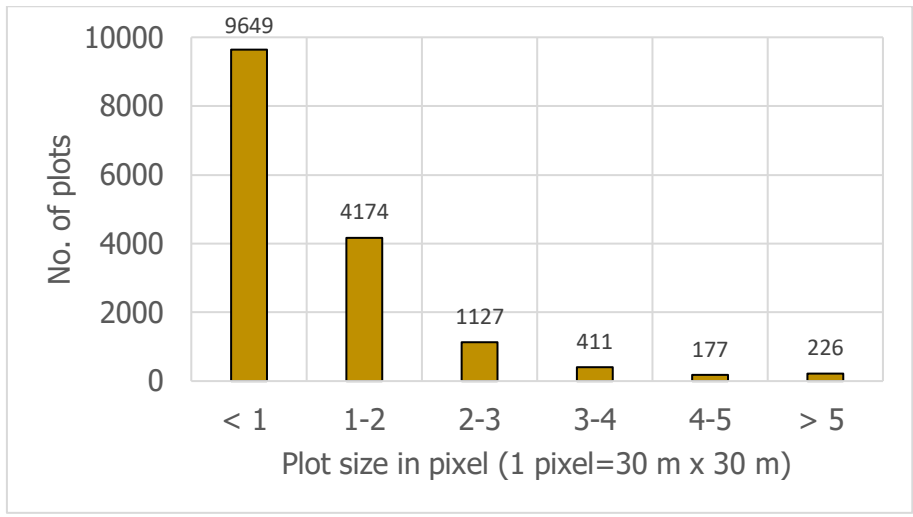


**Figure 5. 5 Histogram showing number of rice plots of varied sizes**

The rice plots either belong to different land owners or are interspersed with different land uses (Figure 5. 6). Individual owners have full discretion on decision about cropping. These differences in them may simply reflect personal choice on behalf of plot owners, and these can potentially contribute to the heterogeneity of the pixels in the images. The problems of mixed pixels when classifying medium-resolution satellite images was stressed by Butt et al. (2015) when using Landsat-5 TM imagery. In situations where fields are small, like the Paro Valley, Landsat imagery with 30 m spatial resolution does not appear suitable for mapping crops because the signature of rice is "corrupted" by signatures of other land cover (often bare soil, tracks, paths) between the rice plots.

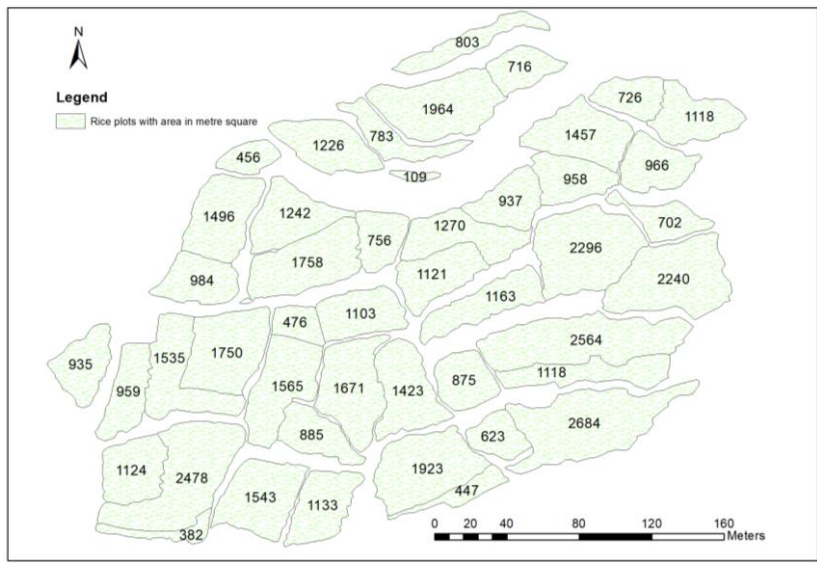


**Figure 5. 6 A typical example of rice plots interspersed by other land uses (white areas). The area of each plot in m<sup>2</sup> is labelled.**

## **5.3 Change detection**

### **5.3.1 Change in rice fields from 1995 – 2005**

According to the classification results, there was a slight decline in the overall rice cultivation in the decade up to 2005 of about 100 hectares. The area of rice field losing to other land classes was more than the gain in the rice field from other land classes. The conversion of rice into forest was the major change in the rice field during this period. From Appendix E, besides the small areas showing a decrease in rice cultivation along the edge of the rice fields, there are reasonably large clumps of rice pixels in 1995 that became other land cover types in 2005. As reported in the section 4.4.2, some of the changes in rice land cover were due to the error in the classification.

### **5.3.2 Change in rice fields from 2005-2011**

In contrast to the 1995-2005 period, there was a drastic increase in the paddy rice in the 2005-2011 period: it increased by 585 hectares in these six years. The majority of the rice fields that were lost to other land class types in the preceding decade were regained during this period (Appendix F). Approximately 25% of the net increase in rice came from the other crops class.

### **5.3.3 Change in rice fields from 1995-2011**

Overall, rice cultivation increased by 485 hectares during the entire study period. This is equivalent to annual increase in rice of approximately 30 hectares. More than 320 hectares of land which was used for other crops in 1995 had become rice fields by 2011. In addition, about 100 hectares of 'forest' had become rice. The change detection map (Appendix G), small losses in rice fields occurred mostly along the edges of fields.

### **5.3.4 Change detection accuracy**

In computing the accuracies for change detection, the following assumptions were made:

- i. The accuracy of classification for 1995 and 2005 images was assumed to be the same as the 2011 image, i.e., 81.4%.

There were no reference data for 1995 and 2005 to assess the classifications independently. However, since the images were from same sensor, acquired in the same season of the year and the same classification technique was applied, the assumption that a similar level of accuracy to that of the 2011 image classification can be applied to 1995 and 2005 images is justifiable. With these assumptions, the accuracy of change according to the method of Coppin et al. (2004) is around 66%. In other words, it is likely that a change in rice (either a loss or a gain) between any two dates of being correct is approximately 0.66.

ii. Classification errors were treated as random

Checking for the randomness of classification errors was beyond the scope of this study. So, to simplify computation, it was assumed that the errors were numerically random. If this is the case and using the assumption that the measured error in 2011 classification can be equated to the standard deviation and using propagation of variances, then this method of error estimation leads to an accuracy of 73%. Hence, using these two approaches, the accuracy of change lies in the 66-73% range. The percentage net change from 1995-2005, 2005-2011 and 1995-2011 are seven, 47 and 36 respectively. These change percentages are smaller than the change detection error range, that statement applied particularly to the 1995-2005-time period.

Another reason for the low accuracy of the post-classification change detection could be due to the three images not having the exact anniversary dates of acquisition. The first image was acquired on 25 September 1995, the second image was acquired on 3 August 2005 and the last image was acquired on 20 August 2011. Even if images cannot be acquired on the same day of the year, they should be as close as possible to prevent errors due to the phenological changes of vegetation and crops. However, even that assumes that phenology is constant from one year to another, which is not generally the case for seasonal cropping which is a function of rainfall, temperature and planting date.

## **5.4 Drivers for change in rice cultivation**

One of the aims of this study was to try and reveal evidence that could be related to some of the potential major drivers that could have caused change for rice cultivation in Paro Valley over the period of 16 years from 1995. Some of the ancillary data used in this context, showed that variations in temperature and rainfall did not produce a noticeable impact on the rice production in this period, however, socio-economic factors appear to have the potential to explain some of these changes: though more research would be needed to link changes in rice to these factors.

### **5.4.1 Socio-economic factors**

The GDP of Bhutan had shown an upward trend during the study period. Furthermore, with increased road connectivity and improved market facilities, farmers seemed to have focused more on rice than other crops and it considered as a major plank of national agricultural development (Arowolo & Deng 2018). In addition, since 2005, the government has placed a high priority on intensifying farm road construction. The objective of this initiative was to provide easy access to markets in which farmers can sell their agricultural produce and also to ease the transport of farm machinery (Wangchuk & Siebert 2013). It is almost a universal phenomenon that socio-economic factors have far-reaching impacts on the agricultural activities and vice-versa (Lambin, Geist & Lepers 2003).

### **5.4.2 Demographic factors**

Population growth in Bhutan during the study period showed a correlation with the increase in rice field area in the Paro Valley. The increase in population in the region could be responsible for increase in the rice production in the study area. In their research on the rural-to-urban population migration, Gosai and Sulewski (2014) revealed that in 2005 many people were migrating from other parts of Bhutan to the western districts of the country, which includes Paro. Obviously, this would have increased the population in Paro valley and so raised the demand for more rice production and more people to cultivate it. This finding concurs with the trends discovered in some countries like Nepal, Ethiopia and Ghana (Arowolo & Deng 2018), where an increase in population leads to increase in agriculture land under production.

### **5.4.3 Institutional factors**

Prior to 1995, there was no restriction on hunting wild animals or cutting trees in Bhutan. However, with the implementation of the Forest and Nature Conservation Act 1995 of Bhutan, there have been increasing incidences of human-wildlife conflicts have been noted (Wang, Curtis & Lassoie 2006). The increasing wildlife population, which had been an outcome of this act, has led to the destruction of crops on the one hand, while on the other hand, the stringent conservation laws hinder agro-pastoralists (Barua, Bhagwat & Jadhav 2013). In the study area, the rice fields seem to be well located in terms of animal encroachment because majority of them are located along the flat valleys surrounded by settlements and other croplands. That is substantiated by the increase in rice cultivation revealed in this research. The Land Act of 2007 emphasizes the optimal utilization of land to achieve grain self-sufficiency, but it is also expected to have encouraged people to intensify agriculture as a whole. This effect has been manifested in the form of increased rice cultivation in Paro Valley from 1995 to 2011.

## **5.5 Limitations of the study**

Despite the best attempts within the reach of the available resources and time, the author argues that the following limitations have impacted the research and that future research needs to try and overcome these.

- i. The issue of clouds

Due to cloud masking of individual images by the combined cloud quality assessment bands of three images, some areas of rice field had to be masked out. Therefore, the findings of the study are restricted to this sub-set of rice field and are thus potentially affected. Almost seven percent of rice field was masked out by cloud.

## ii. The issue of spatial resolution

Given the relatively small size of rice fields in the Paro Valley, and the heterogeneous cropping practices in the study area, 30 m spatial resolution of Landsat-5 TM image resulted many mixed pixels during classification. This could possibly be one of the reasons for the classification accuracy being quite low. Consequently, this resulted in a low accuracy of change detection, in particular the change in rice fields from 1995 to 2005 where it was much smaller than the error range. In such a scenario, the reliability of outcomes is undoubtedly going to be too poor to be used in decision making. The high-resolution imageries from commercial sensors like Worldview, GeoEye, Ikonos, etc are available but they are quite recent and associated with high cost.

## iii. Lack of some ancillary data specific to the study area

The socio-economic data and the demographic data used were for the entire country. The author could not acquire data specific to the current study area. As a result, the drivers that were identified were generally derived from the national data. Clearly to understand agricultural land use change in the valleys of Bhutan requires more work on the ground in terms of field mapping, household-level socio-economic surveys, and oral histories of land uses over a long-time period for as many fields as is feasible.

## CHAPTER SIX

### 6 CONCLUSION AND RECOMMENDATION

This chapter summarizes and draws conclusions from the whole thesis by briefly reviewing the key findings from the two research questions raised in the Chapter One:

- Which dataset and image processing methods are most suitable for change detection of rice cultivation in Bhutan?
- What are the possible factors that have influenced rice land use change in the study area from 1995 to 2011?

Finally, the chapter concludes by highlighting on some of the important recommendations which could improve the results of the future researches.

#### 6.1 Key findings

##### 6.1.1 Challenge to acquire suitable satellite data

In a change detection study dating back to the days when not many satellites were available, the only choice is to go for the Landsat series. A few contemporary satellites like SPOT and IRS which may have been available; are either expensive or restricted for public access. Other aspects like spatial, spectral, temporal and radiometric resolutions must be appropriately analysed before considering using a particular satellite image (Gilani et al. 2015). Usually, there is a trade-off between the spatial and spectral resolutions and the nature of project at hand and the availability of funds must influence the choice. The summers in the Himalayas, where the study area is located remain mostly cloudy which is the greatest hindrance to optical remote sensing. In trying to get images of different years with minimum cloud coverage, temporal variations between two images dates got increased which is not an ideal condition for the change detection study.

##### 6.1.2 Highest accuracy by supervised classification of original TM image

Contrary to the findings of Bahadur K.C. (2009) and Eiumnoh and Shrestha (2000) which yielded higher accuracy from a PC1-NDVI-DEM data composite, the supervised classification of original Landsat-5 TM image produced highest accuracy of 81.4%. It will be worth mentioning here that the accuracy assessment was performed by comparing the classified rice raster data against the reference raster data for rice. This type of accuracy assessment is considered comprehensive approach and its confidence level is high because in this case the sample size is equal to the population.

However, due to relatively low classification accuracy, the accuracy for the post-classification change detection was intrinsically low at about 70%. One of the reasons for the poor accuracy was due to the spectral heterogeneity produced by small size of rice plots. These individual plots belong to different land owners. It was found that almost 90% of rice plots were smaller than 2-pixel size.

### **6.1.3 Overall increase in rice cultivation during the study period**

Although the accuracy of change detection being quite low, and reliability of the result may remain low, empirically the study indicated an overall increase of nearly 500 hectares of rice in field from 1995 to 2011. There was a marginal decline in the rice cultivation during the first decade of the study period but a drastic increase in the next six years, not only compensated for the apparent loss in the previous period but resulted in an overall increase. This result seems to agree with the findings of Gilani et al. (2015) where a slight increase in agricultural land cover was observed from 2000 to 2010.

### **6.1.4 Possible drivers of increase in the rice cultivation**

The analysis of the change detection result for rice with other data suggests that the increase in the rice cultivation in Paro valley showed some level of correlation with the rise in Bhutan's population. Whilst there was no exact demographic data for the study area, the similar trend in population growth in the Paro district was inferred from the national level population data. This revelation seems to resonate with the findings of Ghimiray, Pandey and Velasco (2013) where a slight increase in the overall area of rice fields in Bhutan from 2004 to 2009 was observed.

The other factor for the increase in the rice cultivation was found due to the economic development which had taken place during the study period and particularly in Paro being one the fast-developing districts in Bhutan, the increasing demand for rice has led to increase in rice production. There were some laws and policies which potentially could impact the agricultural activities in Bhutan, but this has not shown any significant impact on the area of rice cultivation in the Paro valley.

## **6.2 Recommendations**

### **6.2.1 Higher spatial resolution imagery**

Since the spatial resolution of 30 m Landsat pixel size for the small size fields and heterogeneous land use in the study area was seen as the main reason for the substandard accuracy for the change detection, finer spatial resolution imagery with little cost attached can potentially produce a better result. It will be worth exploring the use of time series Synthetic Aperture Radar (SAR) data with optical data, where Park et al. (2018) have reportedly achieved 98.7% accuracy for paddy rice mapping. The use of SAR data can also address the problem of cloud contamination in the optical sensor.

### **6.2.2 Higher spectral resolution**

While the six bands of the level 2 processed Landsat TM image that was used in this study are better than some of the higher spatial resolution imagery like SPOT and GeoEye in terms of spectral resolutions, but still there were issues of mixed spectral classes. This can be resolved with the use of imagery with higher spectral and spatial resolution which is available at high costs for recent times in World View 3. The use of hyperspectral Environmental Mapping and Analysis Programme (EnMAP) at 30 m ground sample distance which is planned to launch soon, is expected to solve the current issues posed by the lower spectral resolution.

### **6.2.3 More specific ancillary data**

To have a better understanding of drivers causing the change in rice cultivation, an exhaustive collection of ancillary data is recommended through interviews with local farmers and consultation with relevant government agencies. Due to the obvious reason of time and budget constraint, this approach of data collection could not be incorporated into the methodology of this study.

### **6.2.4 Change trajectory analysis**

Land use land cover trajectory analysis which is a recently developed methodology for change detection could be used. This method performs a search for the idealized spectral signature in the entire temporal trajectories, rather than looking for single change event between two dates.

### **6.2.5 Control illegal cropping**

If remote sensing techniques can map the rice field with reasonable accuracy, it can be used to map illegal cropping in government land by overlaying with the cadastral data. The field verification survey of such encroachment is both time consuming and labour intensive which ultimately adds to the cost.

## REFERENCES

- Abd El-Kawy, OR, Rød, JK, Ismail, HA & Suliman, AS 2011, 'Land use and land cover change detection in the western Nile delta of Egypt using remote sensing data', *Applied Geography*, vol. 31, no. 2, pp. 483-94.
- Adam, E & Mutanga, O 2009, 'Spectral discrimination of papyrus vegetation (*Cyperus papyrus* L.) in swamp wetlands using field spectrometry', *Isprs Journal of Photogrammetry and Remote Sensing*, vol. 64, no. 6, pp. 612-20.
- Anderson, JR, Hardy, EE & Roach, JT 1972, *A land-use classification system for use with remote sensor data*, vol. 671, US Geological Survey.
- Arowolo, AO & Deng, X 2018, 'Land use/land cover change and statistical modelling of cultivated land change drivers in Nigeria', *Regional Environmental Change*, vol. 18, no. 1, pp. 247-59.
- Baban, SM & Wan Yusof, K 2001, 'Mapping land use/cover distribution on a mountainous tropical island using remote sensing and GIS', *International Journal of Remote Sensing*, vol. 22, no. 10, pp. 1909-18.
- Bahadur K.C., K 2009, 'Improving Landsat and IRS Image Classification: Evaluation of Unsupervised and Supervised Classification through Band Ratios and DEM in a Mountainous Landscape in Nepal', *Remote Sensing*, vol. 1, no. 4, p. 1257.
- Banskota, A, Kayastha, N, Falkowski, MJ, Wulder, MA, Froese, RE & White, JC 2014, 'Forest monitoring using Landsat time series data: A review', *Canadian Journal of Remote Sensing*, vol. 40, no. 5, pp. 362-84.
- Barua, M, Bhagwat, SA & Jadhav, S 2013, 'The hidden dimensions of human–wildlife conflict: health impacts, opportunity and transaction costs', *Biological Conservation*, vol. 157, pp. 309-16.

Bewket, W & Abebe, S 2013, 'Land-use and land-cover change and its environmental implications in a tropical highland watershed, Ethiopia', *International journal of environmental studies*, vol. 70, no. 1, pp. 126-39.

Blanzieri, E & Melgani, F 2008, 'Nearest neighbor classification of remote sensing images with the maximal margin principle', *IEEE Transactions on Geoscience and Remote Sensing*, vol. 46, no. 6, pp. 1804-11.

Bruggeman, D, Meyfroidt, P & Lambin, EF 2016, 'Forest cover changes in Bhutan: revisiting the forest transition', *Applied Geography*, vol. 67, pp. 49-66.

Buffum, B, Gratzner, G & Tenzin, Y 2009, 'Forest grazing and natural regeneration in a late successional broadleaved community forest in Bhutan', *Mountain Research and Development*, vol. 29, no. 1, pp. 30-5.

Butt, A, Shabbir, R, Ahmad, SS & Aziz, N 2015, 'Land use change mapping and analysis using Remote Sensing and GIS: A case study of Simly watershed, Islamabad, Pakistan', *The Egyptian Journal of Remote Sensing and Space Science*, vol. 18, no. 2, pp. 251-9.

Campbell, JB & Wynne, RH 2011, *Introduction to Remote Sensing*, 5th edn, Guilford Press, New York.

Cassman, KG, Wood, S, Choo, P, Cooper, H, Devendra, C, Dixon, JA, Gaskell, J, Khan, S, Lal, R & Lipper, L 2005, 'Cultivated systems', in *Ecosystems and human well being, millennium ecosystem assessment (current state and trends)*, Washington, vol. 1.

Centre for GNH 2018, *What is GNH*, viewed 12 October 2018, <<http://www.gnhcentrebhutan.org/what-is-gnh/>>.

Chaplin-Kramer, R, Sharp, RP, Mandle, L, Sim, S, Johnson, J, Butnar, I, i Canals, LM, Eichelberger, BA, Ramler, I & Mueller, C 2015, 'Spatial patterns of agricultural expansion determine impacts on

biodiversity and carbon storage', *Proceedings of the National Academy of Sciences*, vol. 112, no. 24, pp. 7402-7.

Chhogyel, N, Ghimiray, M, Wangdue, K & Bajgai, Y 2015, 'Enhancing Bhutanese rice in the domestic market through increased production and favorable pricing regime', *Journal of Bhutan Studies*, vol. 32, pp. 26-44.

Chowdhury, RR 2006, 'Landscape change in the Calakmul Biosphere Reserve, Mexico: Modeling the driving forces of smallholder deforestation in land parcels', *Applied Geography*, vol. 26, no. 2, pp. 129-52.

Cingolani, AM, Renison, D, Zak, MR & Cabido, MR 2004, 'Mapping vegetation in a heterogeneous mountain rangeland using landsat data: an alternative method to define and classify land-cover units', *Remote Sensing of Environment*, vol. 92, no. 1, pp. 84-97.

Civco, DL 1989, 'Topographic normalization of Landsat Thematic Mapper digital imagery', *Photogrammetric Engineering and Remote Sensing*, vol. 55, no. 9, pp. 1303-9.

Civco, DL, Hurd, JD, Wilson, EH, Song, M & Zhang, Z 2002, 'A comparison of land use and land cover change detection methods', in *ASPRS-ACSM Annual Conference*.

Clarke, GM 1994, *Statistics and experimental design*, 3rd edn, Edward Arnold., London.

Colby, JD 1991, 'Topographic normalization in rugged terrain', *Photogrammetric Engineering and Remote Sensing*, vol. 57, no. 5, pp. 531-7.

Colditz, RR, Acosta-Velázquez, J, Díaz Gallegos, JR, Vázquez Lule, AD, Rodríguez-Zúñiga, MT, Maeda, P, Cruz López, MI & Ressler, R 2012, 'Potential effects in multi-resolution post-classification change detection', *International Journal of Remote Sensing*, vol. 33, no. 20, pp. 6426-45.

Congalton, RG & Green, K 2008, *Assessing the accuracy of remotely sensed data: principles and*

*practices*, CRC press.

Coppin, P & Bauer, ME 1996, 'Digital change detection in forest ecosystems with remote sensing imagery', *Remote sensing reviews*, vol. 13, no. 3-4, pp. 207-34.

Coppin, P, Jonckheere, I, Nackaerts, K, Muys, B & Lambin, E 2004, 'Review Article Digital change detection methods in ecosystem monitoring: a review', *International Journal of Remote Sensing*, vol. 25, no. 9, pp. 1565-96.

Costa, MH, Botta, A & Cardille, JA 2003, 'Effects of large-scale changes in land cover on the discharge of the Tocantins River, Southeastern Amazonia', *Journal of Hydrology*, vol. 283, no. 1-4, pp. 206-17.

Dai, X & Khorram, S 1998, 'The effects of image misregistration on the accuracy of remotely sensed change detection', *IEEE Transactions on Geoscience and Remote Sensing*, vol. 36, no. 5, pp. 1566-77.

Das, B, Sahoo, R, Biswas, A, Pargal, S, Krishna, G, Verma, R, Chinnusamy, V, Sehgal, VK & Gupta, VK 2018, 'Discrimination of rice genotypes using field spectroradiometry', *Geocarto International*, no. just-accepted, pp. 1-28.

De Fries, R, Hansen, M, Townshend, J & Sohlberg, R 1998, 'Global land cover classifications at 8 km spatial resolution: the use of training data derived from Landsat imagery in decision tree classifiers', *International Journal of Remote Sensing*, vol. 19, no. 16, pp. 3141-68.

De Rosa, M, Vestergaard Odgaard, M, Staunstrup, JK, Trydeman Knudsen, M & Hermansen, JE 2017, 'Identifying Land Use and Land-use Changes (LULUC): a global LULUC matrix', *Environmental Science & Technology*, vol. 51, no. 14, pp. 7954-62.

Dhodhi, MK, Saghri, JA, Ahmad, I & Ul-Mustafa, R 1999, 'D-ISODATA: A distributed algorithm for unsupervised classification of remotely sensed data on network of workstations', *Journal of Parallel*

*and Distributed Computing*, vol. 59, no. 2, pp. 280-301.

Dong, J & Xiao, X 2016, 'Evolution of regional to global paddy rice mapping methods: A review', *Isprs Journal of Photogrammetry and Remote Sensing*, vol. 119, pp. 214-27.

Dong, JW, Xiao, XM, Kou, WL, Qin, YW, Zhang, GL, Li, L, Jin, C, Zhou, YT, Wang, J, Biradar, C, Liu, JY & Moore, B 2015, 'Tracking the dynamics of paddy rice planting area in 1986-2010 through time series Landsat images and phenology-based algorithms', *Remote Sensing of Environment*, vol. 160, pp. 99-113.

Dorji, U, Olesen, JE, Bøcher, PK & Seidenkrantz, MS 2016, 'Spatial variation of temperature and precipitation in Bhutan and links to vegetation and land cover', *Mountain Research and Development*, vol. 36, no. 1, pp. 66-79.

Eiumnoh, A & Shrestha, RP 2000, 'Application of DEM data to Landsat image classification: Evaluation in a tropical wet-dry landscape of Thailand', *Photogrammetric Engineering and Remote Sensing*, vol. 66, no. 3, pp. 297-304.

El-Hattab, MM 2016, 'Applying post classification change detection technique to monitor an Egyptian coastal zone (Abu Qir Bay)', *The Egyptian Journal of Remote Sensing and Space Science*, vol. 19, no. 1, pp. 23-36.

El-Kawy, OA, Rød, J, Ismail, H & Suliman, A 2011, 'Land use and land cover change detection in the western Nile delta of Egypt using remote sensing data', *Applied Geography*, vol. 31, no. 2, pp. 483-94.

ERDAS Field Guide 2003, *ERDAS Field Guide*, 7th edn, Leica Geosystems GIS & Mapping, LLC, Atlanta, Georgia.

FAO 2013, *Statistical Year Book 2013: World Food and Agriculture*, United Nations, Rome, Italy.

Food and Agriculture Organization of the United Nations 2016, *Map Accuracy Assessment and Area Estimation: A Practical Guide*, by —.

Feng, DL, Yu, L, Zhao, YY, Cheng, YQ, Xu, YD, Li, CC & Gong, P 2018, 'A multiple dataset approach for 30-m resolution land cover mapping: a case study of continental Africa', *International Journal of Remote Sensing*, vol. 39, no. 12, pp. 3926-38.

Foley, JA, DeFries, R, Asner, GP, Barford, C, Bonan, G, Carpenter, SR, Chapin, FS, Coe, MT, Daily, GC & Gibbs, HK 2005, 'Global consequences of land use', *Science*, vol. 309, no. 5734, pp. 570-4.

Friedl, MA, McIver, DK, Hodges, JC, Zhang, XY, Muchoney, D, Strahler, AH, Woodcock, CE, Gopal, S, Schneider, A & Cooper, A 2002, 'Global land cover mapping from MODIS: algorithms and early results', *Remote Sensing of Environment*, vol. 83, no. 1-2, pp. 287-302.

Garrard, R, Kohler, T, Price, MF, Byers, AC, Sherpa, AR & Maharjan, GR 2016, 'Land use and land cover change in Sagarmatha National Park, a world heritage site in the Himalayas of Eastern Nepal', *Mountain Research and Development*, vol. 36, no. 3, pp. 299-310.

Ghimiray, M, Pandey, S & Velasco, ML 2013, *Estimating adoption rate of modern rice varieties in Bhutan*, Department of Agriculture, Bhutan.

Gibbs, HK, Ruesch, AS, Achard, F, Clayton, MK, Holmgren, P, Ramankutty, N & Foley, JA 2010, 'Tropical forests were the primary sources of new agricultural land in the 1980s and 1990s', *Proceedings of the National Academy of Sciences*, vol. 107, no. 38, pp. 16732-7.

Gilani, H, Shrestha, HL, Murthy, M, Phuntso, P, Pradhan, S, Bajracharya, B & Shrestha, B 2015, 'Decadal land cover change dynamics in Bhutan', *Journal of Environmental Management*, vol. 148, pp. 91-100.

Goldewijk, KK 2001, 'Estimating global land use change over the past 300 years: the HYDE database', *Global Biogeochemical Cycles*, vol. 15, no. 2, pp. 417-33.

Goncalves, M, Netto, M, Costa, J & Zullo Junior, J 2008, 'An unsupervised method of classifying remotely sensed images using Kohonen self-organizing maps and agglomerative hierarchical clustering methods', *International Journal of Remote Sensing*, vol. 29, no. 11, pp. 3171-207.

Gopal, S, Woodcock, CE & Strahler, AH 1999, 'Fuzzy neural network classification of global land cover from a 1 AVHRR data set', *Remote Sensing of Environment*, vol. 67, no. 2, pp. 230-43.

Gosai, MA & Sulewski, L 2014, 'Urban attraction: Bhutanese internal rural–urban migration', *Asian Geographer*, vol. 31, no. 1, pp. 1-16.

Hall, O & Hay, GJ 2003, 'A multiscale object-specific approach to digital change detection', *International Journal of Applied Earth Observation and Geoinformation*, vol. 4, no. 4, pp. 311-27.

Hamad, R, Balzter, H & Kolo, K 2017, 'Multi-Criteria Assessment of Land Cover Dynamic Changes in Halgurd Sakran National Park (HSNP), Kurdistan Region of Iraq, Using Remote Sensing and GIS', *Land*, vol. 6, no. 1, p. 18.

Hansen, MC, Potapov, PV, Moore, R, Hancher, M, Turubanova, S, Tyukavina, A, Thau, D, Stehman, S, Goetz, S & Loveland, T 2013, 'High-resolution global maps of 21st-century forest cover change', *Science*, vol. 342, no. 6160, pp. 850-3.

Hazell, P & Wood, S 2008, 'Drivers of change in global agriculture', *Philosophical Transactions of the Royal Society of London B: Biological Sciences*, vol. 363, no. 1491, pp. 495-515.

Hussain, M, Chen, D, Cheng, A, Wei, H & Stanley, D 2013, 'Change detection from remotely sensed images: From pixel-based to object-based approaches', *Isprs Journal of Photogrammetry and Remote Sensing*, vol. 80, pp. 91-106.

2012, *Data collection survey report on food self-sufficiency and food security in the Kingdom of Bhutan*, by Japan International Cooperation Agency, Nomura Research Institute Ltd.

Jensen, JR 2005, *Introductory digital image processinga remote sensing perspective*, 3rd edn, Pearson Education, Inc.

— 2009, *Remote sensing of the environment: An earth resource perspective 2/e*, Pearson Education India.

— 2014, *Remote sensing of the environment: an earth resource perspective*, Pearson Education, 1292021705.

Johnson, FA & Hutton, CW 2014, 'Dependence on agriculture and ecosystem services for livelihood in Northeast India and Bhutan: vulnerability to climate change in the Tropical River Basins of the Upper Brahmaputra', *Climatic change*, vol. 127, no. 1, pp. 107-21.

Jolliffe, I 2011, 'Principal component analysis', in *International encyclopedia of statistical science*, Springer, pp. 1094-6.

Kleemann, J, Baysal, G, Bulley, HN & Fürst, C 2017, 'Assessing driving forces of land use and land cover change by a mixed-method approach in north-eastern Ghana, West Africa', *Journal of Environmental Management*, vol. 196, pp. 411-42.

Kontgis, C, Schneider, A & Ozdogan, M 2015, 'Mapping rice paddy extent and intensification in the Vietnamese Mekong River Delta with dense time stacks of Landsat data', *Remote Sensing of Environment*, vol. 169, pp. 255-69.

Kubiszewski, I, Costanza, R, Dorji, L, Thoennes, P & Tshering, K 2013, 'An initial estimate of the value of ecosystem services in Bhutan', *Ecosystem Services*, vol. 3, pp. e11-e21.

Kuenzer, C & Knauer, K 2013, 'Remote sensing of rice crop areas', *International Journal of Remote Sensing*, vol. 34, no. 6, pp. 2101-39.

Kumar, M & Rawat, TK 2015, 'Optimal design of FIR fractional order differentiator using cuckoo search algorithm', *Expert Systems with Applications*, vol. 42, no. 7, pp. 3433-49.

Lambin, EF, Geist, HJ & Lepers, E 2003, 'Dynamics of land-use and land-cover change in tropical regions', *Annual review of environment and resources*, vol. 28, no. 1, pp. 205-41.

Lambin, EF, Gibbs, HK, Ferreira, L, Grau, R, Mayaux, P, Meyfroidt, P, Morton, D, Rudel, T, Gasparri, I & Munger, J 2013, 'Estimating the world's potentially available cropland using a bottom-up approach', *Global environmental change*, vol. 23, no. 5, pp. 892-901.

Lambin, EF & Meyfroidt, P 2011, 'Global land use change, economic globalization, and the looming land scarcity', *Proceedings of the National Academy of Sciences*, vol. 108, no. 9, pp. 3465-72.

Lambin, EF, Turner, BL, Geist, HJ, Agbola, SB, Angelsen, A, Bruce, JW, Coomes, OT, Dirzo, R, Fischer, G & Folke, C 2001, 'The causes of land-use and land-cover change: moving beyond the myths', *Global environmental change*, vol. 11, no. 4, pp. 261-9.

Li, M, Zang, S, Zhang, B, Li, S & Wu, C 2014, 'A Review of Remote Sensing Image Classification Techniques: the Role of Spatio-contextual Information', *European Journal of Remote Sensing*, vol. 47, no. 1, pp. 389-411.

Lillesand, T, Kiefer, RW & Chipman, J 2004, *Remote sensing and image interpretation*, Fifth edn, John Wiley & Sons, USA.

Liu, J, Kuang, W, Zhang, Z, Xu, X, Qin, Y, Ning, J, Zhou, W, Zhang, S, Li, R & Yan, C 2014, 'Spatiotemporal characteristics, patterns, and causes of land-use changes in China since the late 1980s', *Journal of Geographical Sciences*, vol. 24, no. 2, pp. 195-210.

Liu, J, Shao, Q, Yan, X, Fan, J, Zhan, J, Deng, X, Kuang, W & Huang, L 2016, 'The climatic impacts of land use and land cover change compared among countries', *Journal of Geographical Sciences*, vol. 26, no. 7, pp. 889-903.

Lu, D & Weng, Q 2007, 'A survey of image classification methods and techniques for improving classification performance', *International Journal of Remote Sensing*, vol. 28, no. 5, pp. 823-70.

Lunetta, RS & Elvidge, CD 1999, *Remote sensing change detection*, vol. 310, Taylor & Francis.

Manakos, I & Braun, M 2014, *Land Use and Land Cover Mapping in Europe : Practices and Trends*, Dordrecht: Springer.

Minnaert, M 1941, 'The reciprocity principle in lunar photometry', *The Astrophysical Journal*, vol. 93, pp. 403-10.

Mittermeier, RA, Mittermeier, CG, Pilgrim, J, Fonseca, G & Konstant, WR 2002, *Wilderness: Earth's last wild places*, México, MX: CEMEX.

Muthayya, S, Sugimoto, JD, Montgomery, S & Maberly, GF 2014, 'An overview of global rice production, supply, trade, and consumption', *Annals of the new york Academy of Sciences*, vol. 1324, no. 1, pp. 7-14.

Myint, SW, Gober, P, Brazel, A, Grossman-Clarke, S & Weng, Q 2011, 'Per-pixel vs. object-based classification of urban land cover extraction using high spatial resolution imagery', *Remote Sensing of Environment*, vol. 115, no. 5, pp. 1145-61.

National Statistics Bureau 2017, *Statistical Year Book of Bhutan 2017*, 35 edn, vol. 1, 1 vols., National Statistics Bureau, Thimphu, Bhutan.

— 2018, *2017 Population and Housing Census of Bhutan*, National Statistics Bureau of Bhutan, Thimphu, Bhutan.

Netanyahu, NS, Le Moigne, J & Masek, JG 2004, 'Georegistration of Landsat data via robust matching of multiresolution features', *IEEE Transactions on geoscience and remote sensing*, vol. 42, no. 7,

pp. 1586-600.

Oetter, DR, Cohen, WB, Berterretche, M, Maierperger, TK & Kennedy, RE 2001, 'Land cover mapping in an agricultural setting using multiseasonal Thematic Mapper data', *Remote Sensing of Environment*, vol. 76, no. 2, pp. 139-55.

Ostwald, M, Wibeck, V & Stridbeck, P 2009, 'Proximate causes and underlying driving forces of land-use change among small-scale farmers—illustrations from the Loess Plateau, China', *Journal of Land Use Science*, vol. 4, no. 3, pp. 157-71.

Oweis, T 1997, *Supplemental irrigation: A highly efficient water-use practice*, ICARDA, Aleppo, Syria.

Pal, NR & Bhandari, D 1992, 'On object background classification', *International Journal of Systems Science*, vol. 23, no. 11, pp. 1903-20.

Park, S, Im, J, Park, S, Yoo, C, Han, H & Rhee, J 2018, 'Classification and Mapping of Paddy Rice by Combining Landsat and SAR Time Series Data', *Remote Sensing*, vol. 10, no. 3, p. 447.

Peng, S, Huang, J, Sheehy, JE, Laza, RC, Visperas, RM, Zhong, X, Centeno, GS, Khush, GS & Cassman, KG 2004, 'Rice yields decline with higher night temperature from global warming', *Proceedings of the National Academy of Sciences of the United States of America*, vol. 101, no. 27, pp. 9971-5.

Petit, CC & Lambin, EF 2001, 'Integration of multi-source remote sensing data for land cover change detection', *International Journal of Geographical Information Science*, vol. 15, no. 8, pp. 785-803.

Powell, SL, Cohen, WB, Healey, SP, Kennedy, RE, Moisen, GG, Pierce, KB & Ohmann, JL 2010, 'Quantification of live aboveground forest biomass dynamics with Landsat time-series and field inventory data: A comparison of empirical modeling approaches', *Remote Sensing of Environment*, vol. 114, no. 5, pp. 1053-68.

Puletti, N, Perria, R & Storchi, P 2014, 'Unsupervised classification of very high remotely sensed images for grapevine rows detection', *European Journal of Remote Sensing*, vol. 47, no. 1, pp. 45-54.

Radoux, J, Lamarche, C, Van Bogaert, E, Bontemps, S, Brockmann, C & Defourny, P 2014, 'Automated training sample extraction for global land cover mapping', *Remote Sensing*, vol. 6, no. 5, pp. 3965-87.

Rawat, JS & Kumar, M 2015, 'Monitoring land use/cover change using remote sensing and GIS techniques: A case study of Hawalbagh block, district Almora, Uttarakhand, India', *Egyptian Journal of Remote Sensing and Space Sciences*, vol. 18, no. 1, pp. 77-84.

Riaño, D, Chuvieco, E, Salas, J & Aguado, I 2003, 'Assessment of different topographic corrections in Landsat-TM data for mapping vegetation types (2003)', *IEEE Transactions on Geoscience and Remote Sensing*, vol. 41, no. 5, pp. 1056-61.

2008, *The Constitution of the Kingdom of Bhutan* by Royal Government of Bhutan, Royal Government of Bhutan.

Sánchez, B, Rasmussen, A & Porter, JR 2014, 'Temperatures and the growth and development of maize and rice: a review', *Global change biology*, vol. 20, no. 2, pp. 408-17.

Sangay, T & Vernes, K 2008, 'Human–wildlife conflict in the Kingdom of Bhutan: patterns of livestock predation by large mammalian carnivores', *Biological Conservation*, vol. 141, no. 5, pp. 1272-82.

Saxena, KG, Maikhuri, RK & Rao, KS 2005, 'Changes in agricultural biodiversity: Implications for sustainable livelihood in the Himalaya', *Journal of Mountain Science*, vol. 2, no. 1, p. 23.

Shalaby, A & Tateishi, R 2007, 'Remote sensing and GIS for mapping and monitoring land cover and land-use changes in the Northwestern coastal zone of Egypt', *Applied Geography*, vol. 27, no. 1, pp. 28-41.

Shrestha, S, Chapagain, R & Babel, MS 2017, 'Quantifying the impact of climate change on crop yield and water footprint of rice in the Nam Oon Irrigation Project, Thailand', *Science of The Total Environment*, vol. 599-600, pp. 689-99.

Singh, A 1989, 'Review article digital change detection techniques using remotely-sensed data', *International Journal of Remote Sensing*, vol. 10, no. 6, pp. 989-1003.

Singh, T, Singh, S & Tiwari, S 2013, 'Assessment of digital image classification algorithms for forest and land-use classification in the eastern Himalayas using the IRS LISS III sensor', *International Journal of Remote Sensing*, vol. 34, no. 11, pp. 4105-26.

Song, C, Woodcock, CE, Seto, KC, Lenney, MP & Macomber, SA 2001, 'Classification and Change Detection Using Landsat TM Data: When and How to Correct Atmospheric Effects?', *Remote Sensing of Environment*, vol. 75, no. 2, pp. 230-44.

Turvey, CG & Mclaurin, MK 2012, 'Applicability of the Normalized Difference Vegetation Index (NDVI) in index-based crop insurance design', *Weather, Climate, and Society*, vol. 4, no. 4, pp. 271-84.

Uddin, SN, Taplin, R & Yu, X 2007, 'Energy, environment and development in Bhutan', *Renewable and Sustainable Energy Reviews*, vol. 11, no. 9, pp. 2083-103.

USGS 2018a, *Geometry*, USGS, viewed 30 September 2018, <<https://landsat.usgs.gov/geometry>>.

2018b, *Landsat 4-7 Surface Reflectance (LEDAPS) Product Guide*, by —, USGS.

Vogelmann, JE, Howard, SM, Yang, L, Larson, CR, Wylie, BK & Van Driel, N 2001, 'Completion of the 1990s National Land Cover Data Set for the conterminous United States from Landsat Thematic Mapper data and ancillary data sources', *Photogrammetric Engineering and Remote Sensing*, vol. 67, no. 6.

Vogelmann, JE, Xian, G, Homer, C & Tolk, B 2012, 'Monitoring gradual ecosystem change using Landsat time series analyses: Case studies in selected forest and rangeland ecosystems', *Remote Sensing of Environment*, vol. 122, pp. 92-105.

Wang, SW, Curtis, PD & Lassoie, JP 2006, 'Farmer perceptions of crop damage by wildlife in Jigme Singye Wangchuck National Park, Bhutan', *Wildlife Society Bulletin*, vol. 34, no. 2, pp. 359-65.

Wangchuk, S & Siebert, SF 2013, 'Agricultural change in Bumthang, Bhutan: market opportunities, government policies, and climate change', *Society & Natural Resources*, vol. 26, no. 12, pp. 1375-89.

Weng, Q 2002, 'Land use change analysis in the Zhujiang Delta of China using satellite remote sensing, GIS and stochastic modelling', *Journal of Environmental Management*, vol. 64, no. 3, pp. 273-84.

White, J, Wulder, M, Hobart, G, Luther, J, Hermosilla, T, Griffiths, P, Coops, N, Hall, R, Hostert, P & Dyk, A 2014, 'Pixel-based image compositing for large-area dense time series applications and science', *Canadian Journal of Remote Sensing*, vol. 40, no. 3, pp. 192-212.

Xian, G, Homer, C & Fry, J 2009, 'Updating the 2001 National Land Cover Database land cover classification to 2006 by using Landsat imagery change detection methods', *Remote Sensing of Environment*, vol. 113, no. 6, pp. 1133-47.

Xu, M, Watanachaturaporn, P, Varshney, PK & Arora, MK 2005, 'Decision tree regression for soft classification of remote sensing data', *Remote Sensing of Environment*, vol. 97, no. 3, pp. 322-36.

Xue, J & Su, B 2017, 'Significant remote sensing vegetation indices: A review of developments and applications', *Journal of Sensors*, vol. 2017.

Yangchen, U, Thinley, U & Wallentin, G 2015, 'Land Use Land Cover Changes in Bhutan: 2000-2013', in Shahnawaz & U Thinley (eds), *Climate Change, Environment and Development in Bhutan*,

Thimphu.

Yeom, J-M, Hwang, J, Jung, J-H, Lee, K-H & Lee, C-S 2017, 'Initial Radiometric Characteristics of KOMPSAT-3A Multispectral Imagery Using the 6S Radiative Transfer Model, Well-Known Radiometric Tarps, and MFRSR Measurements', *Remote Sensing*, vol. 9, no. 2, p. 130.

## Appendix A: Crop calendar for Paro district

Crop	Jan	Feb	Mar	Apr	May	Jun	Jul	Aug	Sep	Oct	Nov	Dec
Maize												
Rice												
Winter Wheat / Barley												
Spring wheat												
Buckwheat												
Mustard												
Potato												



Source: Ministry of Forest and Agriculture, Royal Government of Bhutan

## Appendix B: Encapsulated Postscript for cloud masking model

```
COMMENT          "Generated          from          graphical          model:
v:\sotepostgrad\mill0646\tash0013\data\crop season\l2 landsat image\spatial
model\combined_cldmasking.gmd";
# 1995 TM IMAGE
# 2005 TM IMAGE
# 2011 TM IMAGE
# CLOUD QA (1995, 2005 & 2011)
# 2011 FIELD DATA (RICE)
# 2011 FIELD DATA (OTHER CROP)
# CLOUD MASK
# PRISM DEM
# RELATIVE DEM
#
# set cell size for the model
#
SET CELLSIZE MIN;
#
# set window for the model
#
SET WINDOW INTERSECTION;
#
# set area of interest for the model
#
SET AOI NONE;
#
# declarations
#
Integer RASTER n1_cloud95 FILE OLD PUBINPUT NEAREST NEIGHBOR AOI NONE
"v:/sotepostgrad/mill0646/tash0013/data/crop season/l2 landsat
image/studyarea/cloud layers/cloud95-05-11-sub.img";
Float RASTER n3_temp;
Integer RASTER n5_tm FILE DELETE_IF_EXISTING PUBOUT IGNORE 0 ATHEMATIC 16 BIT
UNSIGNED INTEGER "v:/sotepostgrad/mill0646/tash0013/data/crop season/l2
landsat image/cloud_masked_raster/tm-1995-cldmsk.img";
Integer RASTER n6_tm FILE OLD PUBINPUT NEAREST NEIGHBOR AOI
"v:/sotepostgrad/mill0646/tash0013/data/crop season/l2 landsat
image/studyarea/final_aoi_paro.aoi"
"v:/sotepostgrad/mill0646/tash0013/data/crop season/l2 landsat image/tm-
1995/datasets/tm-1995-paro-sub.img";
Integer RASTER n9_tm FILE DELETE_IF_EXISTING PUBOUT IGNORE 0 ATHEMATIC 16 BIT
UNSIGNED INTEGER "v:/sotepostgrad/mill0646/tash0013/data/crop season/l2
landsat image/cloud_masked_raster/tm-2005-cldmsk.img";
Integer RASTER n10_tm FILE DELETE_IF_EXISTING PUBOUT IGNORE 0 THEMATIC BIN
DIRECT DEFAULT 8 BIT UNSIGNED INTEGER
"v:/sotepostgrad/mill0646/tash0013/data/crop season/l2 landsat
image/cloud_masked_raster/tm-2011-cldmsk.img";
Integer RASTER n11_tm FILE OLD PUBINPUT NEAREST NEIGHBOR AOI
"v:/sotepostgrad/mill0646/tash0013/data/crop season/l2 landsat
image/studyarea/final_aoi_paro.aoi"
"v:/sotepostgrad/mill0646/tash0013/data/crop season/l2 landsat image/tm-
2011/datasets/tm-2011-sr-band1-2-3-4-5-7-sub.img";
Integer RASTER n12_tm FILE OLD PUBINPUT NEAREST NEIGHBOR AOI
"v:/sotepostgrad/mill0646/tash0013/data/crop season/l2 landsat
image/studyarea/final_aoi_paro.aoi"
```

```

"v:/sotepostgrad/mill0646/tash0013/data/crop season/12 landsat image/tm-
2005/datasets/tm-2005-sr-b1-2-3-4-5-7.img";
Integer RASTER n17_cadastral FILE OLD PUBINPUT NEAREST NEIGHBOR AOI
"v:/sotepostgrad/mill0646/tash0013/data/crop season/12 landsat
image/studyarea/final_aoi_paro.aoi"
"v:/sotepostgrad/mill0646/tash0013/data/crop season/12 landsat image/land
type/cadastral-paro-rice-recode.img";
Integer RASTER n18_cadastral FILE OLD PUBINPUT NEAREST NEIGHBOR AOI
"v:/sotepostgrad/mill0646/tash0013/data/crop season/12 landsat
image/studyarea/final_aoi_paro.aoi"
"v:/sotepostgrad/mill0646/tash0013/data/crop season/12 landsat image/land
type/cadastral-paro-other-crop-recode.img";
Integer RASTER n21_ground FILE DELETE_IF_EXISTING PUBOUT USEALL THEMATIC BIN
DIRECT DEFAULT 8 BIT UNSIGNED INTEGER
"v:/sotepostgrad/mill0646/tash0013/data/crop season/12 landsat
image/cloud_masked_raster/ground-truth-rice-cldmsk.img";
Integer RASTER n22_ground FILE DELETE_IF_EXISTING PUBOUT IGNORE 0 THEMATIC
BIN DIRECT DEFAULT 8 BIT UNSIGNED INTEGER
"v:/sotepostgrad/mill0646/tash0013/data/crop season/12 landsat
image/cloud_masked_raster/ground-truth-other crop-cldmsk.img";
Integer RASTER n29_prism FILE OLD PUBINPUT NEAREST NEIGHBOR AOI
"v:/sotepostgrad/mill0646/tash0013/data/crop season/12 landsat
image/studyarea/final_aoi_paro.aoi"
"v:/sotepostgrad/mill0646/tash0013/data/crop season/12 landsat
image/dem_sub/prism-dem-cldmsk.img";
Integer RASTER n30_rel_height FILE OLD PUBINPUT NEAREST NEIGHBOR AOI
"v:/sotepostgrad/mill0646/tash0013/data/crop season/12 landsat
image/studyarea/final_aoi_paro.aoi"
"v:/sotepostgrad/mill0646/tash0013/data/crop season/12 landsat
image/dem_sub/rel_height-above-river.img";
Integer RASTER n31_prism FILE DELETE_IF_EXISTING PUBOUT USEALL ATHEMATIC 16
BIT UNSIGNED INTEGER "v:/sotepostgrad/mill0646/tash0013/data/crop season/12
landsat image/cloud_masked_raster/prism-dem-cldmsk.img";
Integer RASTER n32_rel FILE DELETE_IF_EXISTING PUBOUT USEALL ATHEMATIC 16 BIT
SIGNED INTEGER "v:/sotepostgrad/mill0646/tash0013/data/crop season/12 landsat
image/cloud_masked_raster/rel-dem-cldmsk.img";
#
# function definitions
#
n3_temp = EITHER 0 IF (($n1_cloud95(1) GE 2 AND $n1_cloud95(1) NE 9) OR
($n1_cloud95(2) GE 2 AND $n1_cloud95(2) NE 9) OR ($n1_cloud95(3) GE 2 AND
$n1_cloud95(3) NE 9)) OR 1 OTHERWISE ;
n5_tm = $n3_temp * $n6_tm;
n32_rel = $n3_temp*$n30_rel_height;
n31_prism = $n3_temp*$n29_prism;
n10_tm = $n3_temp * $n11_tm;
n9_tm = $n3_temp * $n12_tm;
n22_ground = $n3_temp * $n18_cadastral;
n21_ground = $n3_temp * $n17_cadastral;
QUIT;

```

## Appendix C: Python script of the model to extract relative DEM

```
# -*- coding: utf-8 -*-
# -----
-
# Extraction_DEM.py
# Created on: 2018-09-26 12:03:25.00000
# (generated by ArcGIS/ModelBuilder)
# Usage: Extraction_DEM <DEM> <prsm_strmodr> <dem_heightFromRiver>
<Processing_limit>
# Description:
# -----
-

# Set the necessary product code
# import arcinfo

# Import arcpy module
import arcpy

# Script arguments
DEM = arcpy.GetParameterAsText(0)
if DEM == '#' or not DEM:
    DEM = "PRISM_DSM_Sub" # provide a default value if unspecified

prsm_strmodr = arcpy.GetParameterAsText(1)
if prsm_strmodr == '#' or not prsm_strmodr:
    prsm_strmodr = "prsm_strmodr" # provide a default value if unspecified

dem_heightFromRiver = arcpy.GetParameterAsText(2)
if dem_heightFromRiver == '#' or not dem_heightFromRiver:
    dem_heightFromRiver = "V:\\SOTEPstGrad\\mill0646\\tash0013\\Data\\Data.gdb\\dem_heightFromRiver" # provide a default value if unspecified

Processing_limit = arcpy.GetParameterAsText(3)
if Processing_limit == '#' or not Processing_limit:
    Processing_limit = "Processing_limit" # provide a default value if unspecified

# Local variables:
dem_masked = "V:\\SOTEPstGrad\\mill0646\\tash0013\\Data\\Data.gdb\\dem_masked"
dem_points = "V:\\SOTEPstGrad\\mill0646\\tash0013\\Data\\Data.gdb\\dem_points"
dem_points_with_str_FID = dem_points
strOrder = "V:\\SOTEPstGrad\\mill0646\\tash0013\\Data\\Data.gdb\\strOrder"
strOrder_Layer = "strOrder_Layer"
streamPoints = "V:\\SOTEPstGrad\\mill0646\\tash0013\\Data\\Data.gdb\\streamPoints"
dem_points__2_ = streamPoints
dem_points_with_Field = dem_points_with_str_FID
dem_points_calculated = dem_points__2_

# Set Geoprocessing environments
```

```

arcpy.env.scratchWorkspace
"V:\\SOTEPPostGrad\\mill0646\\tash0013\\Data\\scratch.gdb"

# Process: Extract by Mask
arcpy.gp.ExtractByMask_sa(DEM, Processing_limit, dem_masked)

# Process: Raster to Point
arcpy.RasterToPoint_conversion(dem_masked, dem_points, "VALUE")

# Process: Raster to Point (2)
arcpy.RasterToPoint_conversion(prsm_strmodr, strOrder, "VALUE")

# Process: Make Feature Layer
arcpy.MakeFeatureLayer_management(strOrder, strOrder_Layer, "grid_code < 15
AND grid_code > 1", "", "Shape Shape VISIBLE NONE;OBJECTID OBJECTID VISIBLE
NONE;POINTID POINTID VISIBLE NONE;GRID_CODE GRID_CODE VISIBLE NONE")

# Process: Extract Values to Points
arcpy.gp.ExtractValuesToPoints_sa(strOrder_Layer, DEM, streamPoints, "NONE",
"VALUE_ONLY")

# Process: Near
arcpy.Near_analysis(dem_points,
"V:\\SOTEPPostGrad\\mill0646\\tash0013\\Data\\Data.gdb\\streamPoints", "",
"NO_LOCATION", "NO_ANGLE", "PLANAR")

# Process: Add field for height above river
arcpy.AddField_management(dem_points_with_str_FID, "HeightAboveRiver",
"DOUBLE", "", "", "", "", "NULLABLE", "NON_REQUIRED", "")

# Process: Join Field
arcpy.JoinField_management(dem_points_with_Field, "NEAR_FID", streamPoints,
"OBJECTID", "")

# Process: Calculate Field
arcpy.CalculateField_management(dem_points__2_, "HeightAboveRiver",
"[grid_code] - [RASTERVALU]", "VB", "")

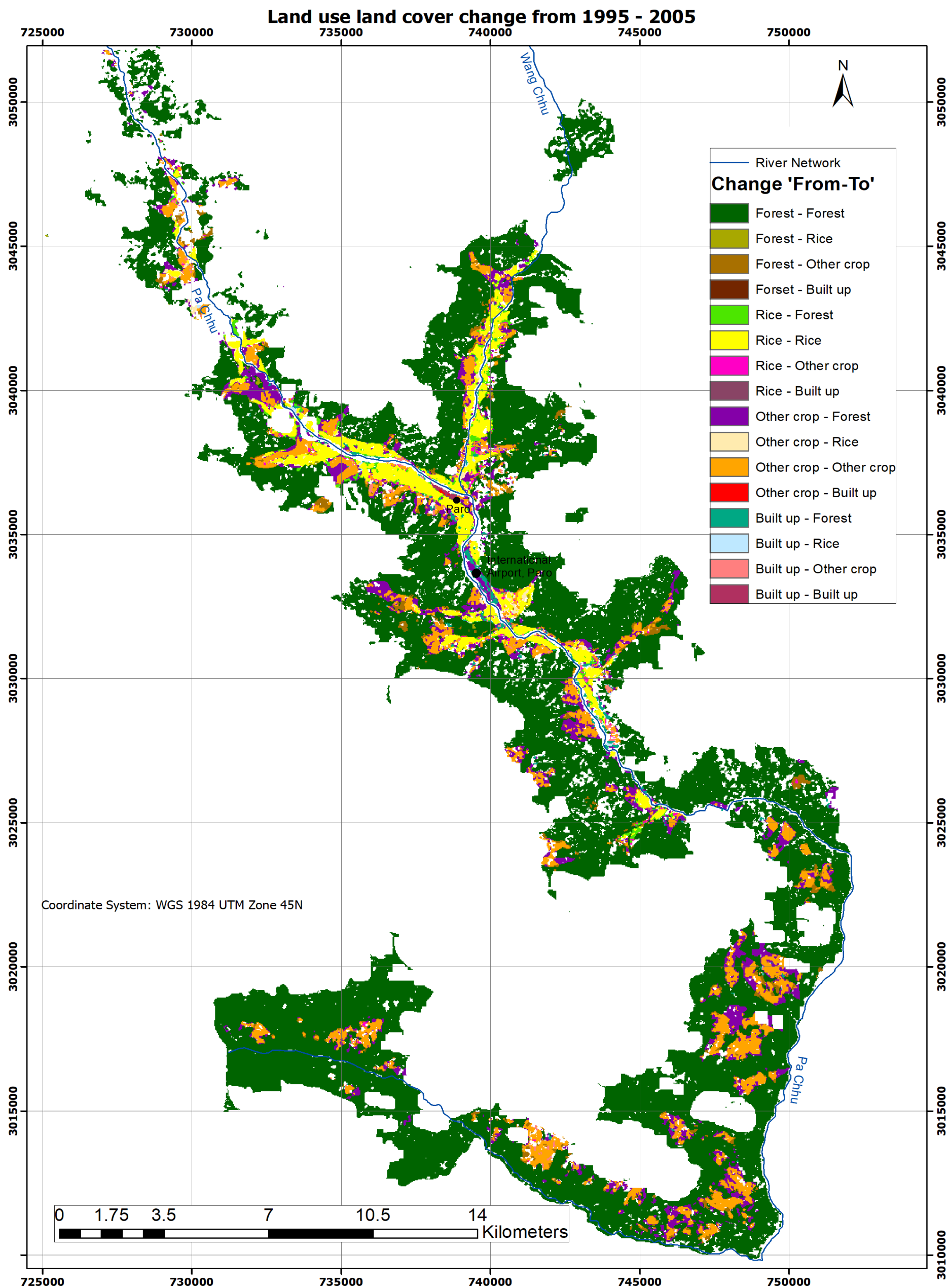
# Process: Point to Raster
arcpy.PointToRaster_conversion(dem_points_calculated, "HeightAboveRiver",
dem_heightFromRiver, "MOST_FREQUENT", "NONE", DEM)

```

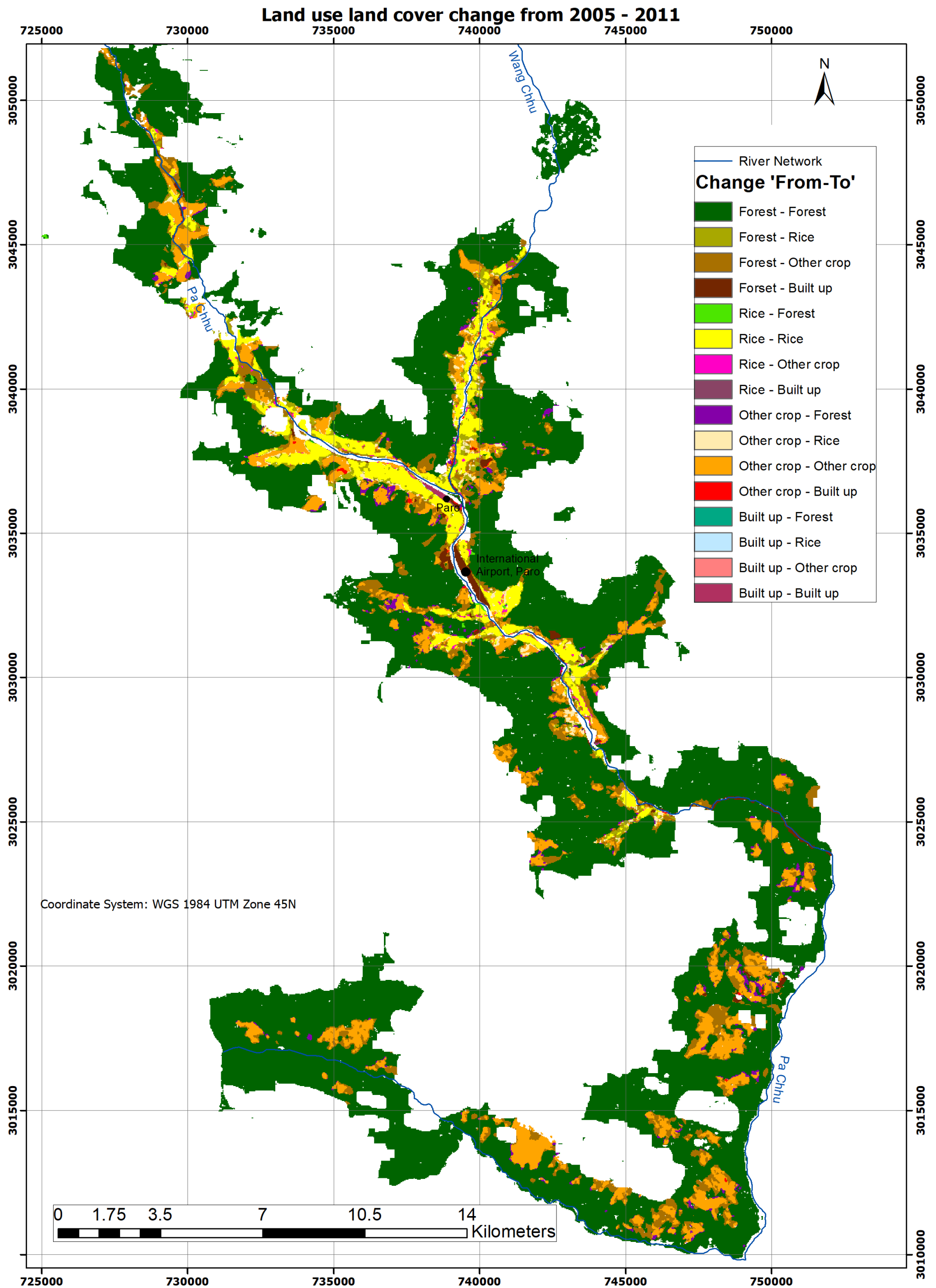
Appendix D: **Encapsulated Postscript for accuracy assessment model**

```
COMMENT          "Generated          from          graphical          model:
v:/sotepostgrad/mill0646/tash0013/data/crop season/l2 landsat image/spatial
model/accuracy assessment.gmd";
# CLASSIFICATION RESULT
# FIELD DATA
#
# set cell size for the model
#
SET CELLSIZE MIN;
#
# set window for the model
#
SET WINDOW INTERSECTION;
#
# set area of interest for the model
#
SET AOI NONE;
#
# declarations
#
Integer RASTER n1_paro FILE OLD PUBINPUT NEAREST NEIGHBOR AOI NONE
"v:/sotepostgrad/mill0646/tash0013/data/crop season/l2 landsat image/post-
classification/thematic lu map/field raster/paro-rice-cldmsk-final.img";
Integer RASTER n2_tm FILE OLD PUBINPUT NEAREST NEIGHBOR AOI NONE
"v:/sotepostgrad/mill0646/tash0013/data/crop season/l2 landsat image/post-
classification/thematic lu map/individual lu/individual lu-2011/tm-2011-rice-
sup-mlc-cldmsk-final.img";
Integer RASTER n3_rice FILE DELETE_IF_EXISTING PUBOUT USEALL ATHEMATIC 8 BIT
SIGNED INTEGER "v:/sotepostgrad/mill0646/tash0013/data/crop season/l2 landsat
image/post-classification/final-accuracy-map/rice-accuracy_positive.img";
#
# function definitions
#
n3_rice = EITHER 3 IF ( $n1_paro==0 AND $n2_tm==0 ) OR (EITHER 2 IF ($n1_paro
- $n2_tm LT 0) OR ($n1_paro - $n2_tm) OTHERWISE) OTHERWISE ;
QUIT;
```

Appendix E: Land use land cover change map from 1995-2005



Appendix F: Land use land cover change map from 2005-2011



Appendix G: Land use land cover change map from 1995-2011

